

AD-A104 312

BELL NORTHERN RESEARCH LTD OTTAWA (ONTARIO)

F/G 16/3

ELECTROMAGNETIC FIELD MAPPING OF CYLINDER AND MISSILE NOSEcone. (U)

JUL 81 R R GOULETTE, K E FELSKA F30602-79-C-0197

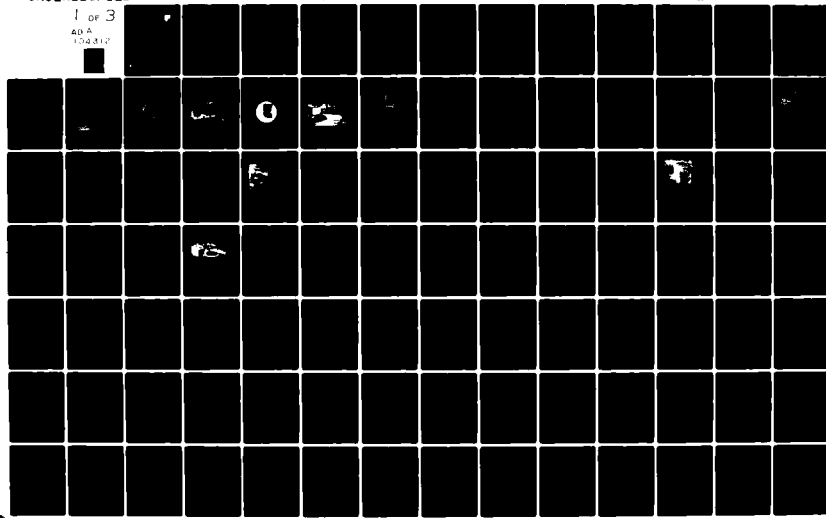
UNCLASSIFIED

RADC-TR-81-179

NL

1 OF 3

4D A
104-812



AD A104312

RADC-TR-81-179
Final Technical Report
July 1981

LEVEL II

(12)



ELECTROMAGNETIC FIELD MAPPING OF CYLINDER AND MISSILE NOSECONE

Bell-Northern Research

Richard R. Goulette
Kent E. Felske

DTIC ELECTE
S SEP 17 1981
E

APPROVED FOR PUBLIC RELEASE; DISTRIBUTION UNLIMITED

DTIC FILE COPY

ROME AIR DEVELOPMENT CENTER
Air Force Systems Command
Griffiss Air Force Base, New York 13441

810 17 23 C 17 81

This report has been reviewed by the RADC Public Affairs Office (PA) and is releasable to the National Technical Information Service (NTIS). At NTIS it will be releasable to the general public, including foreign nations.

RADC-TR-81-179 has been reviewed and is approved for publication.

APPROVED: *Roy F. Stratton*

ROY F. STRATTON
Project Engineer

APPROVED:

David C. Luke

DAVID C. LUKE, Colonel, USAF
Chief, Reliability and Compatibility Division

FOR THE COMMANDER:

John P. Huss

JOHN P. HUSS
Acting Chief, Plans Office

If your address has changed or if you wish to be removed from the RADC mailing list, or if the addressee is no longer employed by your organization, please notify RADC (RBCT) Griffiss AFB NY 13441. This will assist us in maintaining a current mailing list.

Do not return this copy. Retain or destroy.

UNCLASSIFIED

SECURITY CLASSIFICATION OF THIS PAGE (When Data Entered)

19 REPORT DOCUMENTATION PAGE		READ INSTRUCTIONS BEFORE COMPLETING FORM
1. REPORT NUMBER RADCR TR-81-179	2. GOVT ACCESSION NO. AD A104372	3. RECIPIENT'S CATALOG NUMBER
4. TITLE (and Subtitle) ELECTROMAGNETIC FIELD MAPPING OF CYLINDER AND MISSILE NOSECONES		5. TYPE OF REPORT & PERIOD COVERED Final Technical Report Aug 79 - Sep 80
6. AUTHOR(s) Richard R. Goulette Kent E. Felske		7. PERFORMING ORG. REPORT NUMBER N/A
8. CONTRACT OR GRANT NUMBER(s) F3602-79-C-0197		9. PROGRAM ELEMENT, PROJECT, TASK AREA & WORK UNIT NUMBERS 162702F 23380325
10. CONTROLLING OFFICE NAME AND ADDRESS Rome Air Development Center (RBCT) Griffiss AFB NY 13441		11. REPORT DATE July 1981
12. MONITORING AGENCY NAME & ADDRESS (if different from Controlling Office) Same		13. NUMBER OF PAGES 210
14. SECURITY CLASS. (of this report) UNCLASSIFIED		15. SECURITY CLASS. (of the abstract entered in Block 20, if different from Report) UNCLASSIFIED
16. DISTRIBUTION STATEMENT (of this Report) Approved for public release; distribution unlimited.		17a. DECLASSIFICATION/DOWNGRADING SCHEDULE N/A
17. DISTRIBUTION STATEMENT (of the abstract entered in Block 20, if different from Report) Same		
18. SUPPLEMENTARY NOTES RADC Project Engineer: Roy Stratton (RBCT)		
19. KEY WORDS (Continue on reverse side if necessary and identify by block number) Electromagnetic Field Mapping		
20. ABSTRACT (Continue on reverse side if necessary and identify by block number) This technical report describes the technology and instrumentation developed for the measurement of vector electric and magnetic fields with cylindrical configurations, when the configurations are illuminated by a plane electromagnetic wave in the frequency range of 225 to 400 MHz. A set of such contour maps are presented for a missile nosecone and a right circular cylinder illuminated by a 300 MHz planewave.		

DD FORM 1 JAN 73 1473 EDITION OF 1 NOV 68 IS OBSOLETE

UNCLASSIFIED

SECURITY CLASSIFICATION OF THIS PAGE (When Data Entered)

403-0-1

UNCLASSIFIED

SECURITY CLASSIFICATION OF THIS PAGE(When Data Entered)



UNCLASSIFIED

SECURITY CLASSIFICATION OF THIS PAGE(When Data Entered)

PREFACE

Bell-Northern Research is pleased to submit this Final Report on "Electromagnetic Field Mapping of Cylinder and Missile Nosecone", Air Force Contract No. F30602-79-C-0197, to Rome Air Development Centre (RADC/RBCT).

This one year program has demonstrated that electromagnetic probes can be designed with the necessary resolution, sensitivity and accuracy for mapping complex electric and magnetic fields at UHF frequencies within metal structures containing apertures.

Accession For	
NTIS GRA&I <input checked="" type="checkbox"/>	
DTIC TAB <input type="checkbox"/>	
Unannounced <input type="checkbox"/>	
Justification	
By _____	
Distribution/	
Availability Codes	
Dist	Avail and/or
	Special
A	

TABLE OF CONTENTS

	Page
1.0 INTRODUCTION	1
1.1 Background	1
2.0 APPROACH	3
2.1 Considerations in Electromagnetic Field Mapping	3
3.0 EM FIELD MAPPING SYSTEM	6
3.1 General System Description	6
3.2 Electric Field Probe Design	11
3.3 Magnetic Field Probe Design	21
3.4 Signal Conditioning and Transmission	28
3.5 Signal Acquisition and Analysis System	33
3.6 Mechanical Positioning System	37
3.7 Field Illumination System for Mapping	37
4.0 RESULTS	39
4.1 Probe Evaluation	39
4.2 Illumination System Evaluation	42
4.3 Mechanical Positioning System Tests	42
4.4 Field Contours	45
5.0 CONCLUSIONS	47
REFERENCES	48
APPENDIX A Definition of Field Measurement Geometry and Sampling	
APPENDIX B Field Contour Maps for Missile Nosecone and Cylinder	
APPENDIX C Tabulation of E-Field and H-Field Measurement Data	
APPENDIX D Results of E-Field Perturbation Test Conducted in Missile	
APPENDIX E Probe Calibration Curves and Lookup Table (Nosecone Removed)	
APPENDIX F Computer Programs	
APPENDIX G Operating and Maintenance Data for EM Field Mapping Components	

LIST OF ILLUSTRATIONS

<u>FIGURE</u>		<u>Page</u>
1	Missile Nosecone in Position for Field Mapping	6
2	View of Forward Section of Missile with Nosecone Removed, Showing Probe Carriage	7
3	View of Mechanical Positioning Unit, Assembled to Nosecone Bulkhead	8
4	Rear View of Missile, showing Signal Conditioner Installed	9
5	Laboratory Setup Outside of RF Anechoic Chamber	10
6	Block Diagram of Instrumentation Used for Field Mapping	11
7	Equivalent Circuit of E-Field Probe	13
8	E-Field Probe in Holding Fixture	18
9	Mechanical Assembly of E-Field Probe	19
10	DC Characteristics of E-Field Probe	20
11	Equivalent Circuit of H-Field Probe	22
12	H-Field Probe in Holding Fixture	23
13	Mechanical Assembly of H-Field Probe	24
14	DC Characteristic of H-Field Probe	25
15	View of Signal Conditioner, Showing Controls and Signal Ports	29
16	Block Diagram of Signal Conditioner	30
17	Transfer Characteristics of Signal Conditioner	31
18	Frequency Response of Signal Conditioner	32
19	Total Transfer Characteristic of Signal Conditioner and E-Field Probe	34
20	Total Transfer Characteristic of Signal Conditioner and H-Field Probe	35
21	View of Optical Link Receiver Unit connected via Fiber Optic Link to Signal Conditioner	36
22	Frequency Response of E-Field Probe	43
23	Probe Gradient and Resolution	44
24	Frequency Response of H-Field Probe	45

LIST OF TABLES

	<u>Page</u>
TABLE 1 Summary of E-Field Probe Results	40
TABLE 2 Summary of H-Field Probe Results	41

1.0 INTRODUCTION

Bell Northern Research (BNR), under contract to Rome Air Development Center (RADC) has carried out a two-part program for electromagnetic field mapping:

- (a) First, using the EM probing methodology previously developed at BNR, techniques and instrumentation were devised to measure the total vector electric (E) and magnetic (H) fields inside metallic enclosures in the frequency range of 225 MHz to 400 MHz and
- (b) In the second part of the program, these techniques and instrumentation were applied to the mapping of E and H fields within the two metallic enclosures described in this report.

The instrumentation developed by BNR was required to meet the following design objectives:

Frequency range	225-400 MHz
E-field strength	0.19-200 V/m
H-field strength	0.0005-0.52 A/m
Field gradient	10 dB/cm (or more)
Spatial resolution	±0.5 cm
Accuracy	±1 dB
Free of resonance in the range	225-400 MHz

1.1 Background

Measuring electromagnetic field distributions yields accurate results without the need to make assumptions about the enclosing structure or to develop mathematical approximations of complex shapes. On the other hand, there can be severe or even insurmountable physical difficulties to apply the technique within metallic enclosures containing many obstacles.

Prediction techniques avoid this problem and can readily be applied to many complex geometric structures. However, before using a prediction technique with confidence, it is necessary to verify by measurement that the mathematical model accurately portrays reality. It is also useful to learn by measurement which parameters

utilized in the model are most sensitive - that is, in which cases will small changes in parameter value have a significant impact on model results.

The measurement objectives set by RADC which are summarized in paragraph 1.0 were based upon the need to obtain experimental verification for recently developed mathematical modeling techniques developed by Taflove [1].

This is in response to the need for improved high resolution field prediction and measurement techniques in the UHF frequency range. Two "standard cylindrical configurations" were used in comparing various field penetration results. These are described as:

- a) Right Circular Aluminum Cylinder, closed one end, 27-3/16" long by 7-3/16" diameter.
- b) Empty shell of guidance, control, and telemetry section of a missile, subsequently referred to as a "nosecone" as field mapping takes place in this forward section.

The configurations used to obtain the measured results in this report are the identical configurations described in reference [1].

2.0 APPROACH

The approach was to use miniature dipole and loop antennas incorporating detector diodes. This approach permitted the use of a non-perturbing, high-resistance transmission line to transmit demodulated signals to a signal conditioner outside the field measurement zone.

Selection of key elements was carefully optimized in order to meet the requirements for both high sensitivity and high spatial resolution in the UHF frequency band. These stringent requirements for sensitivity and resolution were necessary in order to accurately measure the complex fields within metallic enclosures such as weapon system casings.

2.1 Considerations in Electromagnetic Field Mapping

The design of a high performance electromagnetic field mapping system for use in the UHF frequency range must consider several important factors.

The need for high sensitivity must be carefully balanced against the conflicting need for high spatial resolution. The E-field antenna design in this case uses a biconical dipole in conjunction with a zero-bias schottky diode in order to achieve the required sensitivity at a maximum permissible sensor dimension of one centimeter. For a given physical length, the biconical design exhibits a high antenna effective length and low source impedance, which allow a higher signal to be developed across the detector diode. The H-field antenna employs a resonant coil structure in order to achieve a similar goal.

Some probe requirements arise due to the very complexity of the fields being measured within metallic structures.

When these structures encounter an external radiation field, energy is coupled in a complex way through openings, slits, and seams in the structure to produce concentrated electric and magnetic fields having E/H ratios that depart radically from the usual value of 377 ohms encountered in ideal situations. Accordingly, field probes must be small in order to resolve such

concentrated fields, and must also be free from cross-field sensitivity errors. For example, a high magnetic field could couple to an E-field probe in a region of low electric field strength giving a false reading. Similarly a high electric field could adversely affect an H-field probe.

Since the probes are used to measure only one vector field at a time, it is also important that the polar field pattern of each probe conforms closely to the ideal figure-eight (cosine) field pattern of an infinitesimal dipole (or loop); otherwise the total vector field obtained by summation of the three cartesian coordinate vector fields will be subject to error.

The probes and the mechanical system used to position them must not significantly perturb the very field being measured. Thus, metallic RF transmission cables cannot be used for measurements at UHF frequencies and for high spatial resolutions (e.g., +0.5 cm).

Fibre optic transmission from the probe was also ruled out because of the difficulty in making an RF-to-optical converter sufficiently small. Hence detector diodes coupled to miniature dipoles and wire loops were used. The resulting dc signal developed across the diode is transmitted via high resistance (one kilohm per cm. or greater) conductors out of the field measurement zone to an appropriate high-impedance dc amplifier.

All mechanical parts used within the field measurement zone must be non-metallic and have the smallest size consistent with accurate positioning. This constraint can present design difficulties. For example, reactive torques developed in a carriage pulley drive system can impart a bending moment on long plastic shafts causing deflection; also, using only non-metallic fasteners severely limits the clamping forces available in small non-metallic assemblies.

The illumination system itself may produce radiation at harmonic frequencies. This radiation may cause a problem in regions within the objects under test where high field attenuation exists at the illuminating frequency but not at harmonic frequencies. This situation commonly occurs in coupling through apertures in general and could give false readings where attenuation of 40 dB or more are expected, despite taking normal precautions to filter the radiated signal. The

technique used to minimize this problem, an amplitude-modulated illuminating field, is used together with a narrow-bandwidth filter in the amplifier receiving the signal detected from the antenna probe. In this way, higher transmitter harmonics with multiples of the original modulating frequency are rejected in the amplifier.

This technique also resulted in less background noise and a high signal-to-noise ratio.

Other sources of error include temperature effects, which are controllable for the amplifier system but can be significant in the probe structures. These are systematic errors that can be included in the probe calibrations. It is difficult, however, to add perturbing components to a minuscule antenna structure to compensate automatically for probe temperature effects.

3.0 EM FIELD MAPPING SYSTEM

3.1 General System Description

An overview of the total system configuration used for mapping the missile nosecone and the aluminum cylinder may be obtained by reference to Figures 1 through 6 inclusive. Figure 1 depicts the missile nosecone installed in BNR's RF anechoic chamber in a wooden support rack of peg-and-dowel construction.

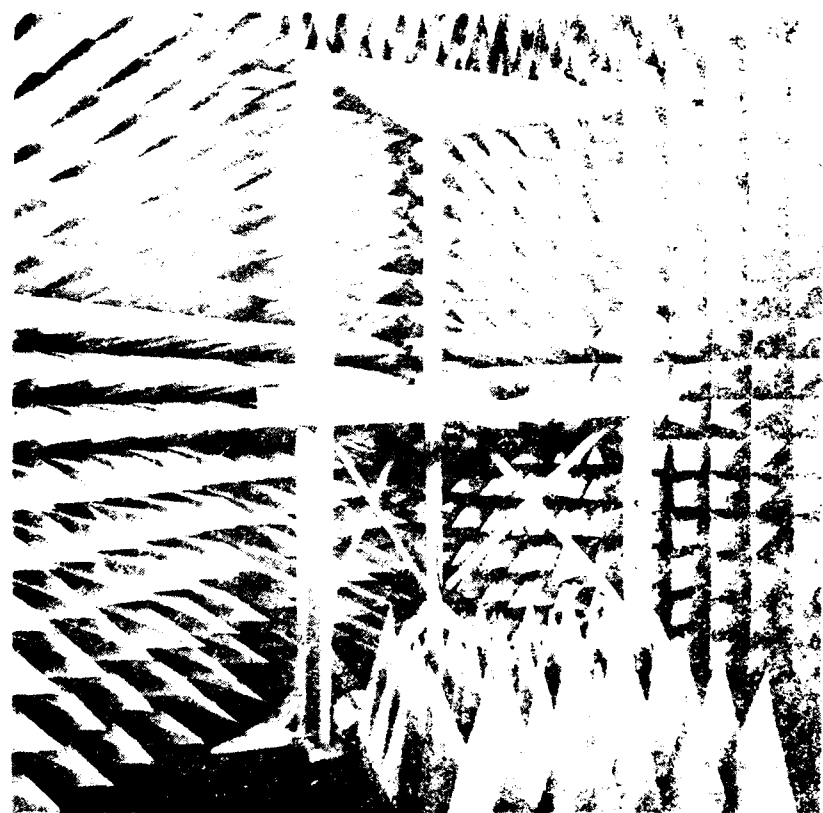


Fig. 1 Missle Nosecone in Position for Field Mapping

Figure 2 shows the nosecone removed from the missile, revealing the probe carriage which is holding the E-field probe.



Fig. 2 View of Forward Section of Missile with Nosecone Removed Showing Probe Mounted on Carriage

Figure 3 shows the mechanical positioner, which is bolted to the rear of the nosecone bulkhead section that is shown in Figure 2.

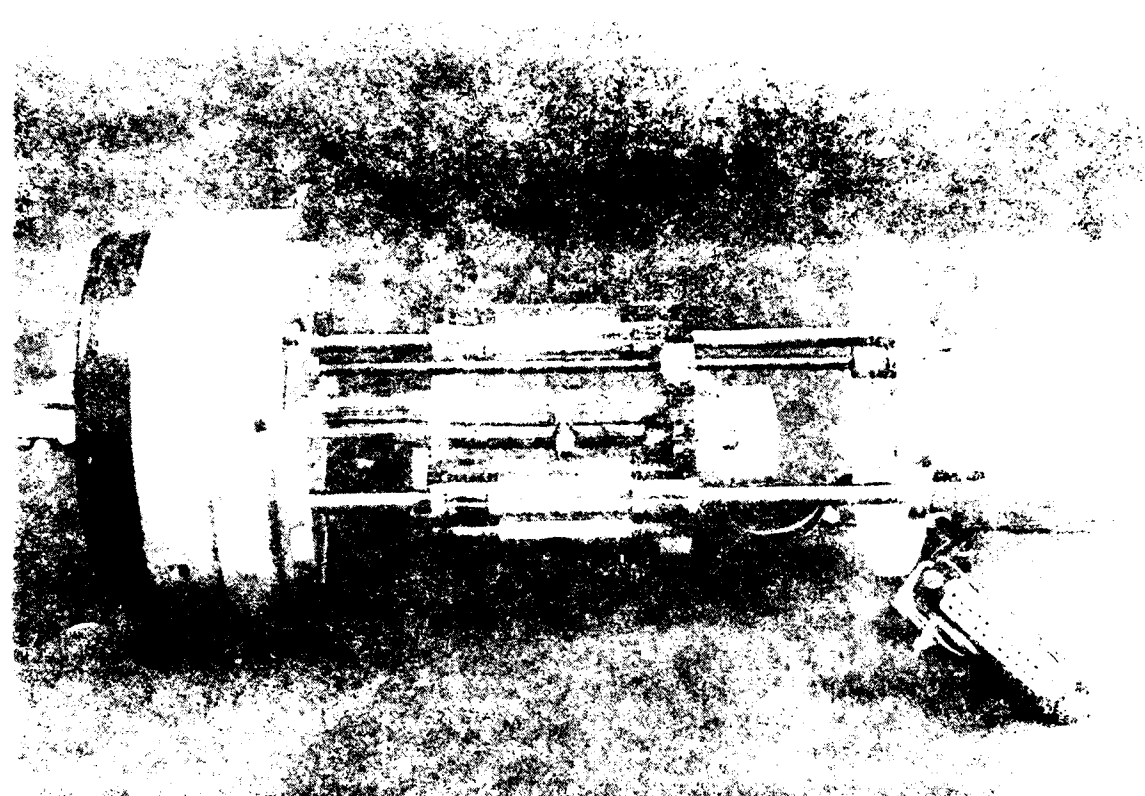


Fig. 3 View of Mechanical Positioning Unit, Assembled to Nosecone Bulkhead

Figure 4 shows the probe signal conditioner, installed in the missile telemetry section, with conductive plastic probe transmission line leads connected to the "in" terminals, a fibre optic link connected to the "out" terminal, and a pneumatic actuator for remote switching of amplifier sensitivity.

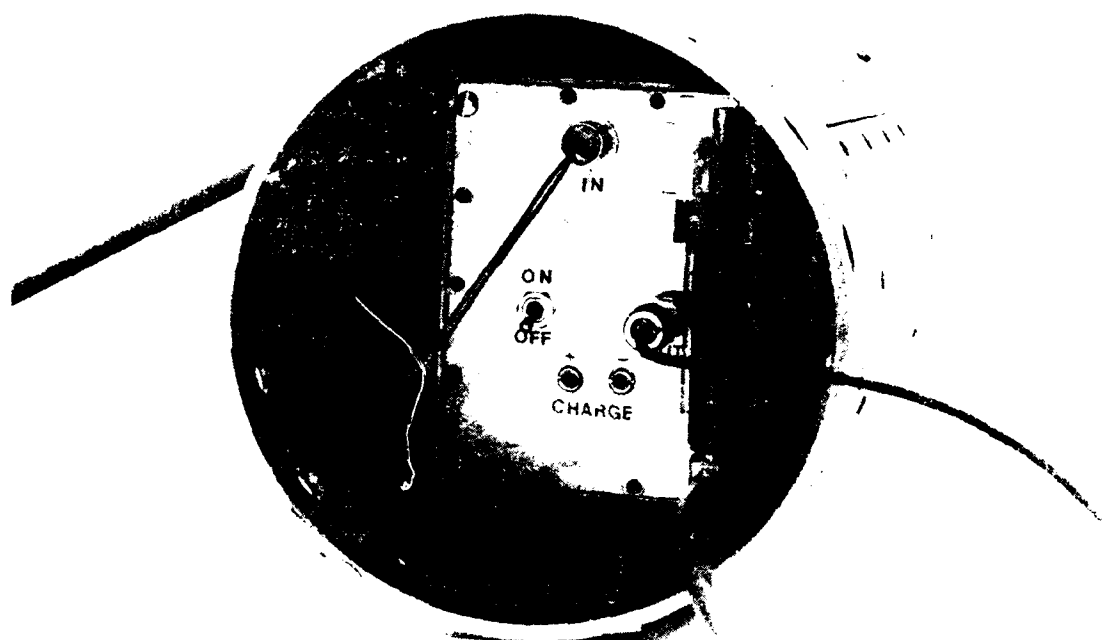


Fig. 4 Rear View of Missile, Showing Signal Conditioner Installed

Figure 5 shows the laboratory setup outside of anechoic chamber. A contour map of a recently completed cylinder may be seen on the computer display screen. The Probe Position Control unit, Optical Link Receiver Unit, Frequency Counter RF Signal Generator, and Computer-controlled relay actuator may also be seen in the photograph.

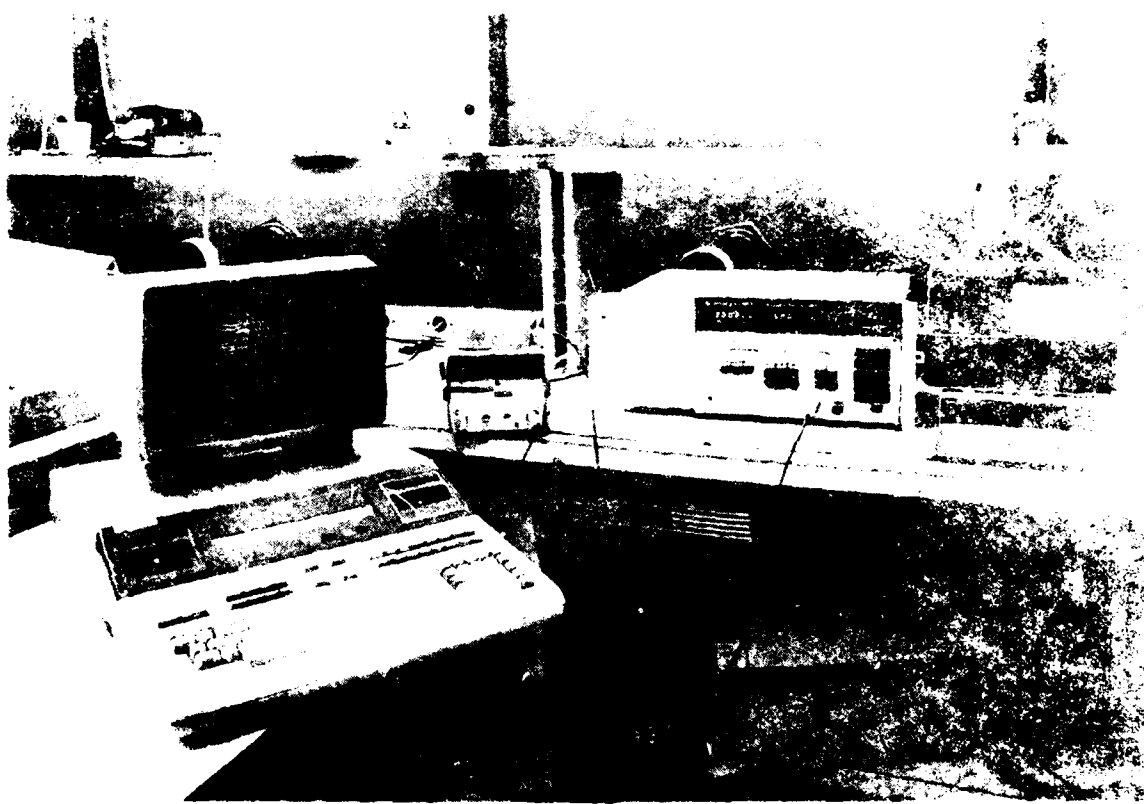


Fig. 5. Laboratory Setup Outside of R.I. Anechoic Chamber

Figure 6 is a block diagram showing how all instrumentation in Figure 5 is functionally interconnected. Details of system function are given in paragraphs 5, 6, 8, and 11.

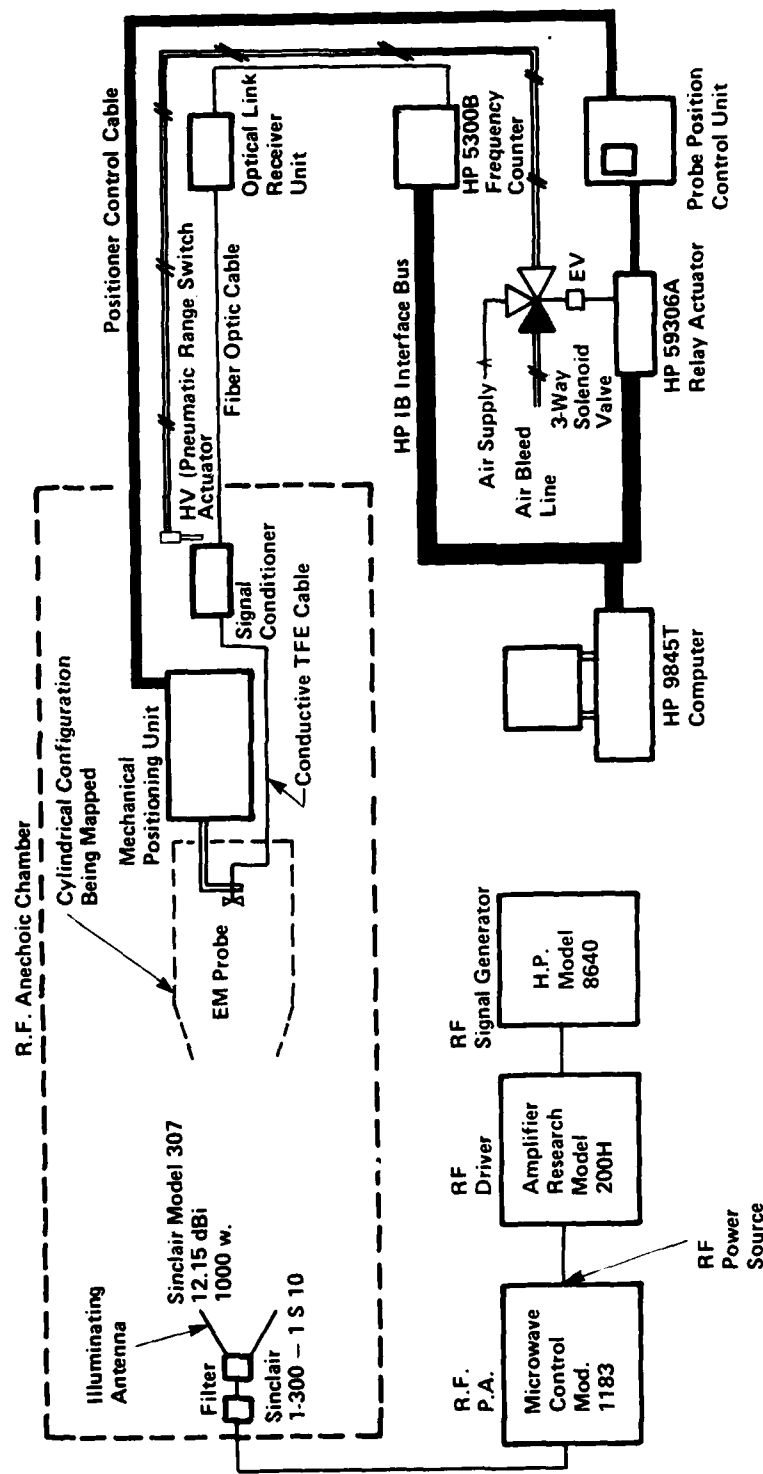


Fig. 6 Block Diagram of Instrumentation Used for Field Mapping

3.2 Electric Field Probe Design

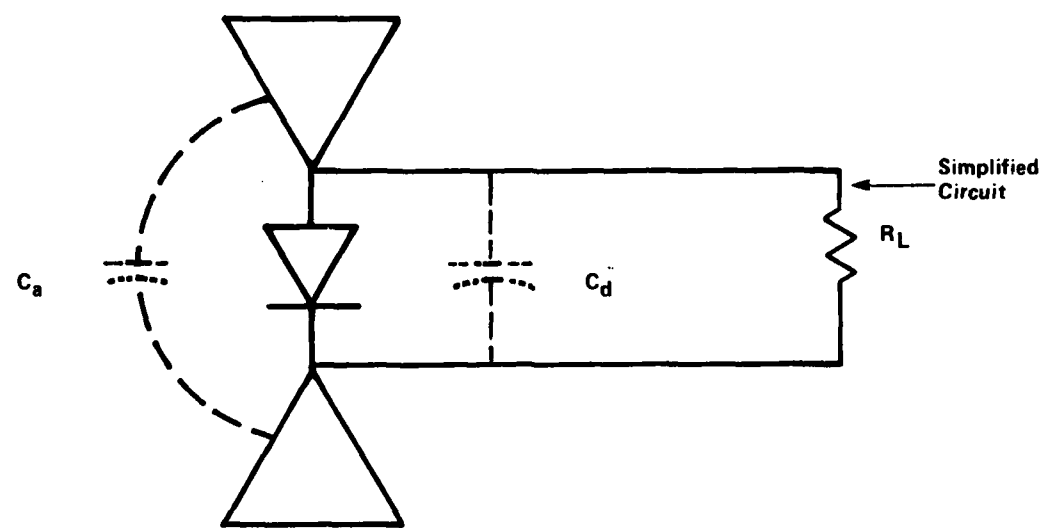
The E-field probe developed under this contract is a small, balanced dipole antenna having a length of one centimeter. The antenna incorporates a zero-bias schottky-diode detector which demodulates the received radio-frequency signal. The demodulated signal is fed to a remote electronic signal conditioner via a high resistance transmission link which provides a high attenuation to radio frequency signals but permits low-loss transmission of dc or low frequency audio signals. The use of this high resistance link minimizes the perturbation of the fields being measured and at the same time provides isolation of RF signals between the probe and its associated electronics. The fundamentals of this technique were first described by Greer [2], and subsequently by several other investigators [7,8].

This section treats the subject of the design of a probe having high sensitivity (better than 0.2 volt/meter), high spatial resolution (better than 0.5 cm), when used for electric field mapping applications in confined metal cylinders in the aeronautical UHF band from 225 to 400 MHz.

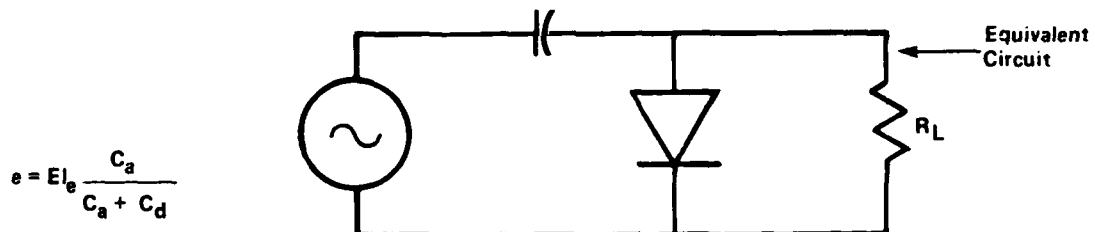
The mapping application described herein employed amplitude-modulated RF illumination, thereby allowing the use of a tuned amplifier to improve the signal-to-noise ratio. However, the probes can be used in other applications to measure unmodulated signals and are discussed in this broader context.

The antenna may be represented by an equivalent Thevenin voltage source e which equals the antenna open-circuit voltage reduced by the capacitive voltage divider actions of the antenna distributed capacitance C_a and the diode detector circuit distributed capacitance C_d . The equivalent source impedance C_{eff} is equal to C_a and C_d connected in parallel. The dc load impedance is represented by the input resistance of the signal conditioner in series with the resistance of the transmission line link.

This simple lumped representation of an essentially distributed network is shown in Figure 7 and accounts for the dominant probe characteristics measured in the UHF region of interest from 225 to 400 MHz.



$$C_{\text{eff}} = C_a + C_d$$



$$e = EI_e \frac{C_a}{C_a + C_d}$$

- E = Incident Field Strength, Volts/Meter
- I_e = Antenna Effective Length, Meters
- C_a = Antenna Distributed Capacitance
- C_d = Diode Distributed Capacitance
- R_L = Load Resistance
- e = Source Voltage of Thevenin Equivalent Circuit
- C_{eff} = Source Impedance of Thevenin Equivalent Circuit

Fig. 7 Equivalent Circuit of E-Field Probe

A closed-form solution for this equivalent circuit may be obtained when the diode is operating in the square law region where diode rectified current is proportional to the square of the applied RF voltage and when the diode is operating in the linear region where rectified current is directly proportional to applied RF voltage.

Starting with the standard diode equation we have:

$$i = i_s \left(\exp \left(\frac{qV}{nKT} \right) - 1 \right) \quad (1)$$

where:

i = dc current flowing through the diode, Amperes

V = dc voltage across the diode junction resulting from dc current " i ", volts

n = constant, ≈ 2 for silicon

q = electron charge = 1.601×10^{-19} coulomb

K = Boltzmann's Constant, 1.38×10^{-23} Joule/ K

T = Temperature, K

i_s = saturation current

The term $\exp\left(\frac{qV}{nKT}\right)$ may be expanded into a Taylor series:

$$1 + \frac{qV}{nKT} + \frac{1}{2!} \left(\frac{qV}{nKT} \right)^2 + \frac{1}{3!} \left(\frac{qV}{nKT} \right)^3 + \dots \quad (2)$$

Accordingly,

$$i = i_s \left(\frac{qV}{nKT} + \frac{1}{2} \left(\frac{qV}{nKT} \right)^2 + \frac{1}{6} \left(\frac{qV}{nKT} \right)^3 + \dots \right) \quad (3)$$

If V is an ac signal, only the even-powered terms in this series can produce rectification.

Also, if $V \lesssim \frac{nKT}{q}$, only the term raised to the power of two need be considered as the sum of the remaining even-powered terms becomes negligible.

In other words, $i_{dc} \approx \frac{i_s}{2} \left(\frac{qV}{nKT} \right)^2$ representing "square law" behavior.

This expression is valid with an error of 8% if $V = \frac{nKT}{q}$

The error diminishes rapidly as V becomes less, and is reduced to 0.015% when:

$$V = \frac{nKT}{q} / 10$$

Now, if $V = (Vm \cos \omega t - iR_L)$ is substituted in this simplified expression, we may solve for:

$$i_{dc} \approx \frac{\frac{q}{nKT} i_s V_m^2}{4 \left(R_L i_s + \frac{nKT}{q} \right)} \quad (4)$$

If $R_L \gg \frac{nKT}{q i_s}$, equation (4) may be simplified to:

$$i_{dc} \approx \frac{\frac{q}{4R_L} \frac{V_m^2}{nKT}}{= \frac{q}{2R_L} \frac{V_{rms}^2}{nKT}} \quad (5)$$

V_{rms} is the root-mean square value of the rf voltage appearing across the diode and R_L is the resistance of the load across the diode.

The quantity $\frac{nKT}{q i_s}$ corresponds to the diode ac resistance when $V < \frac{nKT}{q}$, as derived from the first term of equation (3).

Since: $i_{ac} \approx i_s \frac{qV}{nKT}$ if $V < \frac{nKT}{q}$

Then diode ac resistance $\approx \frac{V}{i_{ac}} = \frac{nKT}{q i_s}$

The RF voltage appearing across the diode may be expressed as a function of the incident electric field strength E (V/m), the antenna effective length ℓ_e , the antenna capacitance C_a and the diode Capacitance C_d , multiplied by the transfer function of the voltage divider formed by the source effective capacitance C_{eff} and the diode effective ac impedance:

$$V_{DIODE} = \frac{C_a}{C_a + C_d} E \ell_e \left[\frac{\left(\frac{nKT}{q\tau_s} \right)}{\left[\left(\frac{nKT}{q\tau_s} \right)^2 + \left(\frac{1}{\omega C_{eff}} \right)^2 \right]^{1/2}} \right] \quad (6)$$

for a 1 cm length biconical antenna with cone angle 30°

$$C_a \approx 0.17 \text{ pf}$$

$$\ell_e \approx 1 \text{ cm} = 0.01 \text{ m}$$

for a MA 40230 schottky diode

$$C_d = 0.2 \text{ pf}, q/nKT = 20 \text{ to } 30,$$

$$\tau_s = 8.9 \times 10^{-5} \text{ to } 1.25 \times 10^{-5} \text{ A}$$

Now at 300 MHz, the right-hand side of equation (6), which is $\frac{nKT}{q\tau_s}$ divided by the denominator, is typically 0.7 for the above antenna and diode.

The RF Voltage across the diode

$$V_{DIODE} = \left(\frac{.17}{.17 + .2} \right) \times E \times .01 \times .7 = 5.2 \times 10^{-5} E \quad (7)$$

Then

$$e_{dc} = \frac{q}{2} \left[5.2 \times 10^{-5} E \right]^2 = 1.28 \times 10^{-4} E^2 \text{ Volts} \quad (8)$$

at 300 MHz

This estimate agrees very closely with Figure 8 which presents measured data. The characteristic gradually changes from a square law characteristic to a linear characteristic above 40 V/m. This corresponds to the region where:

$$\begin{aligned} V_{\text{DIODE}} &> \frac{nKT}{q} \text{ Volts} = \frac{1}{25} \text{ Volt} \\ &= 40 \text{ mV} \\ &= 3.2 \times 10^{-3} E \end{aligned}$$

then

$$E > \frac{40 \times 10^{-3}}{3.2 \times 10^{-3}} \approx 12.5 \text{ V/m}$$



Fig. 2. - A cigarette holder.

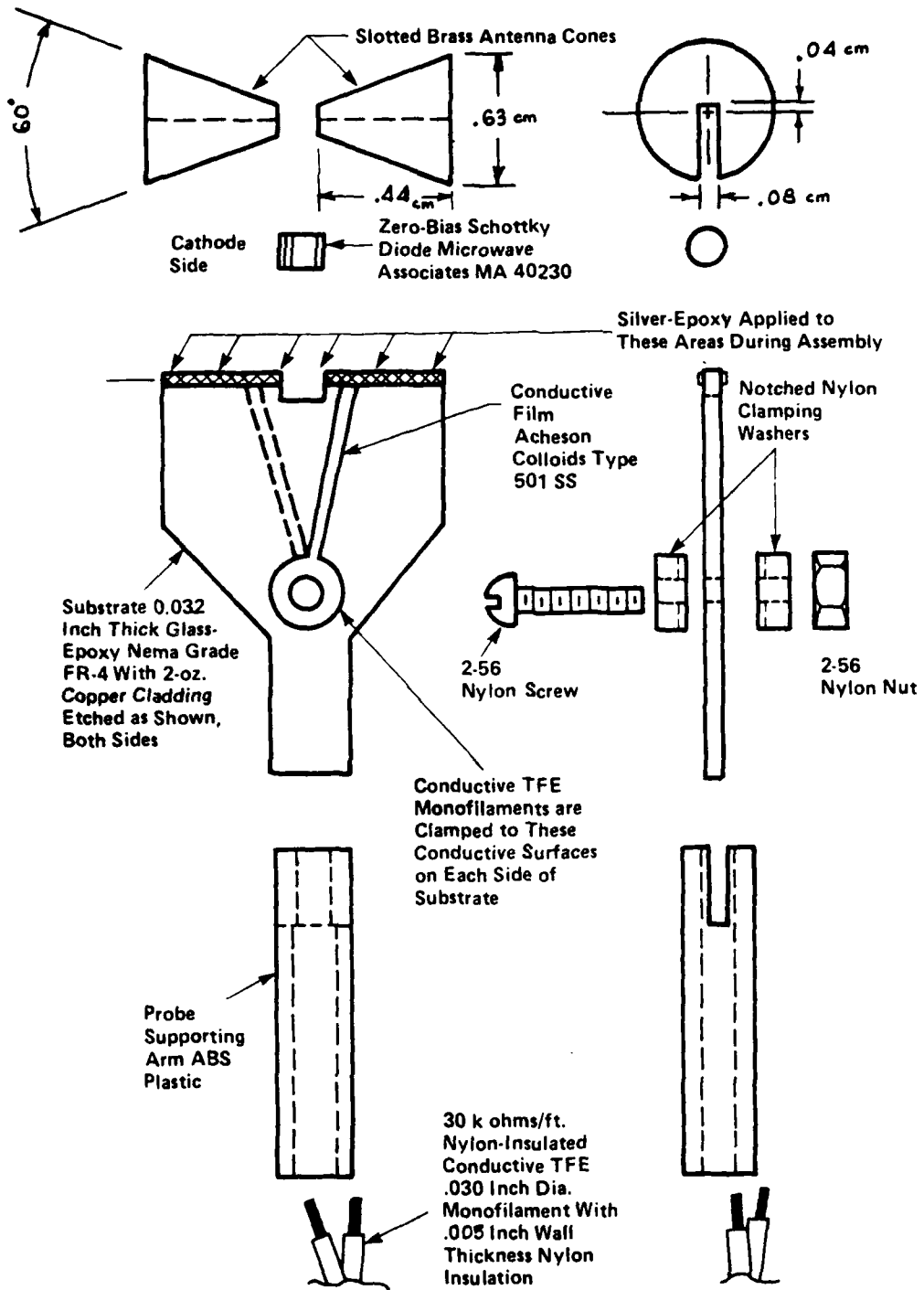


Fig. 9 Mechanical Assembly of E-Field Probe

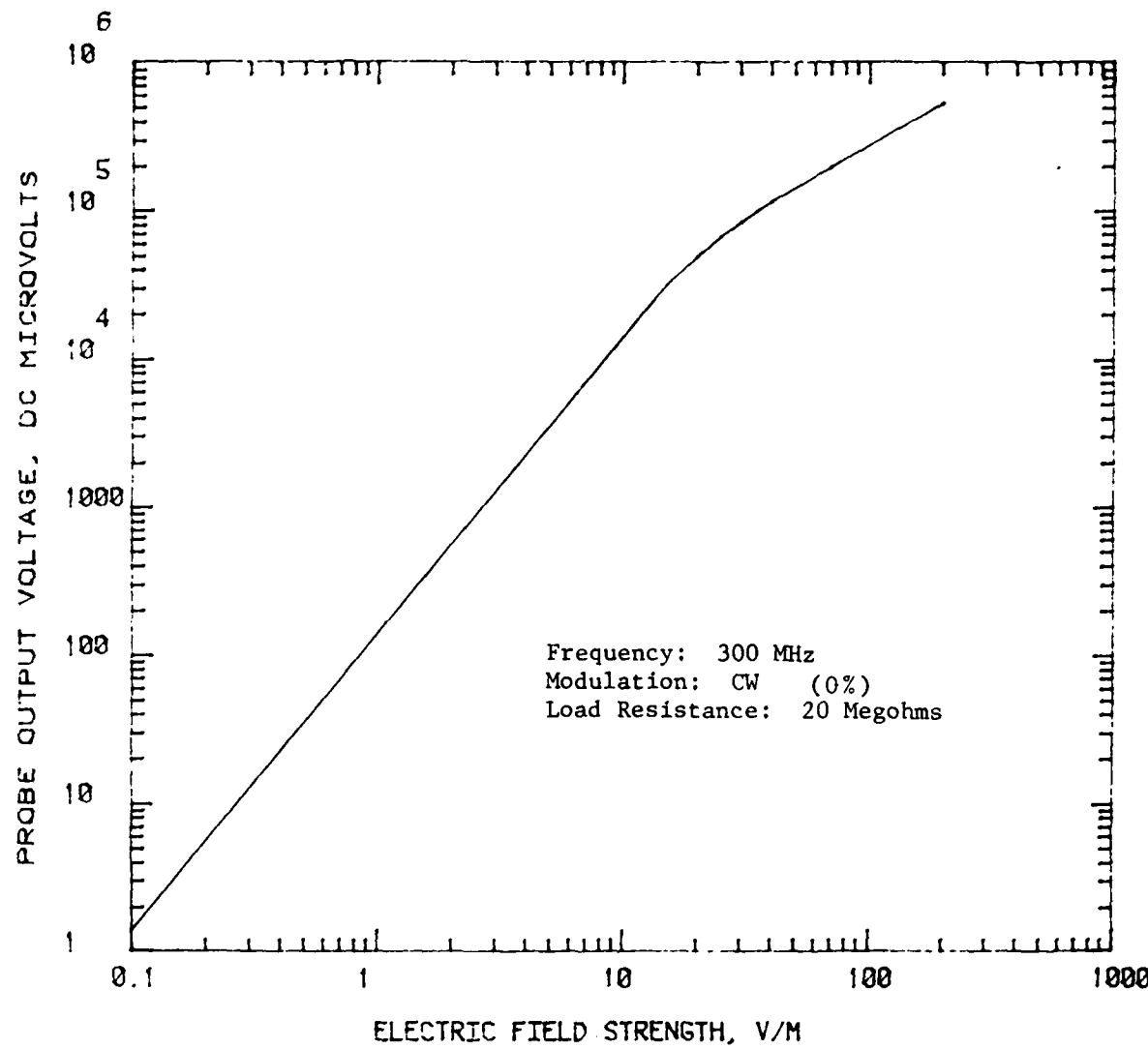
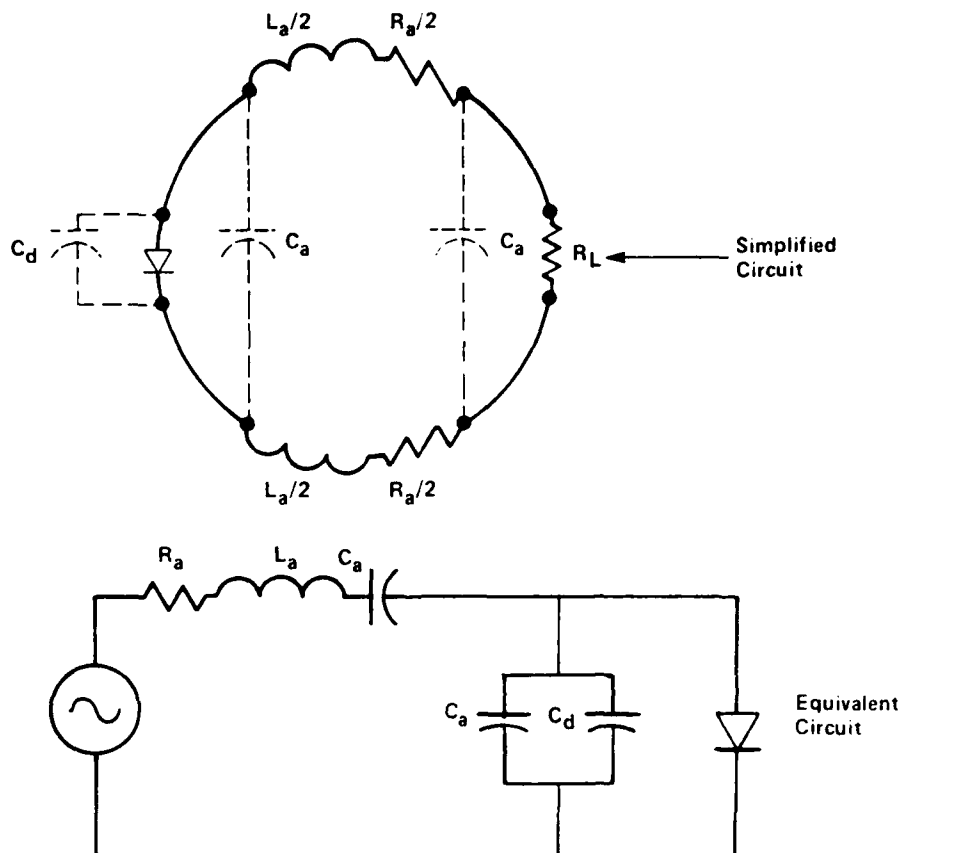


Fig. 10 DC Characteristics of E-Field Probe

3.3 Magnetic Field Probe Design

The H-field probe developed under this contract is a small, balanced loop antenna having an inner diameter of 0.5 centimeter. The antenna incorporates a zero-bias schottky diode detector which demodulates the received radio frequency signal. The construction and use of the probe is identical in all respects to the E-field probe described in paragraph 3.2 except for the coil-diode configuration and probe response to the H-field component of the electromagnetic field. Magnetic field probes of this type have been described by Green [4].

The H-field probe may be represented in simplified form as shown in Figure 11. An equivalent Thevenin voltage source e_0 is formed which consists of the antenna open circuit voltage $\mu_0 \omega H_{\text{AN}}$ which is further reduced by the voltage dividing action of the diode, its connection capacitance and the impedance of the resonant circuit formed by the antenna inductance and total stray circuit capacitance.



$$e_o = \frac{\mu_0 \omega H A N \left[\frac{1}{\omega(C_a + C_d)} \right]}{[(\omega L - 1/\omega C_{eff})^2 + R_a^2]^{1/2}} \quad C_{eff} = \frac{C_a (C_a + C_d)}{2C_a + C_d}$$

ω = Angular Frequency	L_a = Antenna Inductance
μ_0 = Permeability of Free Space	R_a = Effective Resistance in Antenna Resonant Circuit
H = Incident Field Strength, Amperes/Meter	C_d = Diode Distributed Capacitance
A = Antenna Loop Area, Square Meters	R_L = Load Resistance
N = Number of Turns in Antenna Coil	C_{eff} = Effective Antenna Capacitance Which Resonates With L_a
C_a = Antenna Distributed Capacitance	e_o = Source Voltage of Thevenin Equivalent Circuit

Fig. 11 Equivalent Circuit of H-Field Probe

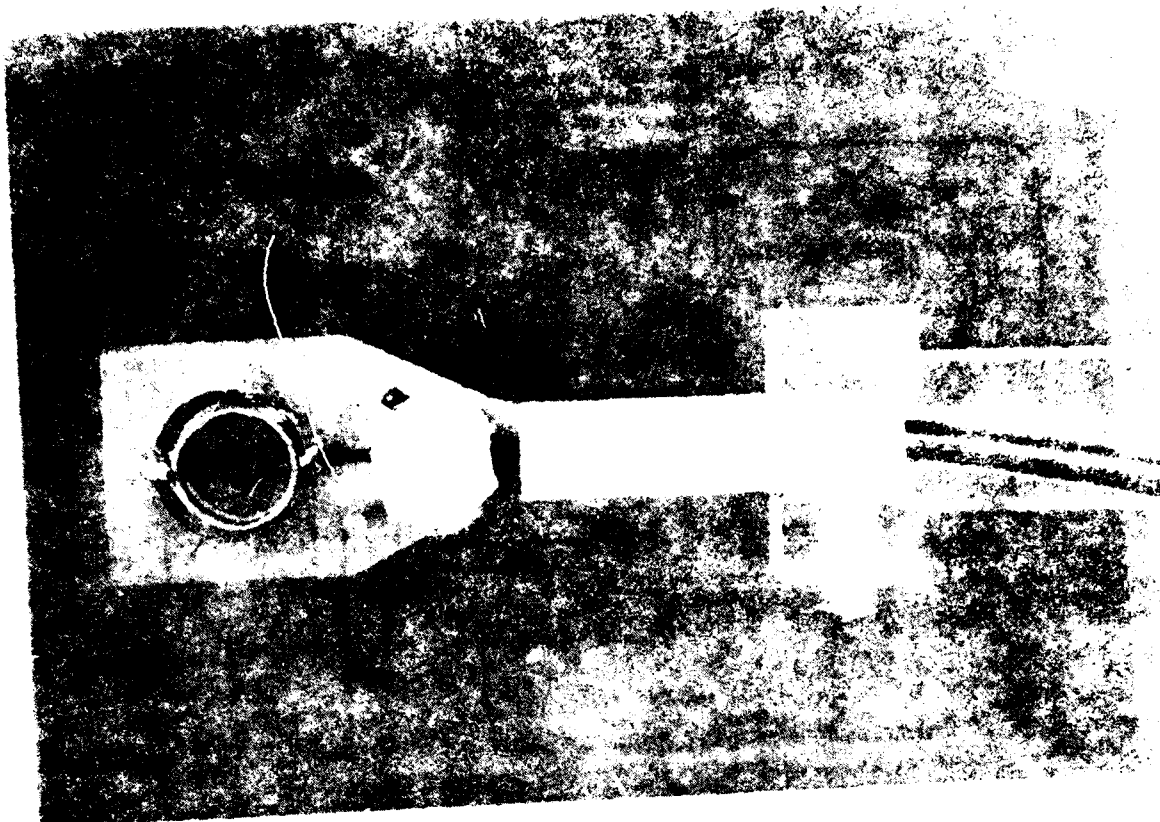


Fig. 12. H-field Probe in Holding Fixture

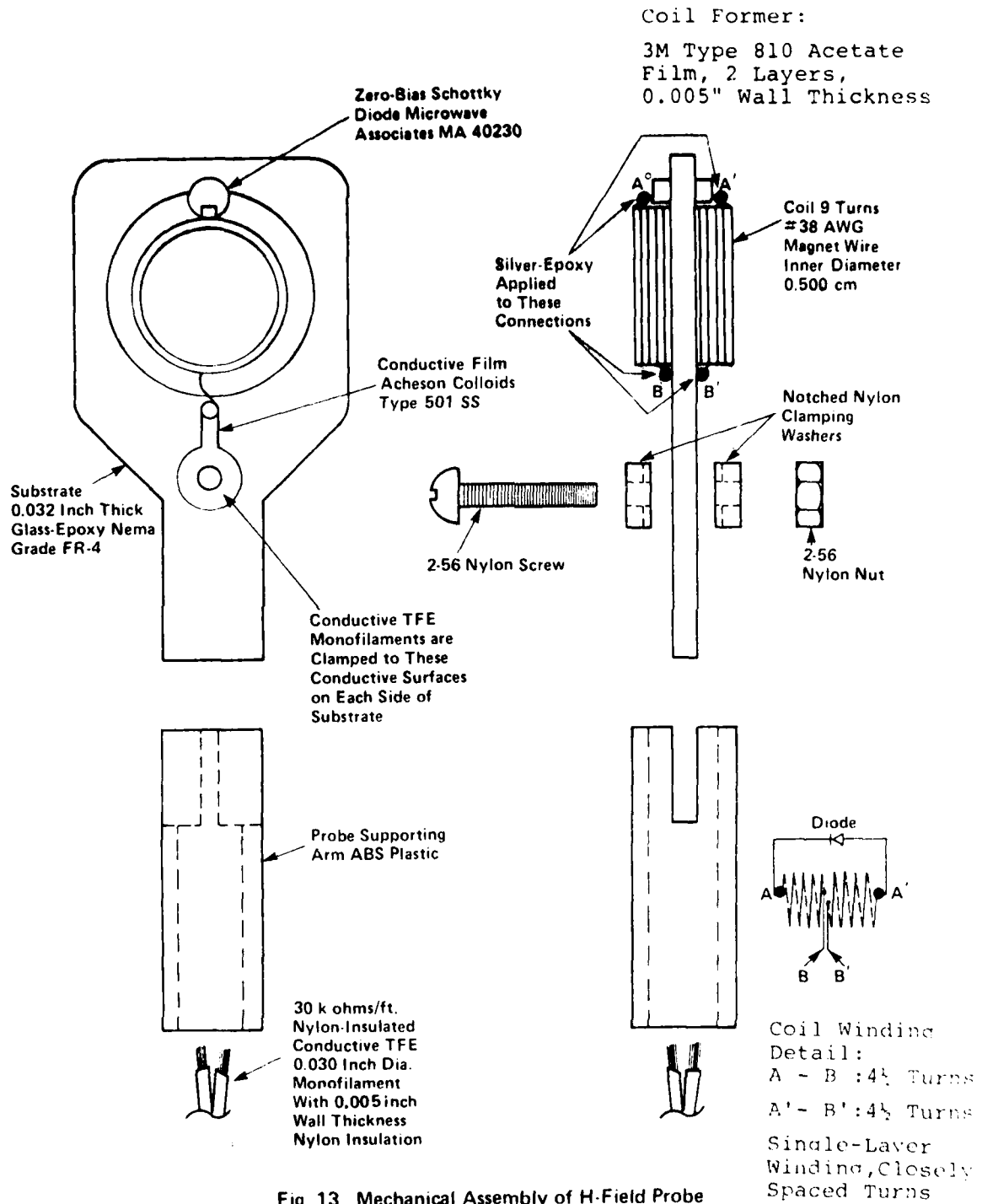


Fig. 13 Mechanical Assembly of H-Field Probe

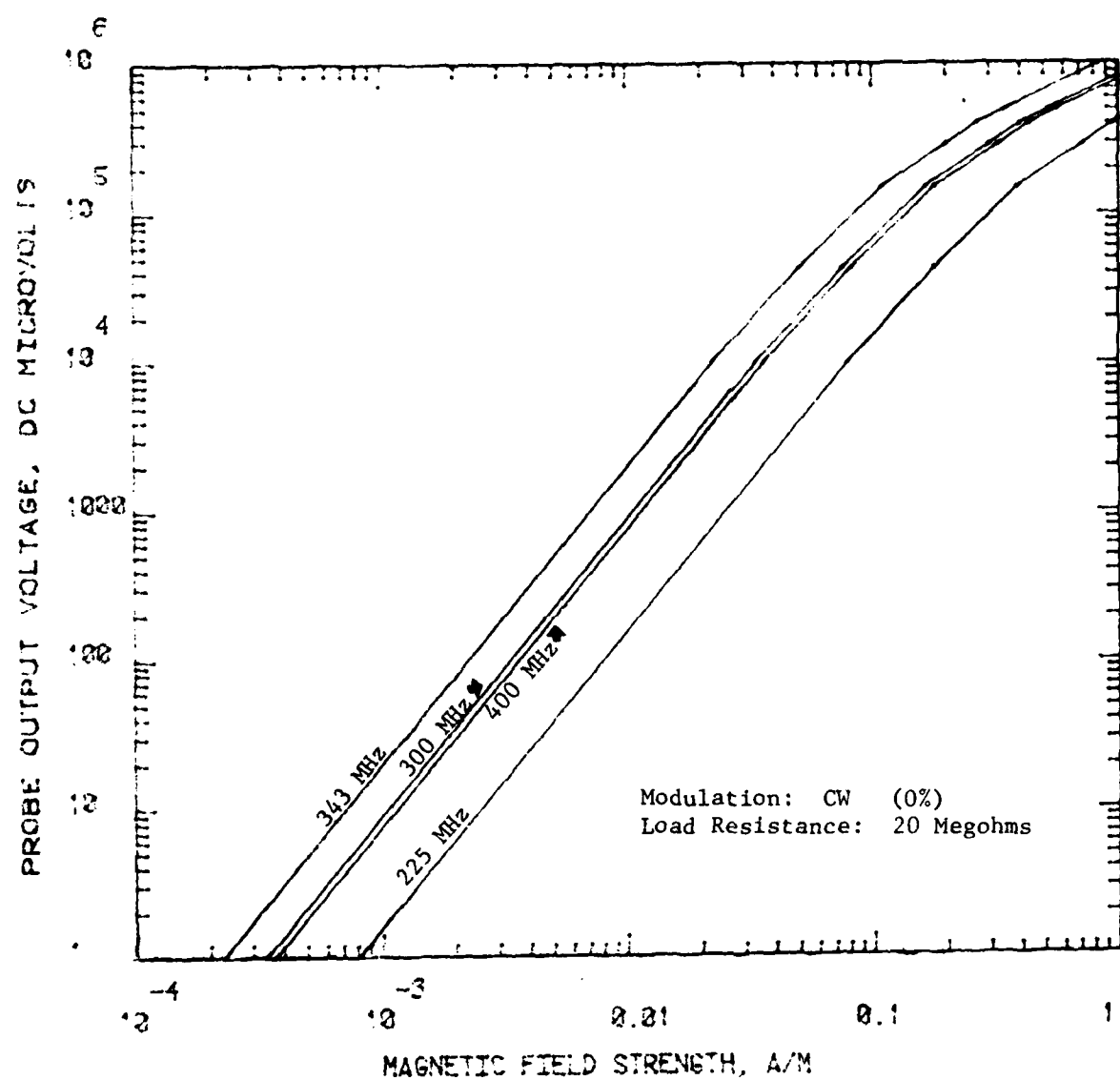


Fig. 14 DC Characteristic of H-Field Probe

The RF voltage appearing across the diode may be expressed as a function of the incident magnetic field strength H and the antenna characteristics, as follows:

$$e_{\text{diode rms}} = e_{\text{antenna}} \frac{\frac{-j}{\omega(C_a + C_d)}}{j(\omega L - \frac{1}{\omega C_{\text{eff}}}) + R_a}$$

$$\begin{aligned} e_{\text{antenna}} &= NHA \omega \times 4\pi \times 10^{-7} \\ &= 1.55031 \times 10^{-4} \text{ NHF} \end{aligned}$$

$$e_{\text{dc}} = \frac{q}{2nKT} \times [e_{\text{diode rms}}]^2$$

$$= \frac{16.2866}{2} \left[1.55031 \times 10^{-4} \text{ NHF} \frac{\frac{1}{\omega(C_a + C_d)}}{\left(\omega L - \frac{1}{\omega C_{\text{eff}}} \right)^2 + R_a^2} \right]^{1/2}$$

(Note: A value of 16.2866 was used for $\frac{q}{2nKT}$, based upon diode measurements at T = 298K.)

where:

C_a = portion of coil distributed capacitance shunting diode
 C_{eff} = effective distributed capacitance associated with coil self-resonance (.3365 pf)
 C_d = diode capacitance (.2 pf)
 H = incident magnetic field, Amperes/m
 λ = area of loop, m²
 ω = angular frequency
 F = frequency, MHz
 L = self inductance of loop ≈ 628.786 nH
 N = number of turns in loop = 9
 R_a = effective resistance in resonant circuit of loop
 $R_a \approx$
 160 ohms at 10°C
 250 ohms at 20°C
 415 ohms at 30°C

This estimate agrees very closely with Figure 10 which presents measured data. The characteristic gradually changes from a square law characteristic to a linear characteristic above 0.1 A/m.

3.4 Signal Conditioning and Transmission

The signal conditioner, into which the signals from the probe are fed, is a high-gain, high input impedance audio amplifier, fixed-tuned to the modulating frequency of the r.f. illuminating signal.

The output of the amplifier is in the form of a pulsed optical signal whose pulse repetition frequency corresponds to the full wave rectified average value of the modulated input signal.

As discussed in paragraph 2-1, an amplitude-modulated RF illuminating field, in conjunction with a narrow-bandwidth filter in the probe signal conditioner, was used to provide a better signal-to-noise ratio by eliminating the effect of unwanted harmonics in the received signal. This technique also helped to reduce the effects of other low-frequency noise sources including stray 60 Hz fields, electrostatic fields and cable microphonics associated with the floating high resistance transmission line.

A nominal amplitude-modulating frequency of 550 Hz was chosen as it was sufficiently low to avoid significant signal loss in the one meter long resistive transmission line connecting the field probes to the signal conditioner. Actual testing was conducted at 552 Hz as this was found by measurement to be the fixed center frequency of the above narrowband filter.

The attenuation characteristics and design of a resistive transmission line using conductive plastic of a similar diameter and resistance per unit length have been described by Greene [4]. The attenuation of a one-meter length of such a line is estimated to be less than one dB at 550 Hz. This is based upon a line resistance of 60 Kilohms per foot (including return path) and a line capacitance of 10 pf per foot.

A twin-lead resistive transmission line was fabricated by bonding the nylon jackets of two parallel conductive monofilaments at five centimeter intervals with an adhesive. The monofilament material is described in Figures 9 and 13. This construction provided a line of sufficient lightness and flexibility to prevent undue mechanical strain on the delicate plastic probe positioning mechanisms required for this non-perturbing field mapping application. A pressure contact was used to electrically connect this line to the field probes, as shown in Figures 9 and 13. At the signal conditioner end

of the line, connection was achieved by crimping metal connector pins onto the ends of the monofilament. Further details on transmission line materials are provided in appendix G.

A photograph of the signal conditioner is shown in Figure 15. All controls and input/output connections appear on the front panel. A power on-off switch, a high-low range switch with pneumatic actuator for remote control, an input signal connector and a connector for the fibre optic transmission cable appear on the front panel. Two jacks are provided for charging an internal nickel-cadmium battery pack. In order to achieve a high degree of shielding the box is completely sealed with a joint between the front panel and flange.

The operation of this circuit can be described with reference to the block diagram shown in Figure 16. Figure 17 through 19 give the input/output characteristics. The demodulated signal from the probe, which is a variable amplitude 552 Hz signal, is amplified by the low-noise instrumentation amplifier consisting of two LF353 W dual FET operational amplifiers. This amplifier provides two ranges of sensitivity selectable by the front panel switch.

The signal is then fed to a single stage active band pass filter which is fixed-tuned to the centre frequency of 552 Hz. The filter has a 3 dB bandwidth of 23 Hz and provides more than 30 dB rejection at the harmonics of the modulated signal.

The filter output is then fed to an AC-DC converter which consists of an operational amplifier rectifier filter stage.

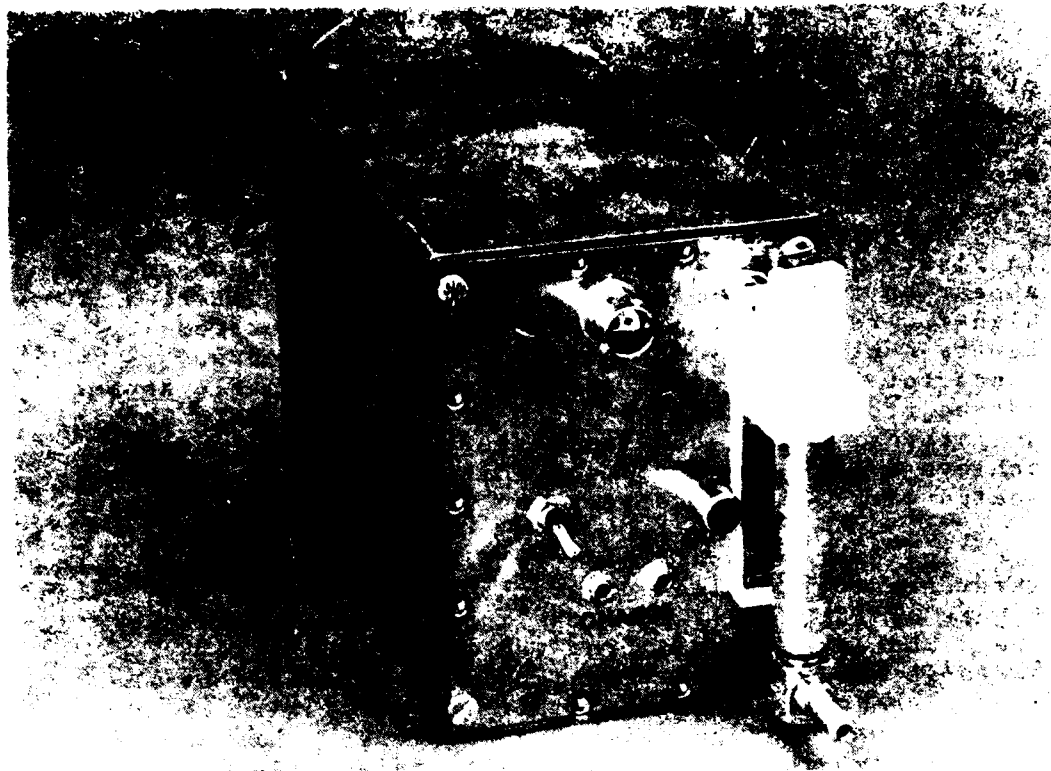


Fig. 15 View of Signal Conditioner, Showing Controls and Signal Ports

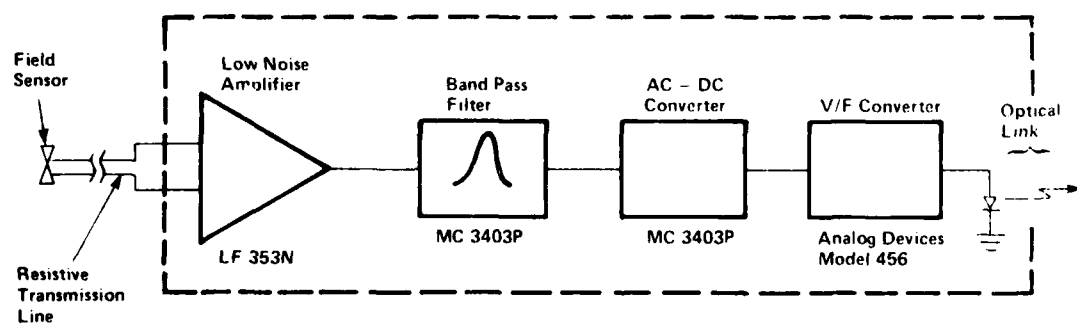


Fig. 16 Block Diagram of Signal Conditioner

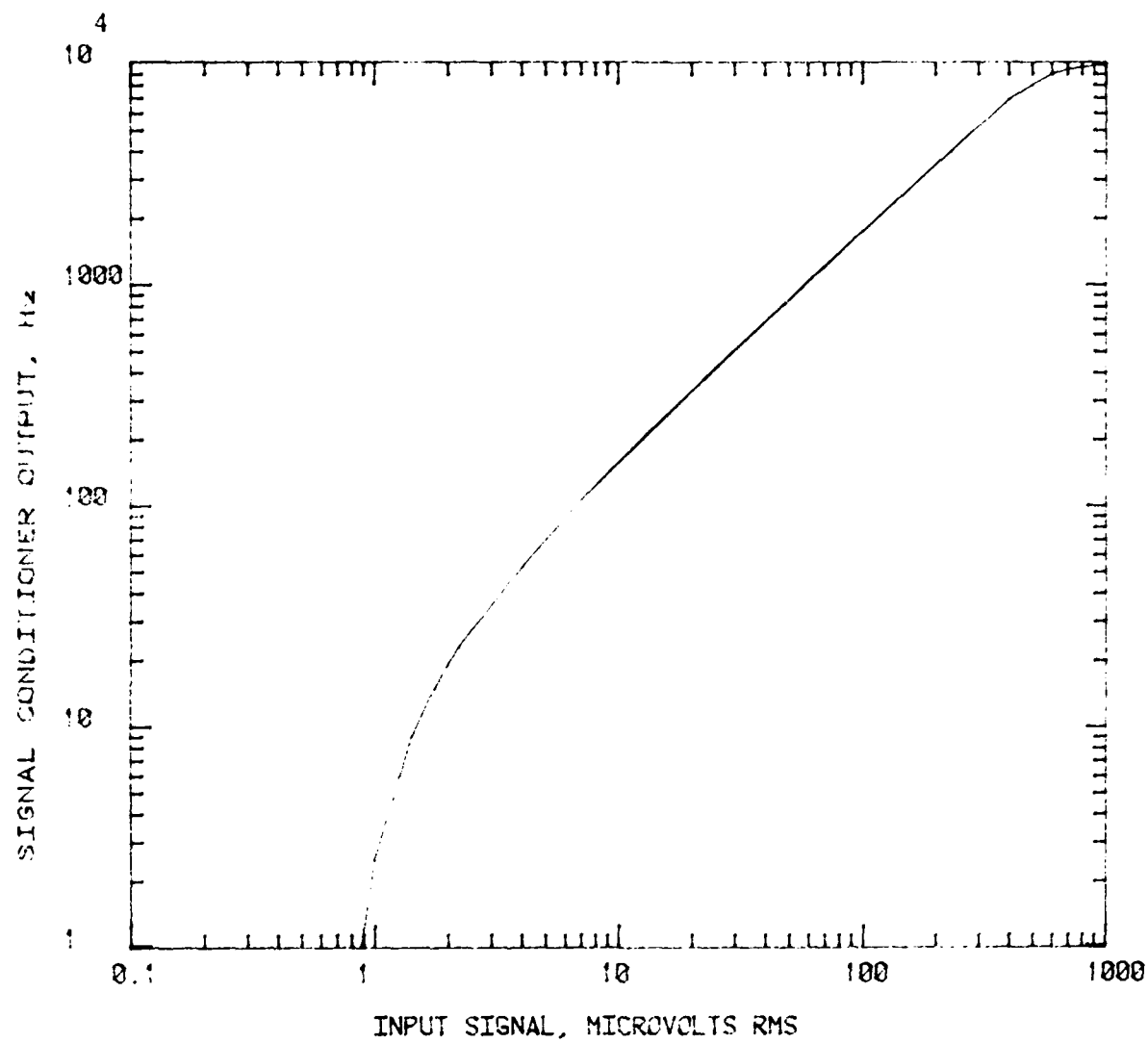


Fig. 17 Transfer Characteristic of Signal Conditioner

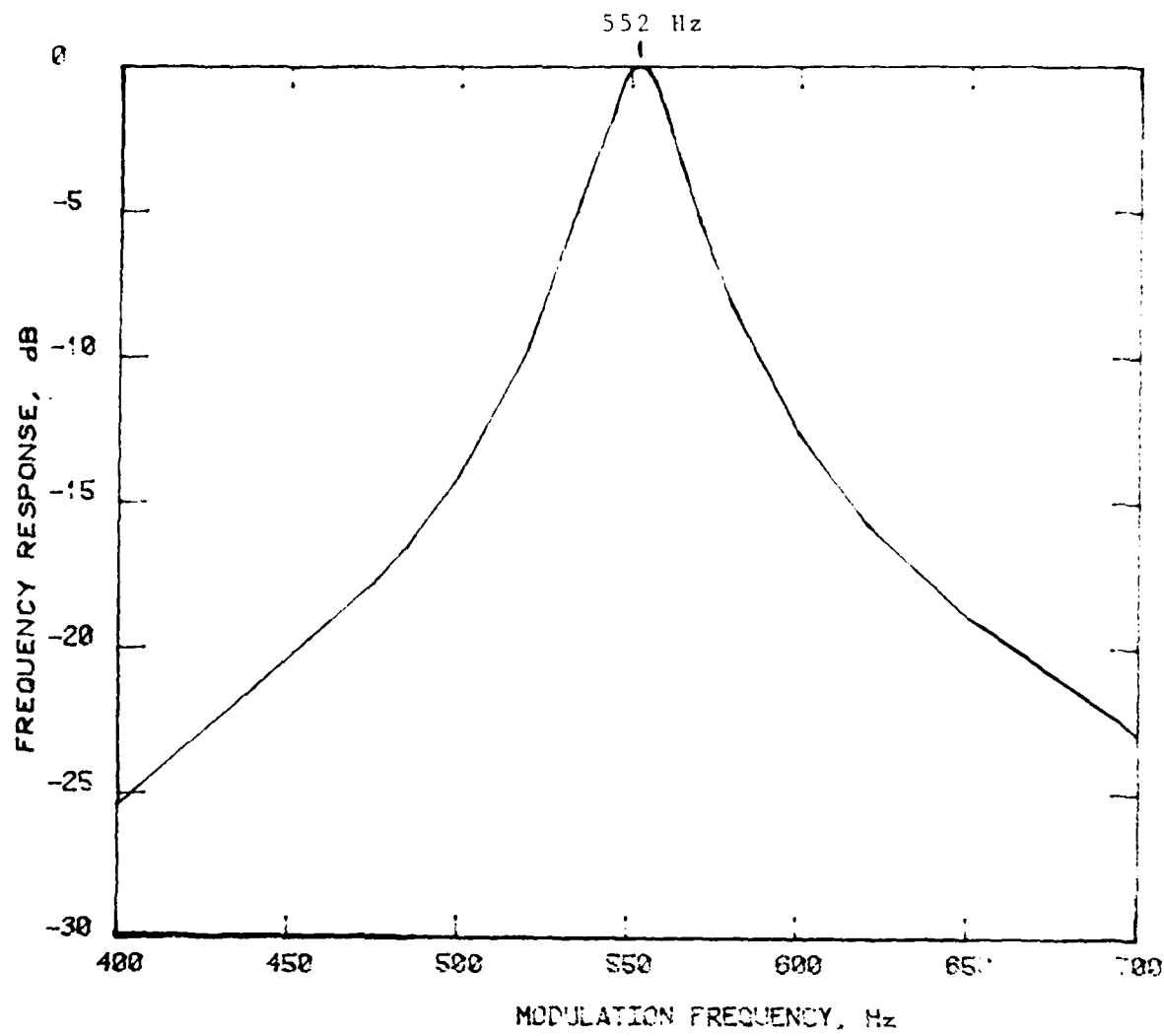


Fig 18 Frequency Response of Signal Conditioner

The DC output of this stage is then converted to a 0-10 KHz variable frequency signal by a voltage-to-frequency converter. This converts the output pulses from a light emitting diode to produce a variable frequency optical signal which is then transmitted over a fibre optic link to an optical receiver unit. The optical signal is then transformed back to a standard TTL level pulse train. The pulse train is fed to a standard frequency counter which forms part of the signal acquisition system described in paragraph 3.5.

3.5 Signal Acquisition and Analysis System

The signal conditioner output is fed to a frequency counter which displays the signal for monitoring purposes and provides the interface to the computer for data storage and analysis. The elements of this system are shown in Figure 5 and 6.

The main functions of the computer includes: -

- (i) conversion of the frequency counter output, in Hz, to the appropriate field parameter (V/m or A/m) by use of a probe calibration look-up table stored in the computer.
- (ii) control of an external relay actuator to sequentially step the mechanical positioner through the 73 positions of the measurements grid shown in Figure A-1, Appendix A.
- (iii) recording, storing and printing the field strength measurements at each grid point.
- (iv) calculations of contours of constant field strength by use of linear interpolation for terminal display and for hard copy.
- (v) performing automatic range switching when the signal conditioner output exceeds a given level as shown in Figure 19 and 20.
- (vi) performing signal averaging to further improve noise rejection.

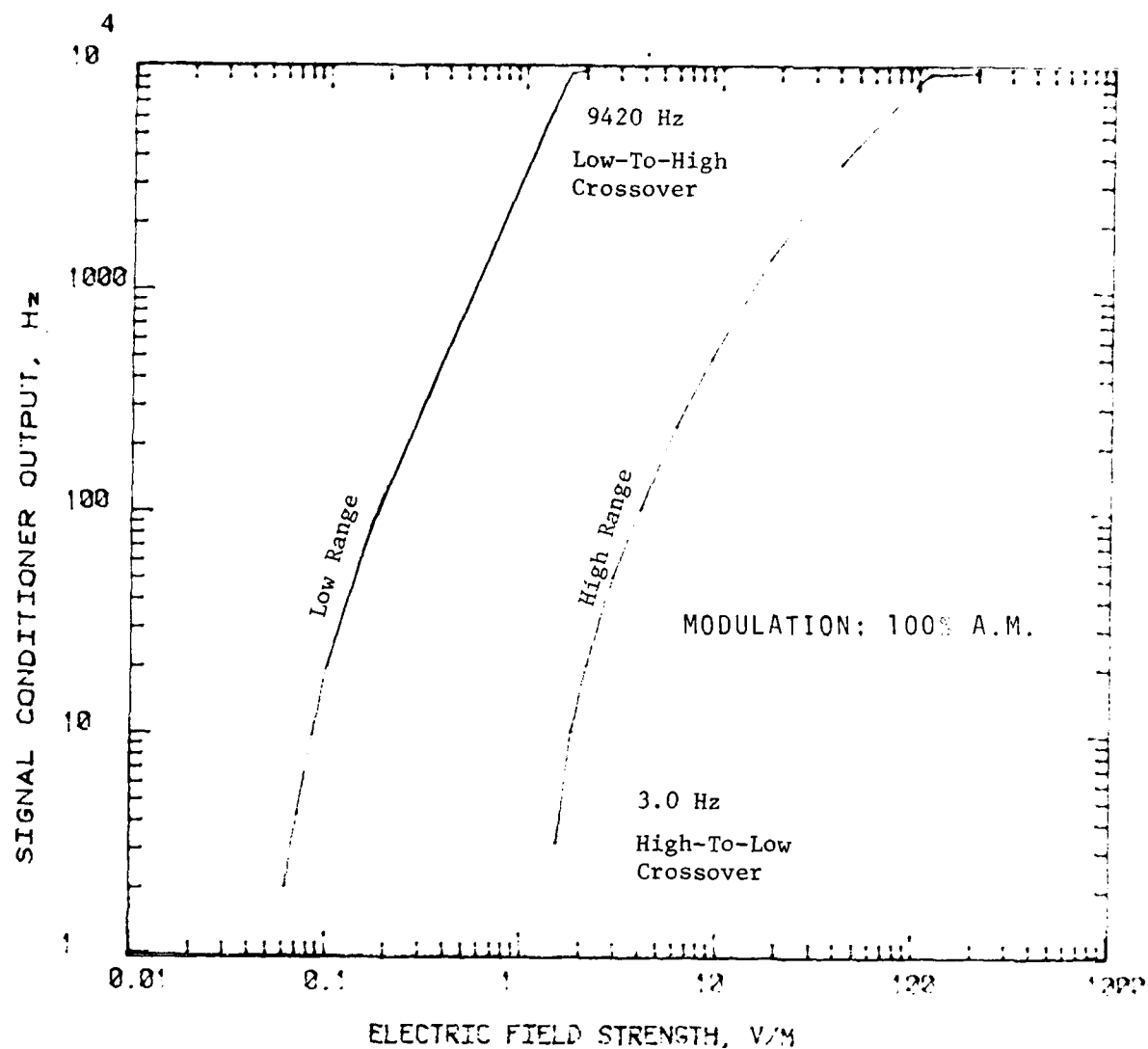


Fig. 19 Total Transfer Characteristic of Signal Conditioner and E-Field Probe

NOTE: Crossover levels shown were implemented in the computer programs of Appendix F for automatic range switching purposes; a small degree of range overlap is provided.

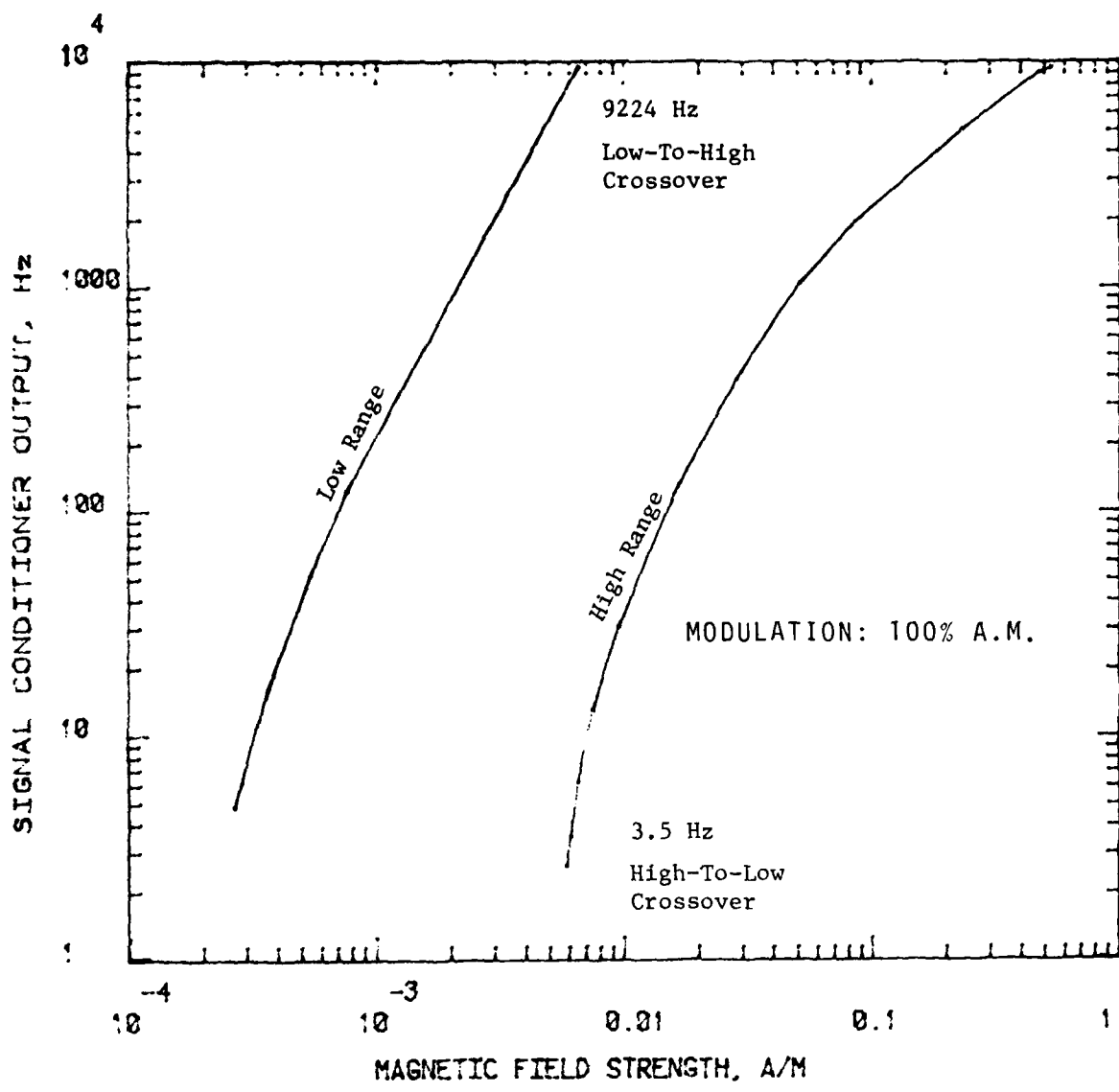


Fig. 20 Total Transfer Characteristic of Signal Conditioner and H-Field Probe

NOTE: Crossover levels shown were implemented in the computer programs of Appendix F for automatic range switching purposes; a small degree of range overlap is provided.

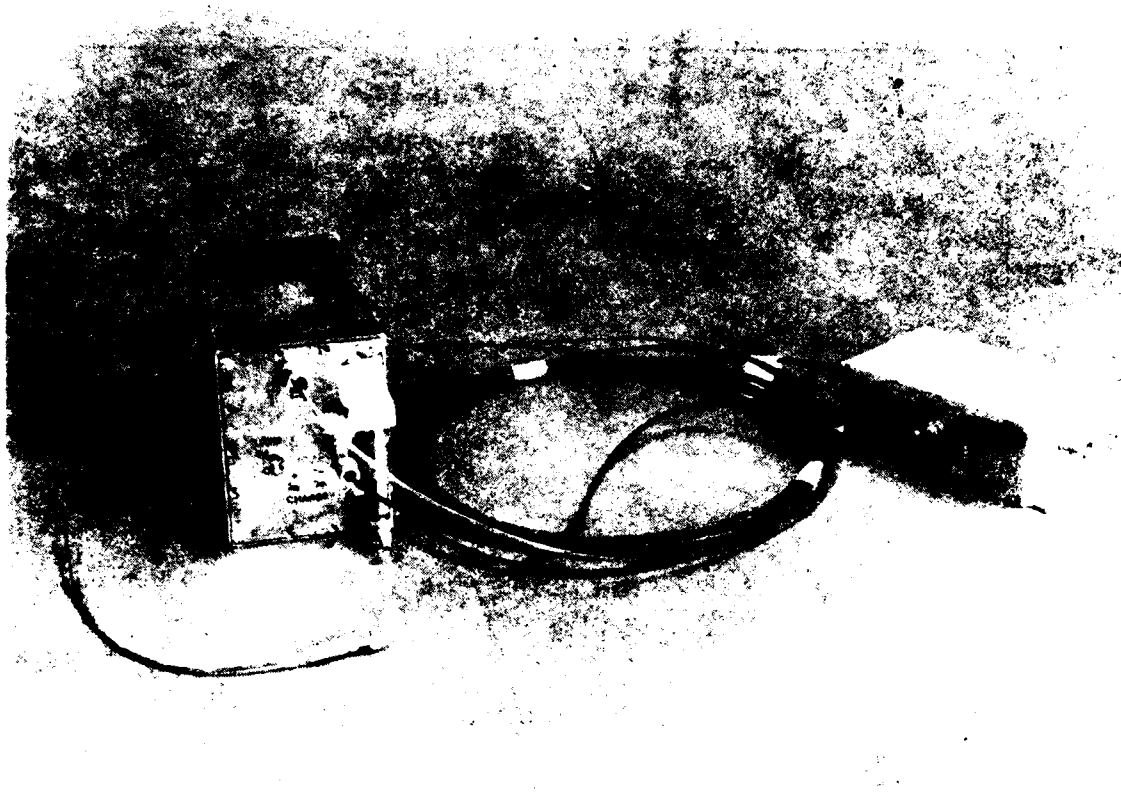


Fig. 21 View of Optical Link Receiver Unit, Connected via Fiber Optic Link to Signal Conditioner

3.6 Mechanical Positioning System

The function of the positioning system is to translate the probes over a 5 cm X 5 cm two dimensional scanning grid with 73 positions as defined in Figure A-1 of Appendix A. This translation is performed by stepper motors and sliding carriage mechanisms which move in axial and radial directions.

The axial motion is achieved by a direct worm-gear drive moving a carriage sliding on two ground steel shafts or four linear motion bearings. The radial movement uses a pulley drive system which moves a small probe mounting block back and forth on two parallel glass shafts. This is shown in Figure 2.

The motors are remotely controlled by a probe position and control unit (PPCU) which is preprogrammed with hard-wired logic to transmit the appropriate number of pulses to the stepping motors. The PPCU lends itself to both manual and automatic control.

In operation the positioning system has to be so mounted that the motors are placed where they can have no influence on the field being mapped.

3.7 Field Illumination System for Mapping

The cylindrical configurations required RF plane wave illumination at 300 MHz for mapping purposes. BNR used its RF anechoic chamber having internal dimensions of 20 x 20 x 12 feet to contain the radiation and to provide an environment relatively free of stray reflections. The chamber is treated with pyramidal absorber cones 26 inches in length. The cylindrical objects to be illuminated were mounted at a height of five feet on a wooden support fixture at one corner of the chamber, as shown in Figure 1. The support fixture used peg-and-dowel construction in order to avoid field perturbations due to metal fasteners or brackets.

The illuminating antenna was mounted at the diagonally opposite corner of the chamber with its nearest surface 3 meters from the geometric centre of the

object under illumination.

At this distance, the normal $\frac{2D^2}{\lambda}$ or 3λ criteria for plane wave illumination was satisfied, as well as a test requirement that the longitudinal field gradient over the 1.13 meter maximum length of the missile nosecone was not to exceed ± 1 dB.

The elements of the illuminating system are shown in schematic form in Figure 6.

A high gain 12.15 dBi Yagi-Uda antenna designed for operation at 300 MHz was used to illuminate the cylindrical configurations with a horizontally polarized plane wave during mapping. The antenna was fed by a 10 dB gain R.F. Power Amplifier via a 300 MHz tuned filter used to lower harmonic content of radiated signals. This power amplifier required up to 100 watts of drive provided by a 200 watt broadband R.F. Amplifier. The signal source feeding the RF driver was an H.P. Model 8640 signal generator which was capable of providing a high stability, 300 MHz signal with 552 Hz amplitude modulation.

The illumination level was checked at the configuration geometric centre using a calibrated dipole and receiver.

4.0 RESULTS

This section presents in summary form the results of tests to characterize the probes, the mechanical positioning system, the illumination system, and actual field mapping of the cylinder and nosecone. Details of results are given in Appendix B for the contour maps, Appendix C for numerical values of measurements made at the various grid points, Appendix D for field illumination tests and Appendix E for probe evaluation tests.

4.1 Probe Evaluation

Characterization tests were performed for both the E-field and H-field probes using a TEM Cell in laboratory ambient conditions and at high and low temperatures.

The results are given in Table 1 for the E-field probe and Table 2 for the H field probe.

The TEM Cell used for the majority of tests had a rectangular cross-section and was based upon a design described by Crawford [9].

The cell dimensions are 9 cm high by 15 cm wide with a total length of 38 cm. Over the frequency band 225 to 400 MHz the VSWR measured was less than 1.1.

The dimensions of the cell are small enough that no propagation of higher modes exists; consequently the main source of error is due to inaccuracy of cell plate spacing and width, and discontinuities at input and output terminations.

The probes were installed in the upper half of the cell midway between the centre plate and the top inner surface. The probes were oriented for maximum pick up for all tests except those requiring probe rotation, i.e., directional pattern tests.

In order to establish the probe errors due to operation in fields of high gradient a special coaxial TEM Cell was used to produce the variation in gradients required for the tests. This consisted of an outer cylinder of 8 cm diameter with a centre No. 12 AWG

TABLE 1
Summary of E-Field Probe Results

Dynamic Range: 0.07 V/m to 1.6 V/m Low Range 100% Modulation
 1.6 V/m to 200 V/m High Range 100% Modulation

Sensitivity: 0.07 V/m at 10 dB $\frac{S+N}{N}$ Ratio 100% M
(Low Range) 0.14 V/m at 10 dB 50% M

Frequency Response: -.7 dB + .3 dB Referred to 300 MHz

Directional Field Pattern:

Cosine θ ± 0.35 dB for $\theta = 0 \pm 60^\circ$
Cosine θ ± 0.90 dB for $\theta = 60$ to 80°

Cross Sensitivity to H-Fields:

E-field measurement error *less than 4.4 V/m per A/m H-field.

* Determination of this value limited by measurement technique.

Spatial Resolution: ± 0.5 cm

Gradient Error:

± 0.5 dB in Fields of 10 dB/cm gradient

Temperature Stability: -0.02 dB/ $^\circ$ C

TABLE 2
Summary of H-Field Probe Results

Dynamic Range: 0.36 mA/m to 6.5 mA/m Low Range 100% Modulation
(300 MHz)

6.5 mA/m to 520 mA/m High Range 100% Modulation

Sensitivity: 0.36 mA/m at 10 dB $\frac{S+N}{N}$ Ratio
100% Modulation
300 MHz

0.72 mA/m at 10 dB $\frac{S+N}{N}$ 50% Modulation
300 MHz

Frequency Response: (Referred to 300 MHz)

225 MHz	- 12.2 dB
300 MHz	0 dB (Resonant Frequency)
343 MHz	+ 5.1 dB is 343 MHz
400 MHz	+ 0.2 dB

Directional Field Pattern:

Cosine θ ± 0.4 dB for $\theta = 0 \pm 80^\circ$

Cross-Sensitivity to E-Fields:

H-field measurement error *less than 8.7×10^{-5} A/m per V/m E-field.

* Determination of this value limited by measurement technique.

Spatial Resolution: ± 0.5 cm

Gradient Error: ± 0.5 dB in Fields of 10 dB/cm gradient

Temperature Stability: 260 MHz - .10 dB/ $^\circ$ C
300 MHz - .13 dB/ $^\circ$ C
346 MHz - .35 dB/ $^\circ$ C
400 MHz - .17 dB/ $^\circ$ C

copper wire. This fixture was also used for directional pattern measurement of the H-field probe to take advantage of the field orientation which allowed easy rotation of the magnetic probe through the lateral access port in the cell.

TEM cells were terminated in their characteristic impedance except during cross-sensitivity tests when open and short circuit stubs were used to produce standing wave minima and maxima.

The influence of the opposite field component (ie. E-field effects or H field probes and vice versa) were measured at these locations.

4.2 Illumination System Evaluation

The longitudinal and lateral field gradients were measured to verify the uniformity of plane waves incident upon the test configuration. This was accomplished by measuring the field strength at all six locations displaced ± 50 cm from the geometric centre of the test configuration along the X, Y and Z coordinate axes, with the level at the geometric centre serving as reference. Measurements were made with a calibrated dipole and tuned receiver. The variation in field strength was within +1 dB for all cases.

4.3 Mechanical Positioning System Tests

The ability of the mechanical positioning system to accurately move the field probes to the specific locations on the scanning grid was determined by use of a vernier caliper. This measurement confirmed that the displacement of the probe mounting carriage in the axial and radial directions was within the required ± 0.5 mm tolerance, when the carriage was moved in 1 cm steps following the prescribed scanning sequence. (See Fig. 1A, Appendix A).

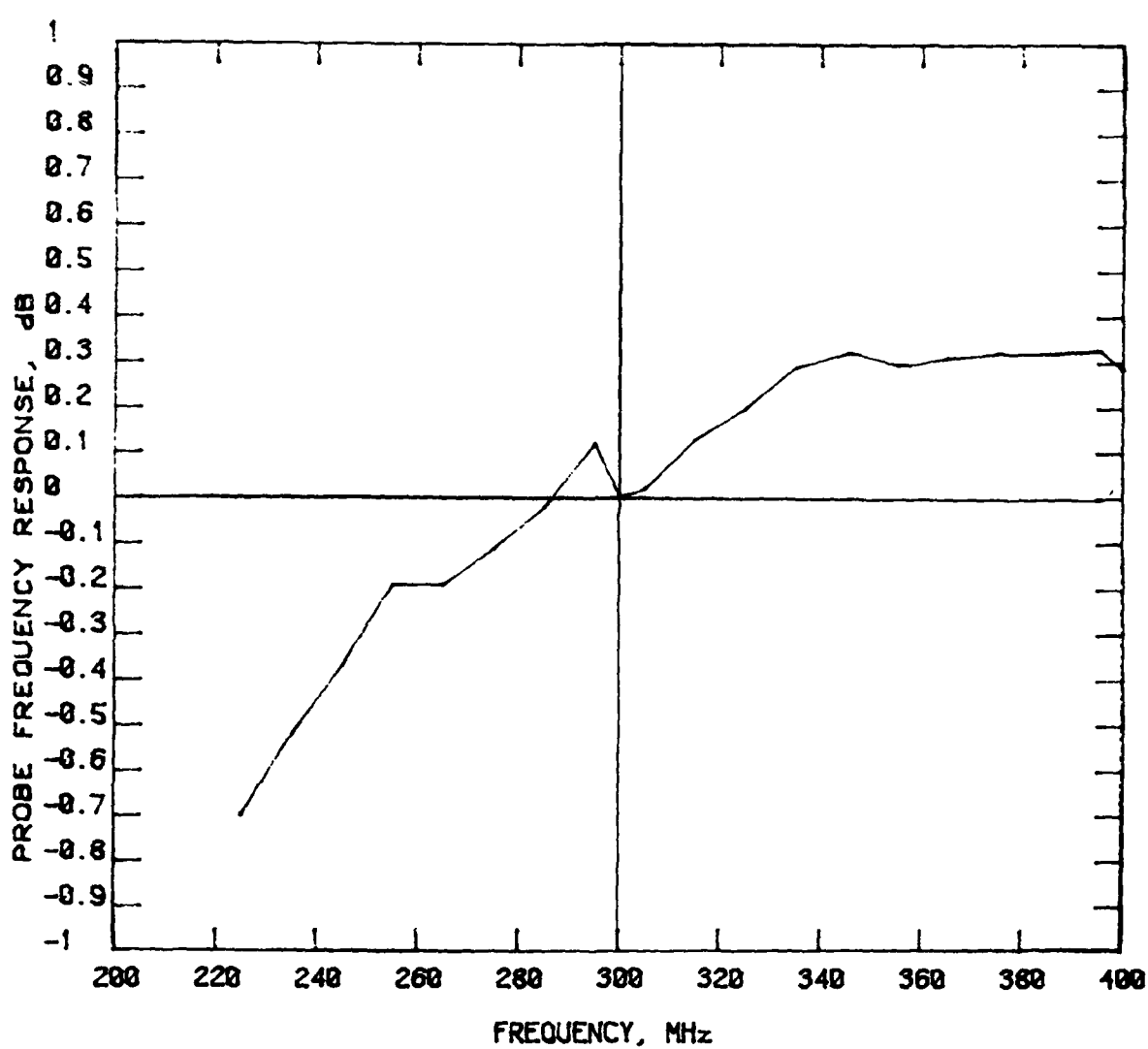


Fig. 22 Frequency Response of E-Field Probe

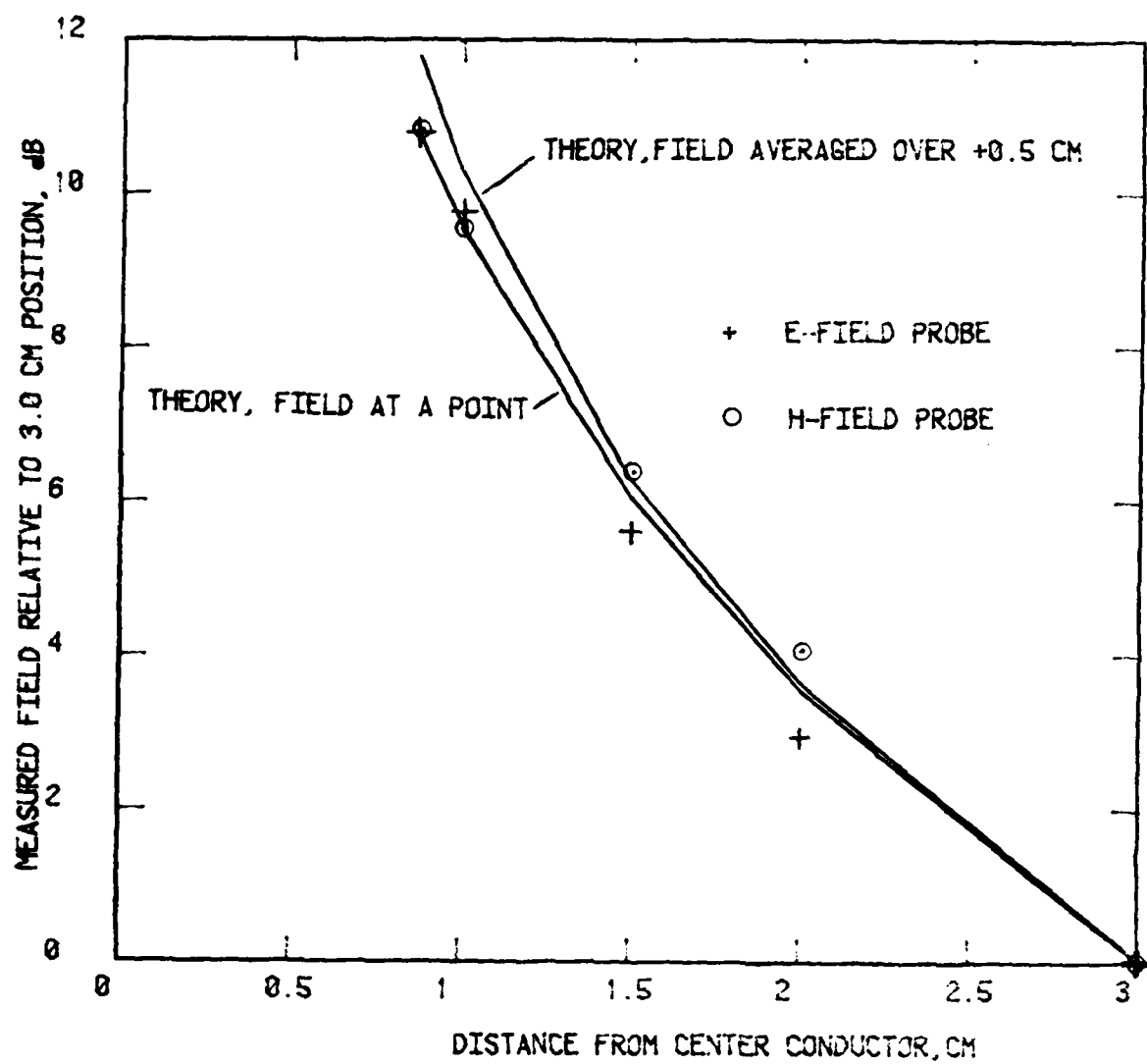


FIG 23 PROBE GRADIENT AND RESOLUTION

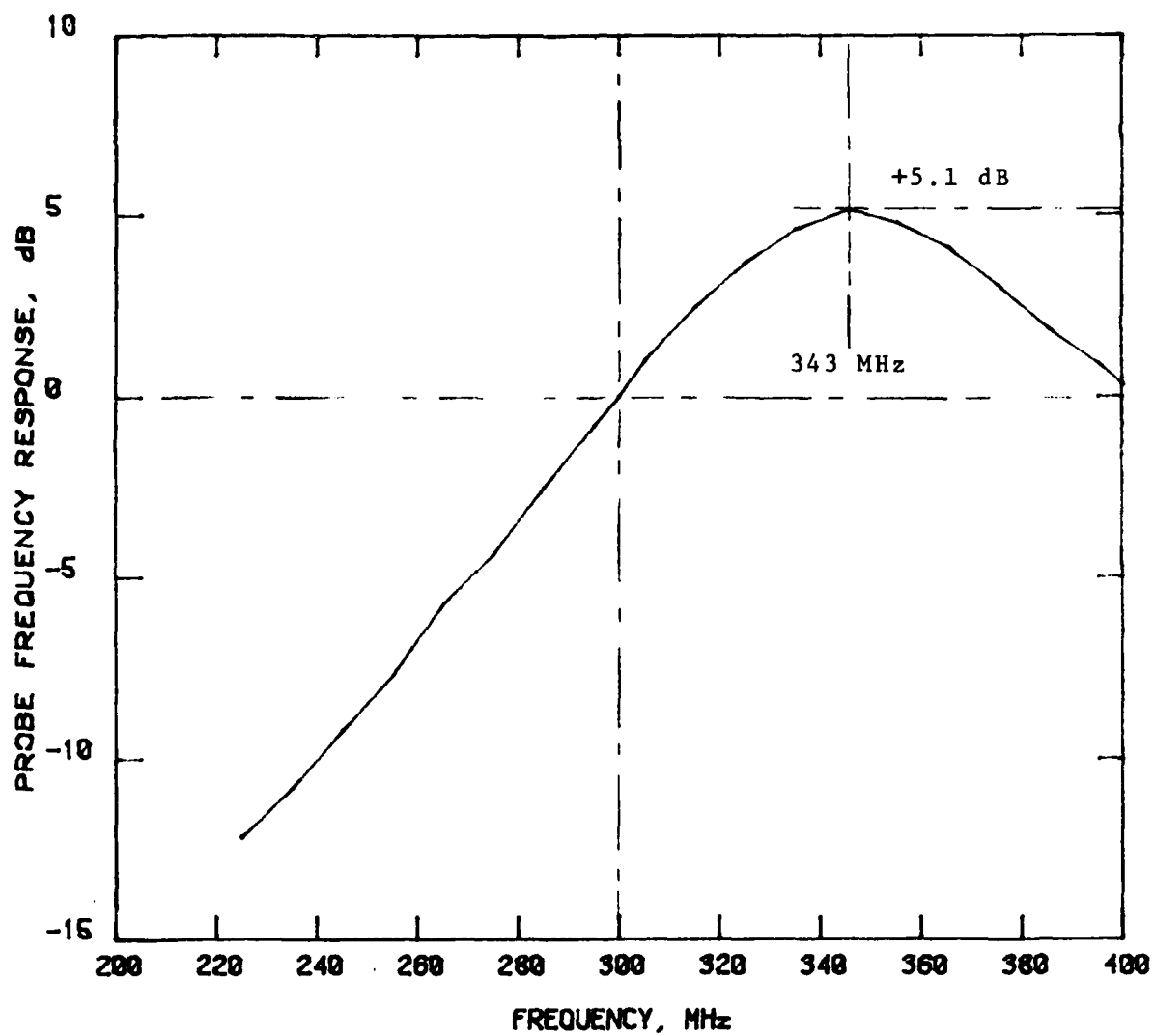


Fig. 24 Frequency Response of H-Field Probe

4.4 Field Contours

The detailed results of field measurements conducted in the missile nosecone and the aluminum cylinders are presented in Appendices A, B, and C.

Appendix A defines the geometry of field measurement for these structures and gives a matrix defining all 36 test combinations.

Appendix B presents the measurement data in the form of contour maps of the measured vector electric and magnetic fields.

Appendix C presents the source data for the contour maps in numerical form.

5.0 CONCLUSIONS

The program has demonstrated that electromagnetic probes can be designed with the necessary resolution, sensitivity and accuracy for mapping complex electric and magnetic fields at UHF frequencies and within metal structures containing apertures.

The appropriate instrumentation has also been developed for the application of the probes to map the variation in field strength in typical equipment enclosures such as weapons systems casings.

Preliminary inspection of maps obtained by theoretical analysis [1] indicates a reasonable agreement with the measured data, however it is beyond the scope of this report to present a detailed analysis of correlation.

The techniques developed will be invaluable for establishing the validity of the assumptions used in mathematical modelling techniques. They will improve the capability to measure and control field strength distributions in general and should be particularly useful in radiated susceptibility testing. Additionally the methodology shows great promise for extension into the gigahertz frequency region and for applications requiring wide frequency band sensors.

REFERENCES

- (1) TAFLOVE, A., "Time Domain Solutions for Electromagnetic Coupling," Document No. RADC-TR-78-142, Rome Air Development Center (RBCT) Griffiss AFB, NY 13441
- (2) GREENE, F.M., "A New Near-Zone Electric Field Strength Meter", NBS J. of Res., Vol. 71-C (Eng. and Instr.), No. 1, pp. 51-57, (Jan.-Mar. 1967).
- (3) GREENE, F.M., "NBS Field-Strength Standards and Measurements," Proc. IEEE, Vol. 55, No. 6, pp. 970-981 (June 1967).
- (4) GREENE, F.M., "Development of Electric and Magnetic Near-Field Probes", NBS Technical Note 658, U.S. Dept. of Commerce/National Bureau of Standards.
- (5) WHITESIDE, H., and KING, R.W.P., "The Loop Antenna as a Probe," IEEE Trans. on Antennas and Propagation, Vol. AP-12, No. 3, pp. 291-297, May 1964.
- (6) BAUM, C.E., et al, "Sensors for Electromagnetic Pulse Measurements both Inside and Away from Nuclear Source Regions", IEEE Trans. Ant. and Propagation, Vol. AP-26, No. 1, Jan. 1978.
- (7) KERNS, D.R. and BRONAUGH, E.L., "A Non-obstructive Remote Indicating Instrument for Probing EM Fields Having Potentially Hazardous levels," IEEE Int. SYMP. on EMC, Atlanta, GA., p.p. 133-136, June 20-22, 1978.
- (8) BASSEN, H., et. al., "EM Probe with Fiberoptic Telemetry System," Microwave Journal, Vol. 20, No. 4, pp. 35-47, April 1977.
- (9) CRAWFORD, M.I., "Generation of Standard EM Fields using TEM Transmission Cells," IEEE Transactions on EMC, Vol. EMC-16, No. 4, pp. 189-195, Nov. 1974.

APPENDIX A

DEFINITION OF FIELD MEASUREMENT GEOMETRY AND SAMPLING

A.1 INTRODUCTION

This appendix defines the conventions used to describe probe orientation and location with respect to the cylinder and missile nosecone structures and with perfect to incident field polarization.

A complete test matrix of all mapping configurations used is also given which defines the extent of the data sample obtained within the cylinder and missile nosecone structures.

TABLE A-1
FIELD CONTOUR MEASUREMENT DATA INDEX

TEST NUMBER	CONFIGURATION	SCAN LOCATION	E-FIELD	H-FIELD	SCANNING PLANE	VECTOR FIELD BEING MEASURED		
			X	X	A	X	X	Z
1	CYLINDER	AT OPEN END	X		A	X	X	
2			X		A			X
3			X		A			X
4				X	A	X	X	
5				X	A		X	
6				X	A			X
7		AT OPEN END	X		B	X	X	
8			X		B			X
9			X		B			X
10				X	B	X	X	
11				X	B		X	
12				X	B			X
13	NOSECONE	NEAR BULKHEAD	X		A	X	X	
14			X		A			X
*15			X		A			X
16				X	A	X	X	
17				X	A			X
*18				X	A			
19		NEAR BULKHEAD	X		B	X	X	
20			X		B			X
*21			X		B			X
22				X	B	X	X	
23				X	B			X
*24				X	B			
25		NEAR TIP	X		C	X	X	
26			X		C			X
27			X		C			X
28				X	C	X	X	
29				X	C			X
30				X	C			
31		NEAR TIP	X		D	X	X	
32			X		D			X
33			X		D			X
34				X	D	X	X	
35				X	D			X
36				X	D			

* Z-AXIS Data for these locations not available due to Limited Mechanical Clearance for Fixturing.

V = VERTICAL

H = HORIZONTAL

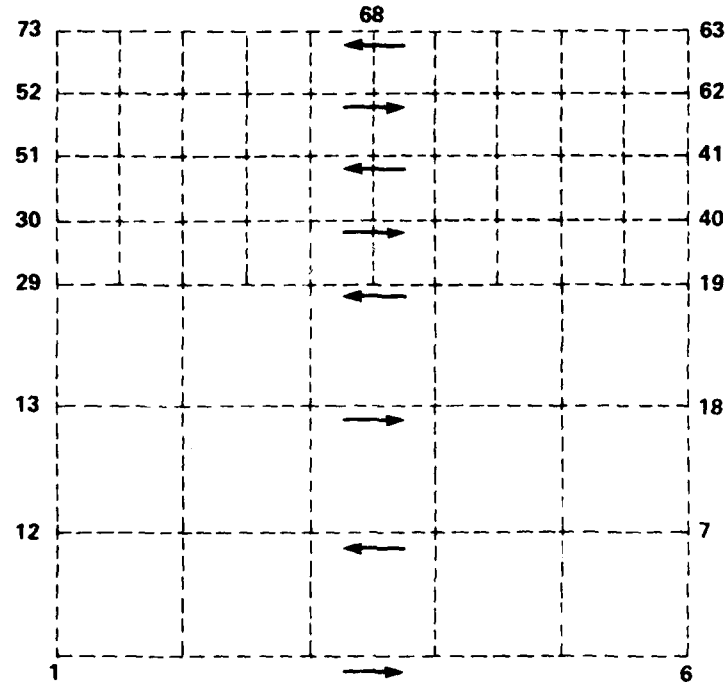
HORIZONTAL (X)

Illuminating Signal Polarization:

Illuminating Signal Intensity at Configuration Centre:

43.65 V/M CARRIER

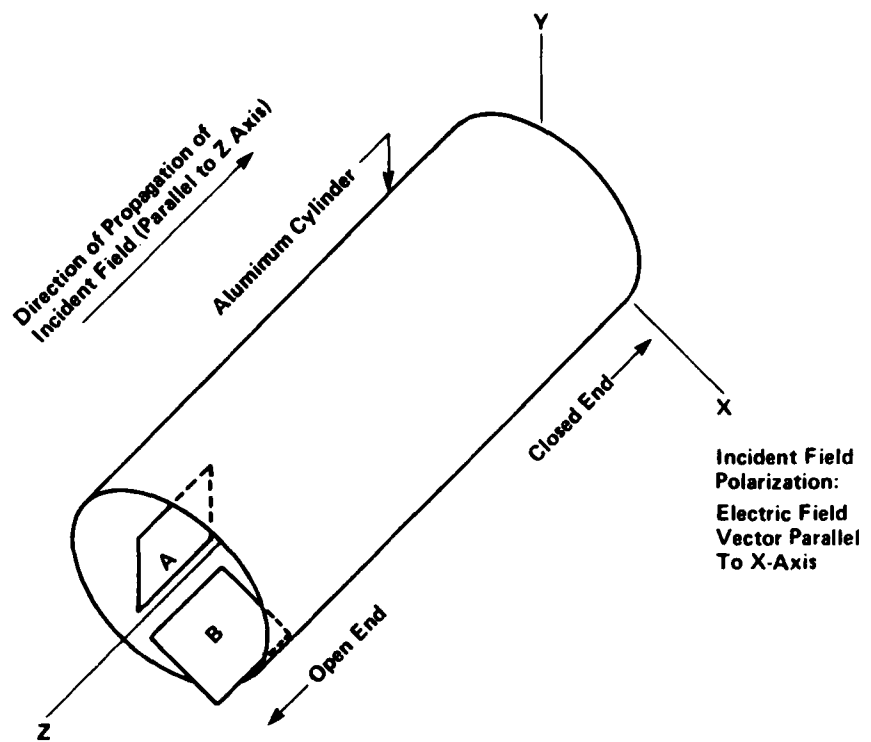
100% A.M. MODULATION



Notes:

1. Arrows indicate direction of probe motion during field mapping.
2. Numbers indicate sequence of measurements and correspond with tabulated measurement points shown in the tables of Appendix "B".

Fig. A-1 Definition of Reference Grid Used for Field Mapping



Note: Letters A, B refer to grid locations; refer to Fig. A-3 for detail view.

Grid "A" is Parallel to Y-Z Plane,
Grid "B" is Parallel to X-Z Plane

Fig. A-2 Reference Axes and Scanning Grid Locations for Aluminum Cylinder

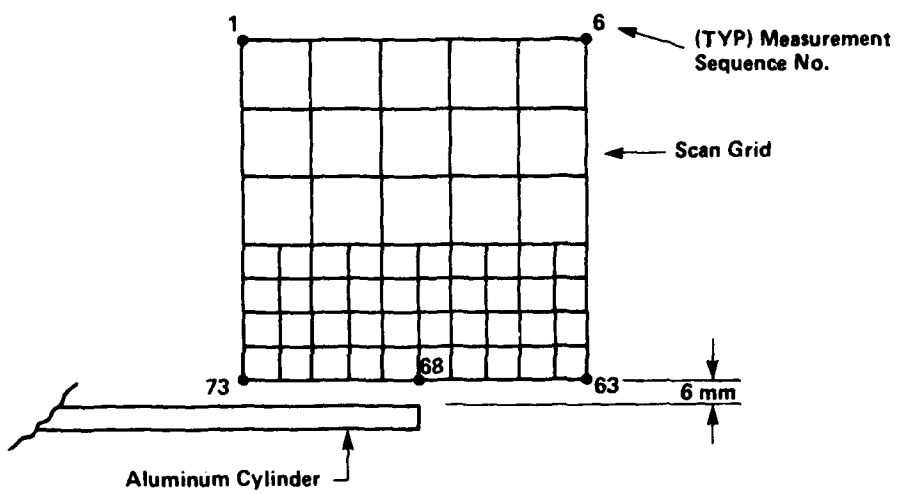
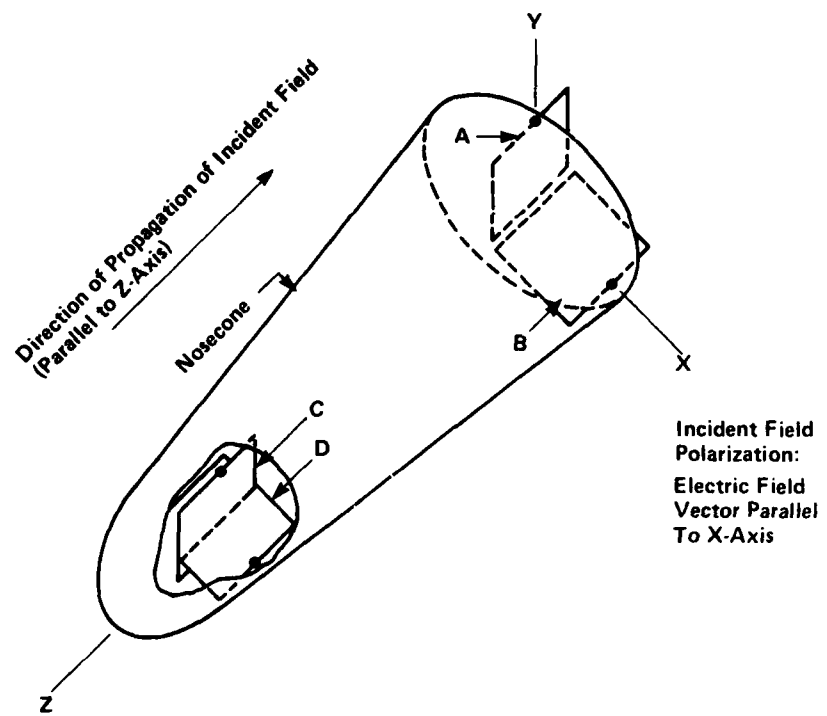


Fig. A-3 Scanning Grid Location Details for Aluminum Cylinder



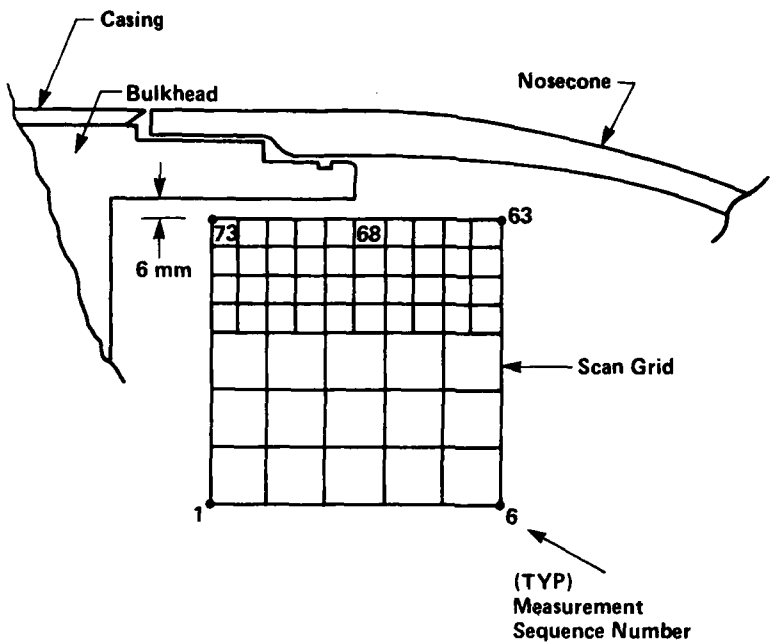
Note: Letters A, B, C, D refer to grid locations; refer to Fig. A-5 for detail views.

Grids "A" and "C" are Parallel to Y-Z Plane,

Grids "B" and "D" are Parallel to X-Z Plane

Fig. A-4 Reference Axes and Scanning Grid Locations for Missile Nosecone

Detail: Grids A, B as Shown on Fig. A-4



Detail: Grids C, D as Shown on Fig. A-4

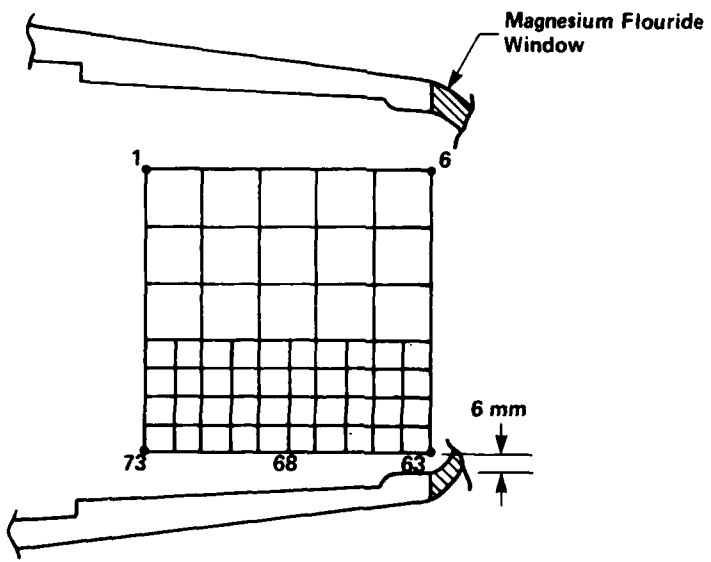


Fig. A-5 Scanning Grid Location Details for Missile Nosecone

APPENDIX B

FIELD CONTOUR MAPS FOR MISSILE NOSECONE AND CYLINDER

B.1 INTRODUCTION

This appendix contains the final field contour maps obtained for the cylinder and missile nosecone configurations.

Contours indicate that vector E or H field component measured, in dB referred to the incident field strength measured at the geometric centre of the configuration. Geometry of measurement is described in Appendix A.

Some contour information is not complete due to the difficulties of positioning probes for Z-axis measurements in the narrow confines of the nosecone tip and base. Figs. B-29 and B-34 were associated with a mechanical coupling failure and are valid for grid points between corners 1 and 73 only. Figs. B-27, 30, 33 and 36 are partial scans due to limited room for scanning in the nosecone tip. Figs. B-15, 18, 21 and 24 are not available due to limited space in the nosecone base for probe fixture clearance.

The numerical suffixes of the figure numbers correspond to the test numbers defined in Table A-1 of Appendix A.

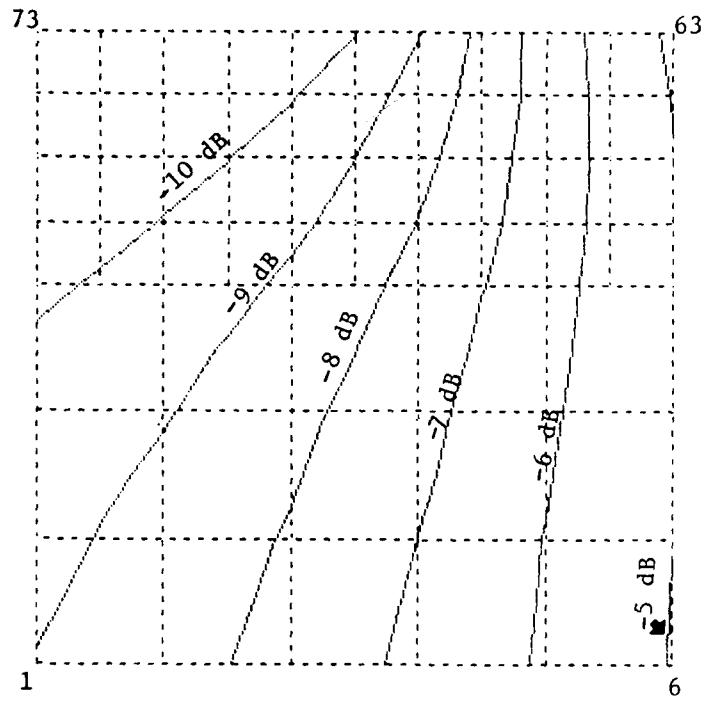


Figure B-1
CYLINDER MAP Ex

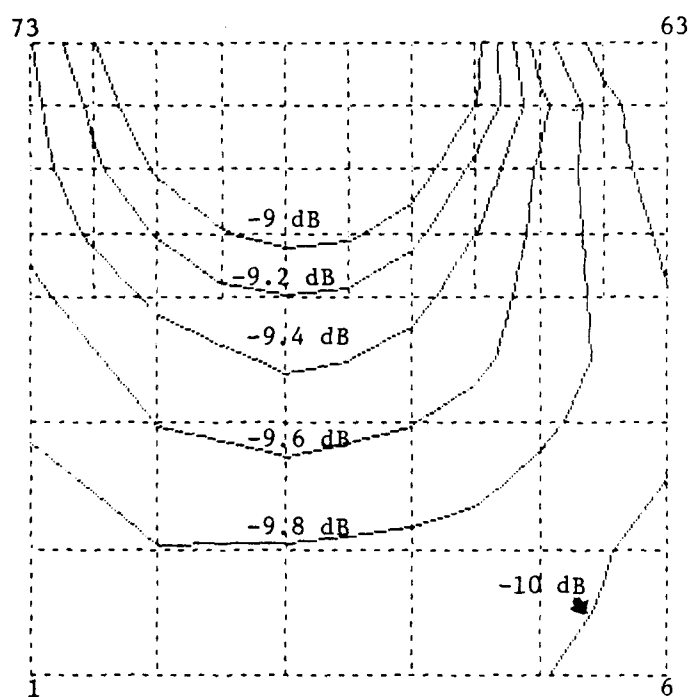


Figure B-2
CYLINDER MAP Ey

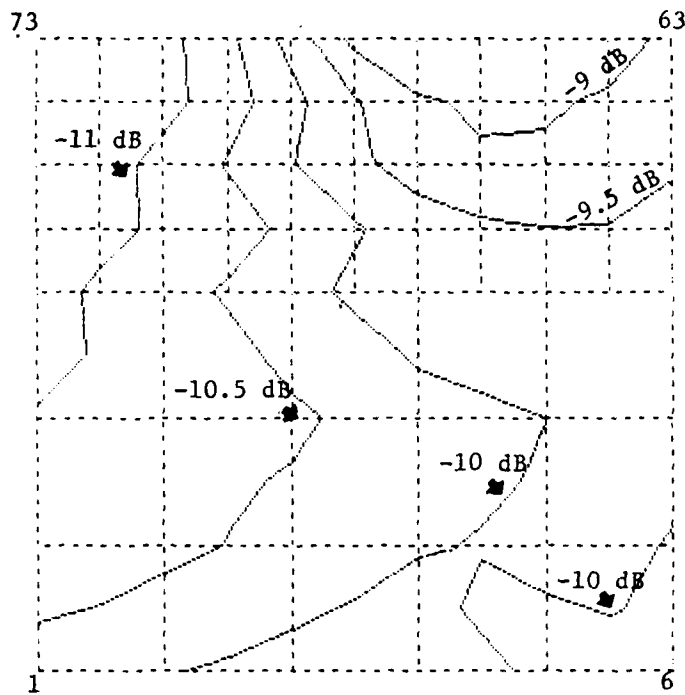


Figure B-3
CYLINDER MAP Ez

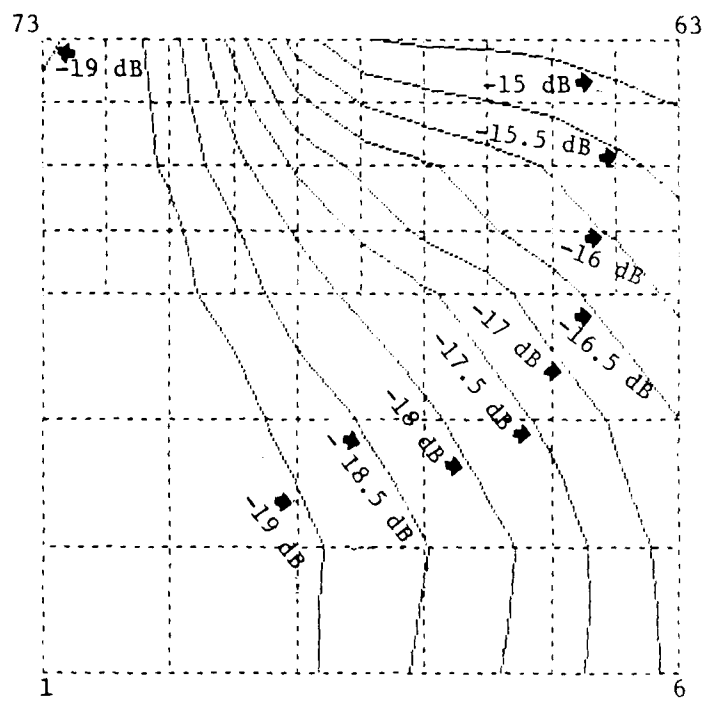


Figure B-4
CYLINDER MAP H_x

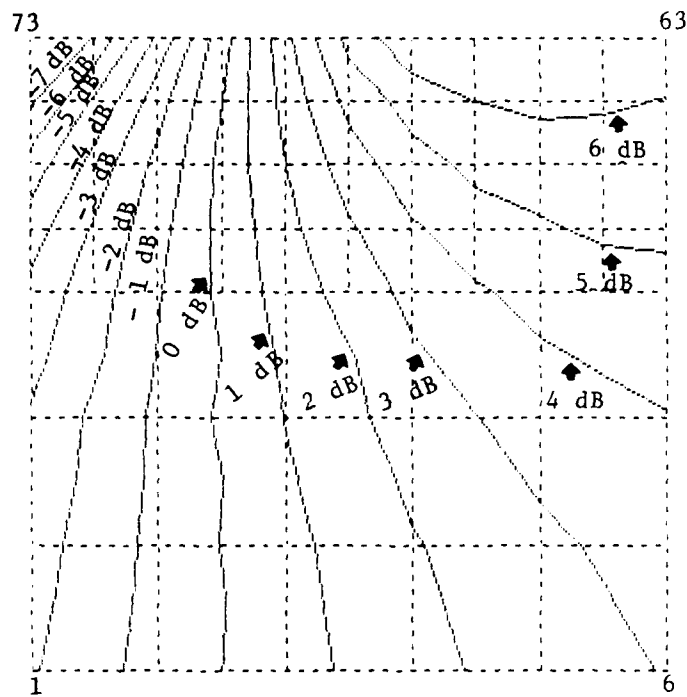


Figure B-5
CYLINDER MAP Hy

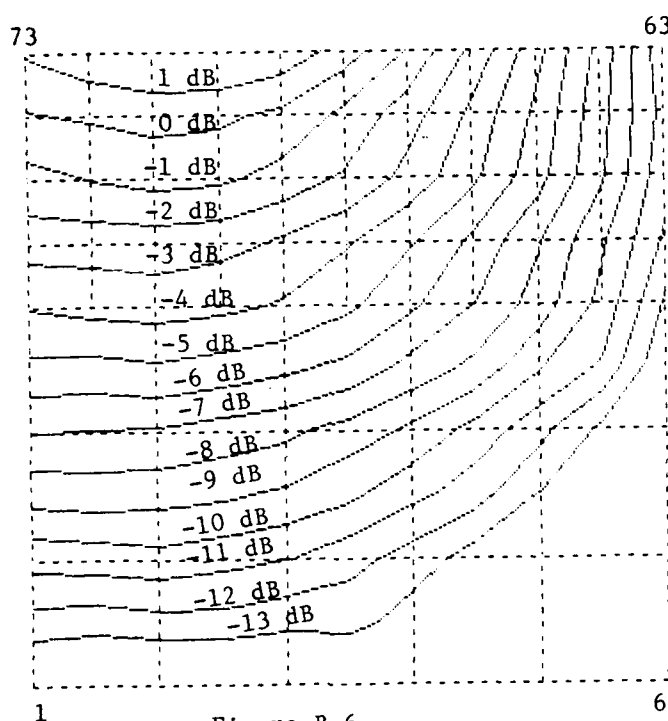


Figure B-6
CYLINDER MAP Hz

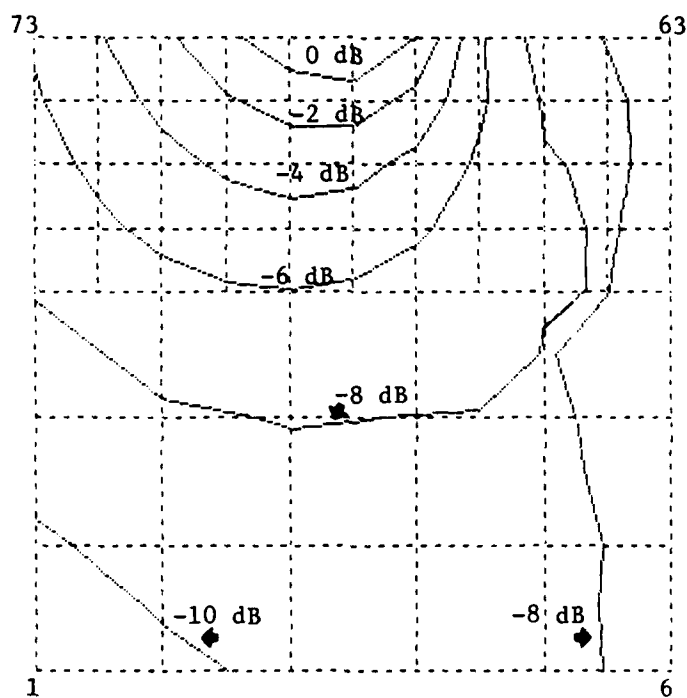


Figure B-7
CYLINDER MAP Ex

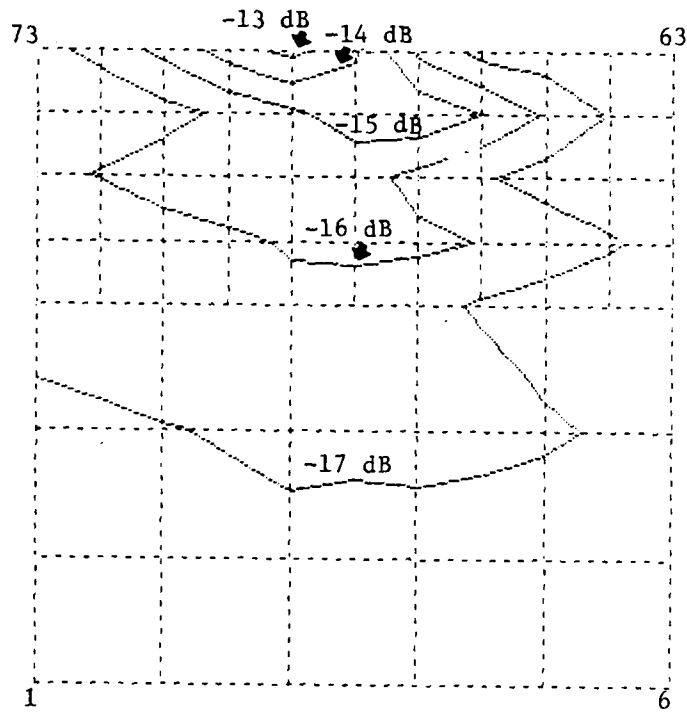


Figure B-8
CYLINDER MAP Ey

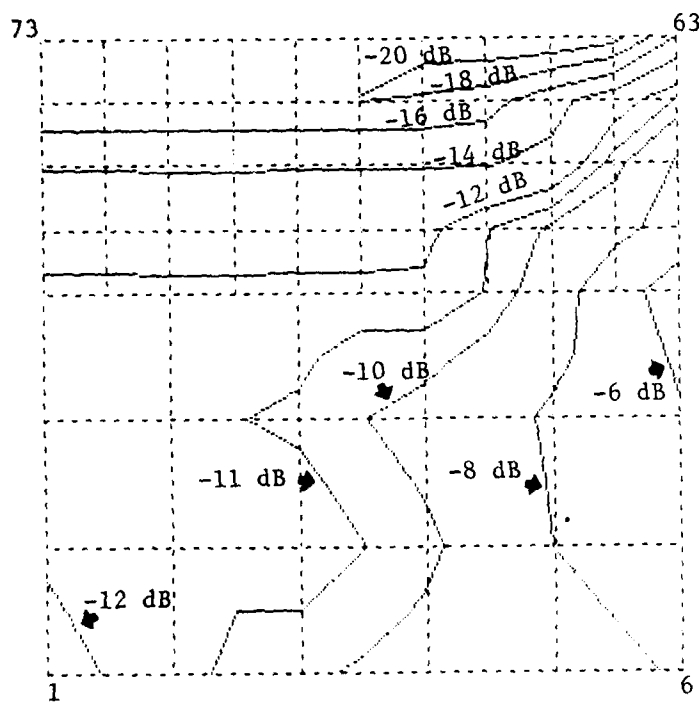


Figure B-9
CYLINDER MAP Ez

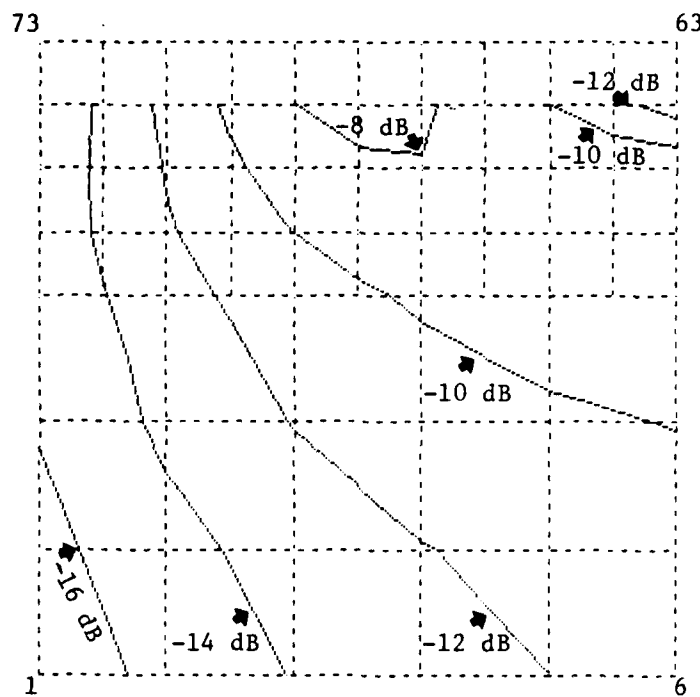


Figure B-10
CYLINDER MAP Hx

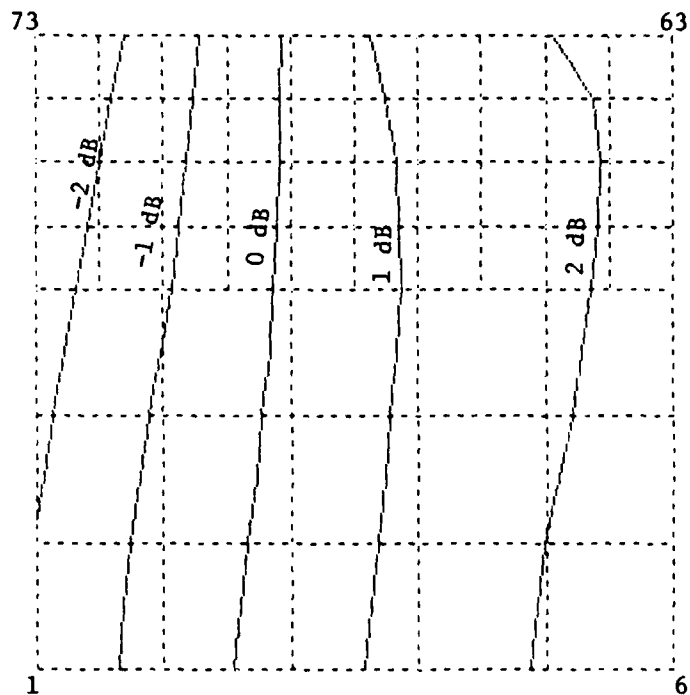


Figure B-11
CYLINDER MAP Hy

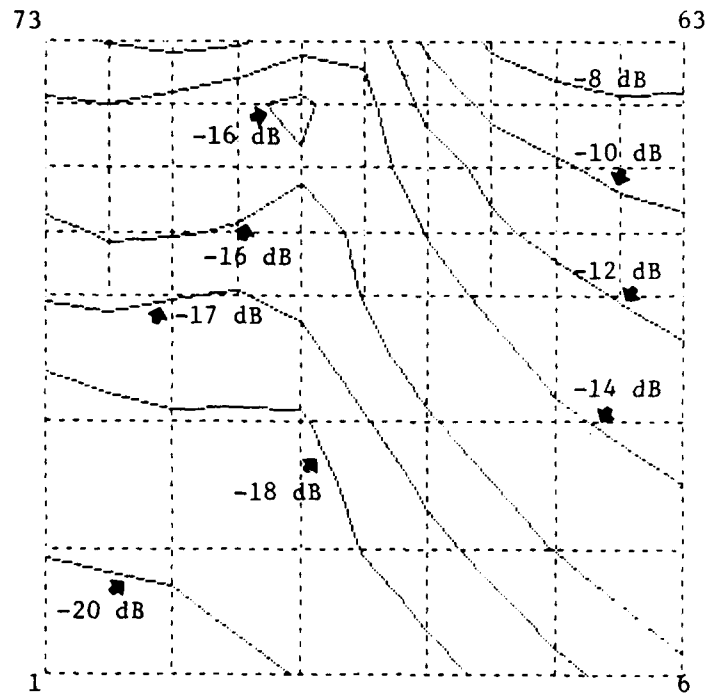


Figure B-12
CYLINDER MAP Hz

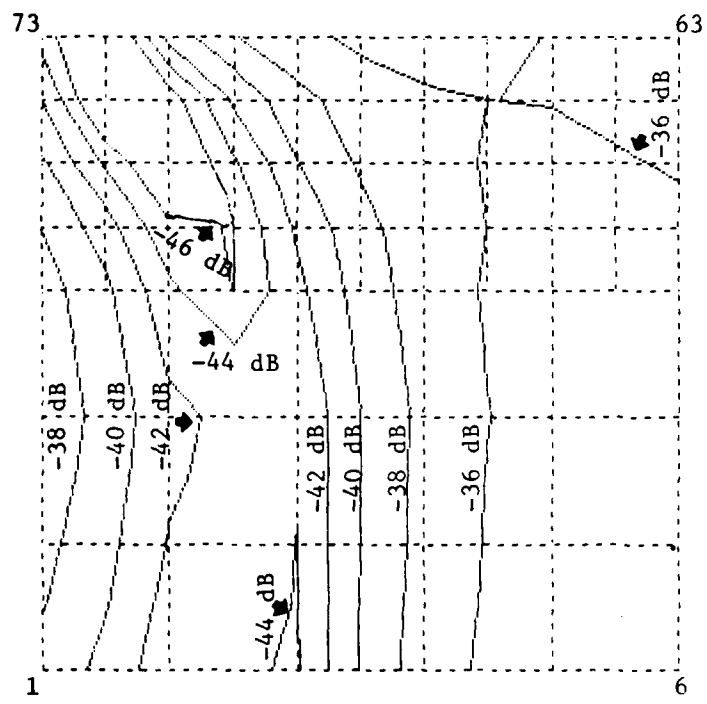


Figure B-13
NOSECONE MAP Ex

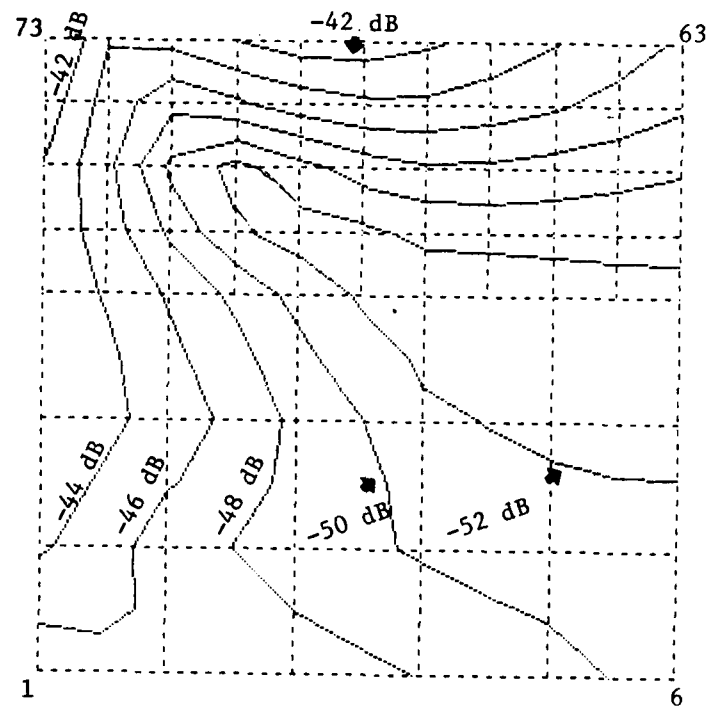


Figure B-14
NOSECONE MAP Ey

**SEE APPENDIX B
B.1 INTRODUCTION FOR EXPLANATION
FOR FIGURE B-15**

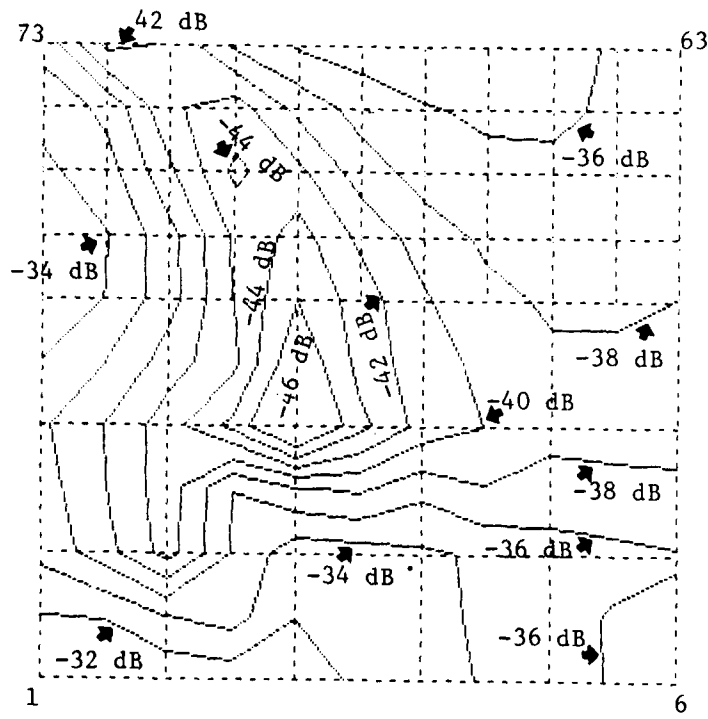


Figure B-16
NOSECONE MAP Hx

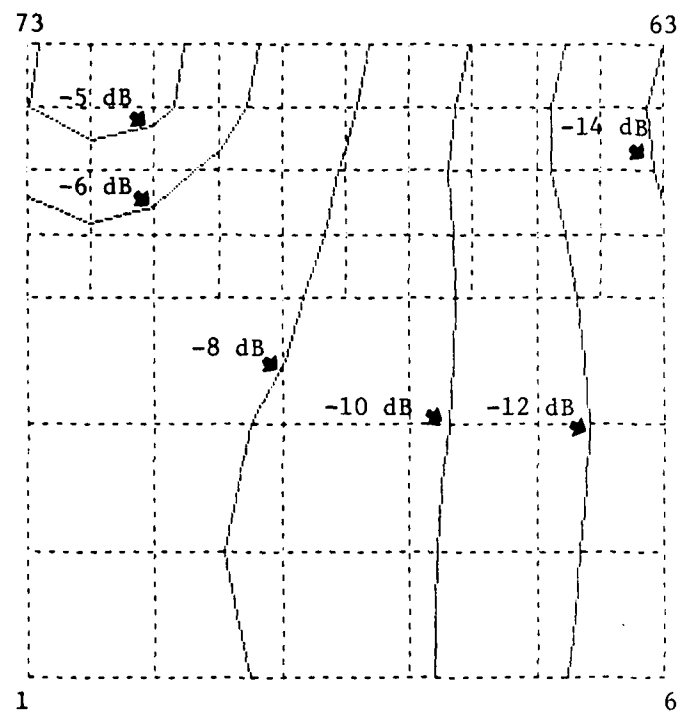


Figure B-17
NOSECONE MAP Hy

SEE APPENDIX B

B.1 INTRODUCTION FOR EXPLANATION
FOR FIGURE B-18

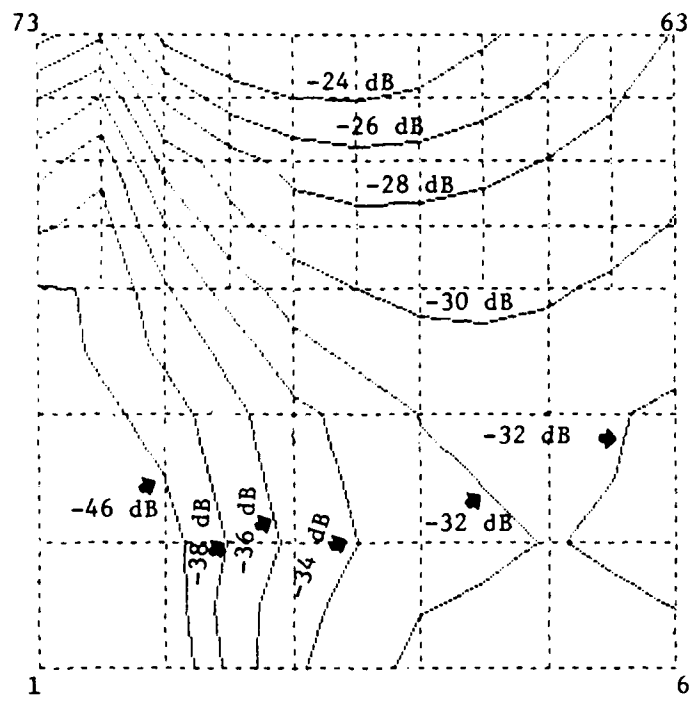


Figure B-19

NOSECONE MAP Ex

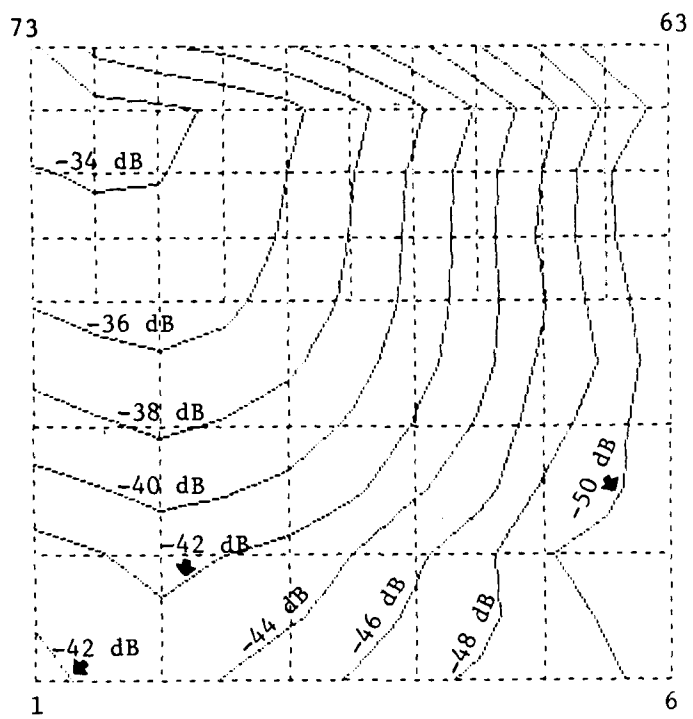


Figure B-20
NOSECONE MAP EY

SEE APPENDIX B
B.1 INTRODUCTION FOR EXPLANATION
FOR FIGURE B-21

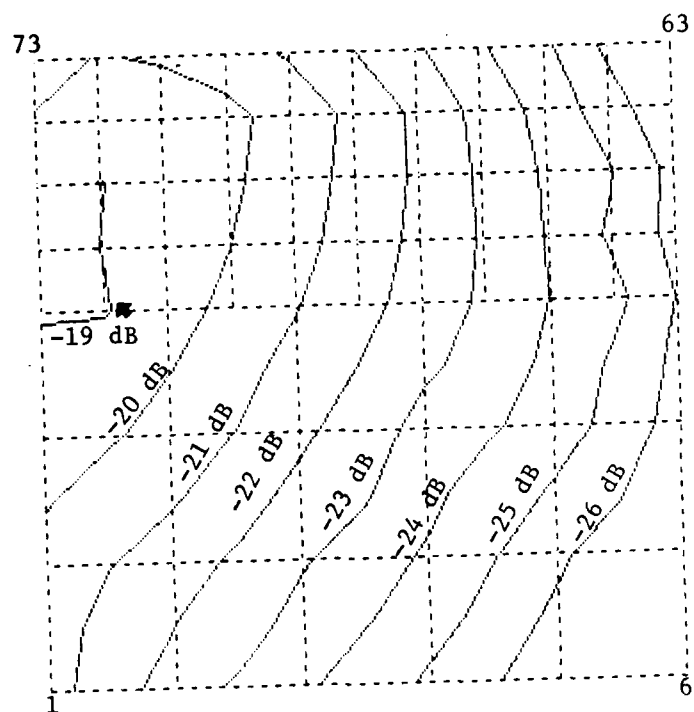


Figure B-22
NOSECONE MAP Hx

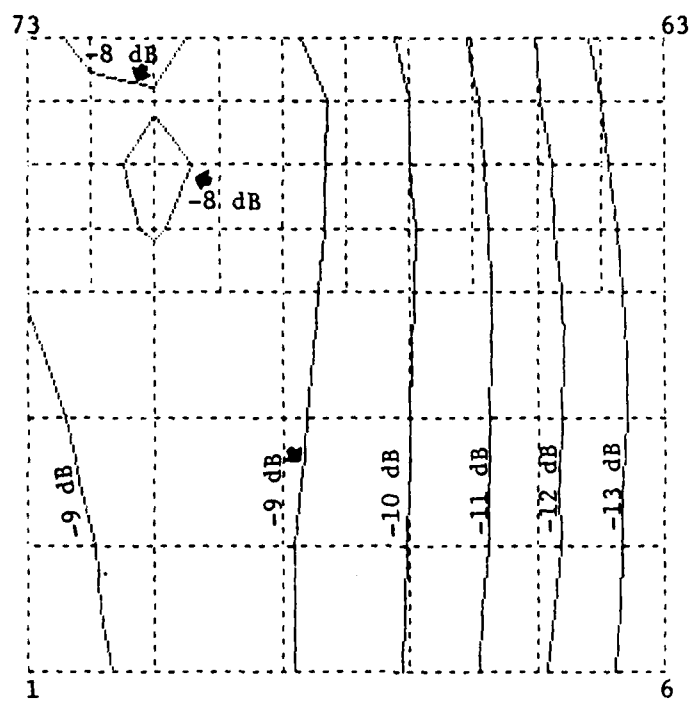


Figure B-23
NOSECONE MAP Hy

SEE APPENDIX B
B.1 INTRODUCTION FOR EXPLANATION
FOR FIGURE B-24

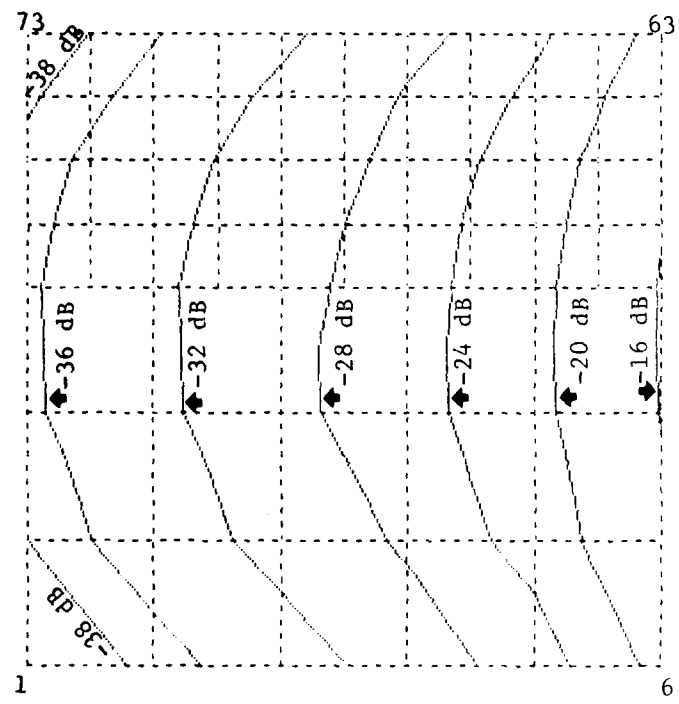


Figure B-25
NOSECONE MAP Ex

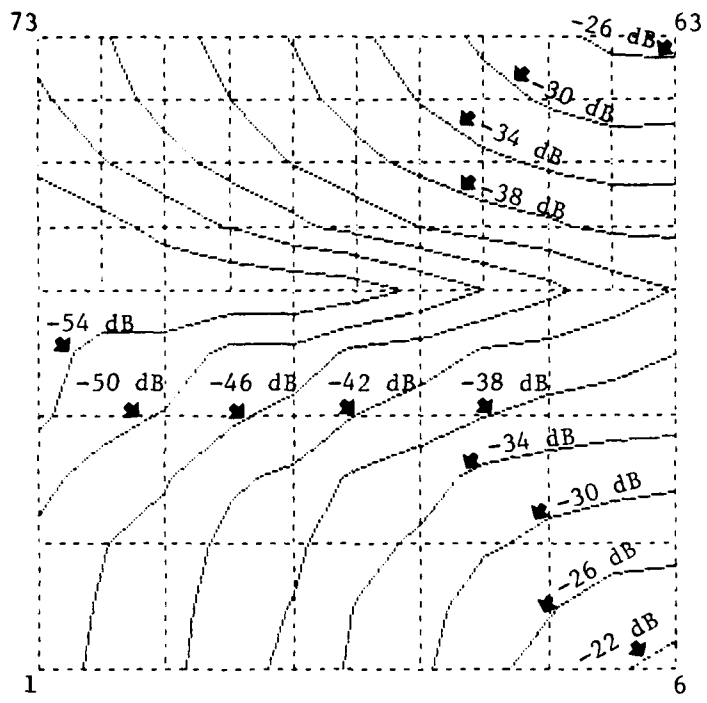


Figure B-26
NOSECONE MAP Ey

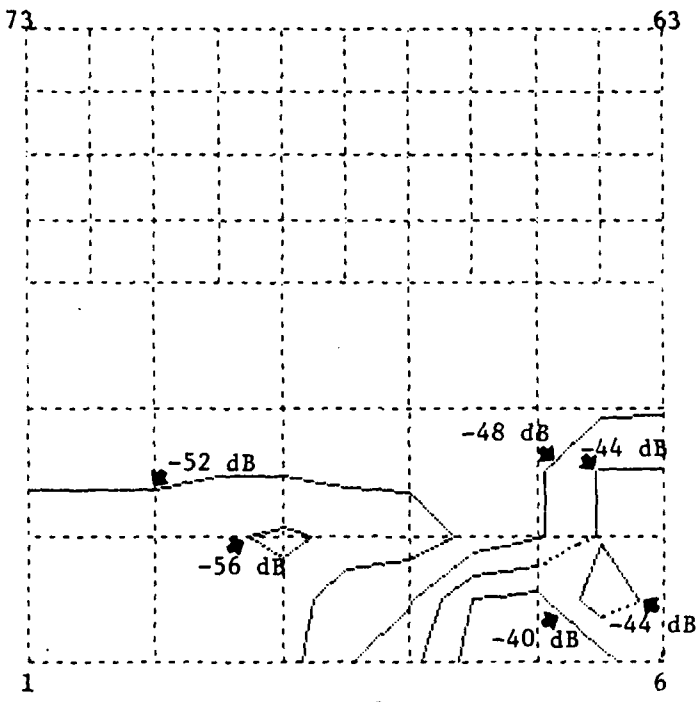


Figure B-27
NOSECONE MAP Ez

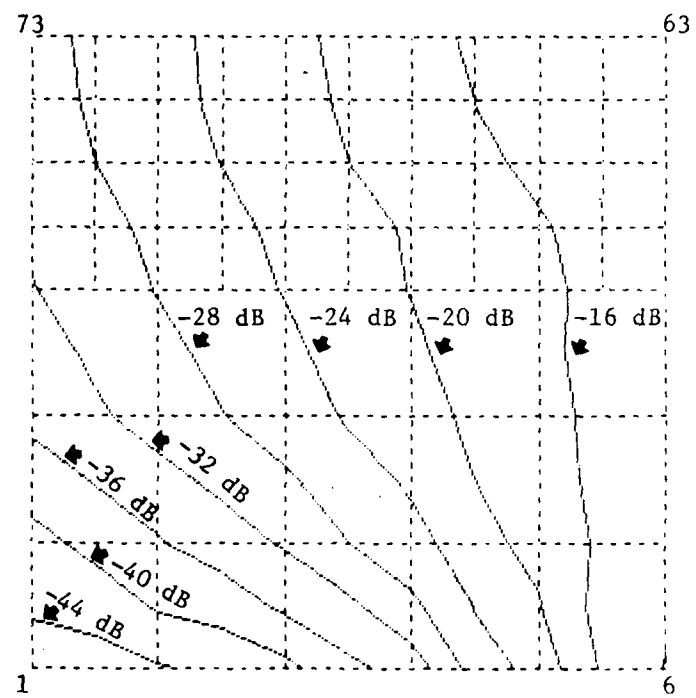


Figure B-28
NOSECONE MAP Hx

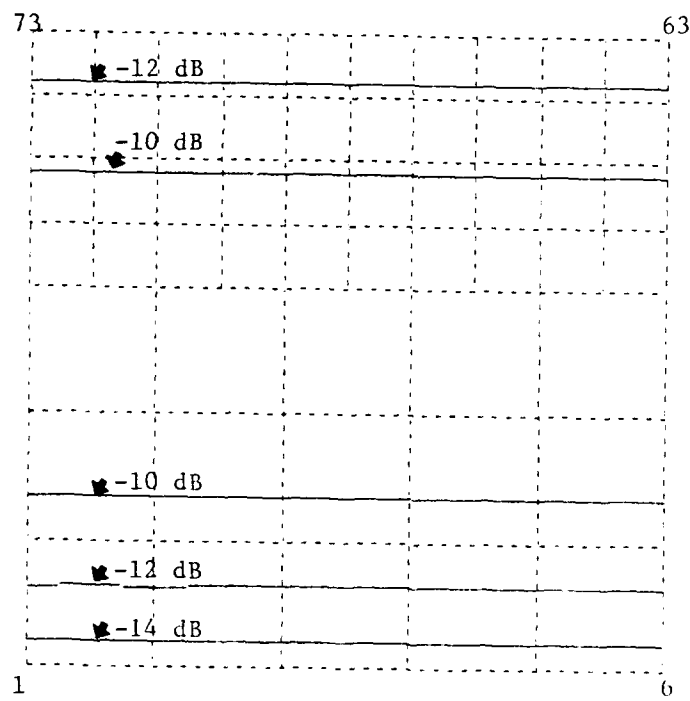


Figure B-29
NOSECONE MAP llly

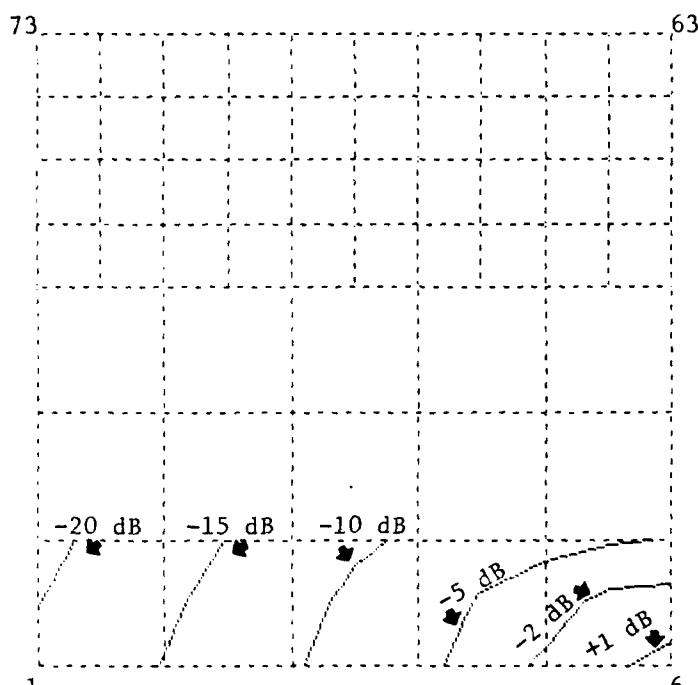


Figure B-30
NOSECONE MAP Hz

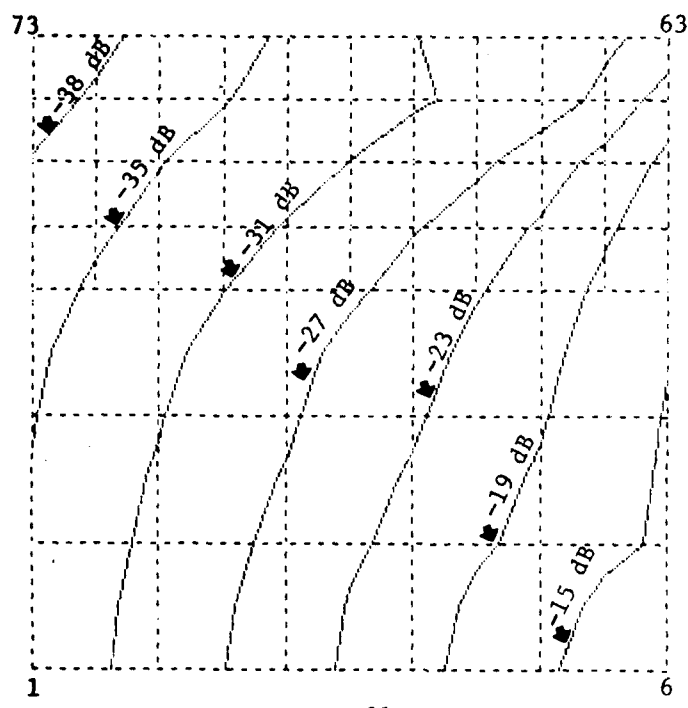


Figure B-31
NOSECONE MAP Ex

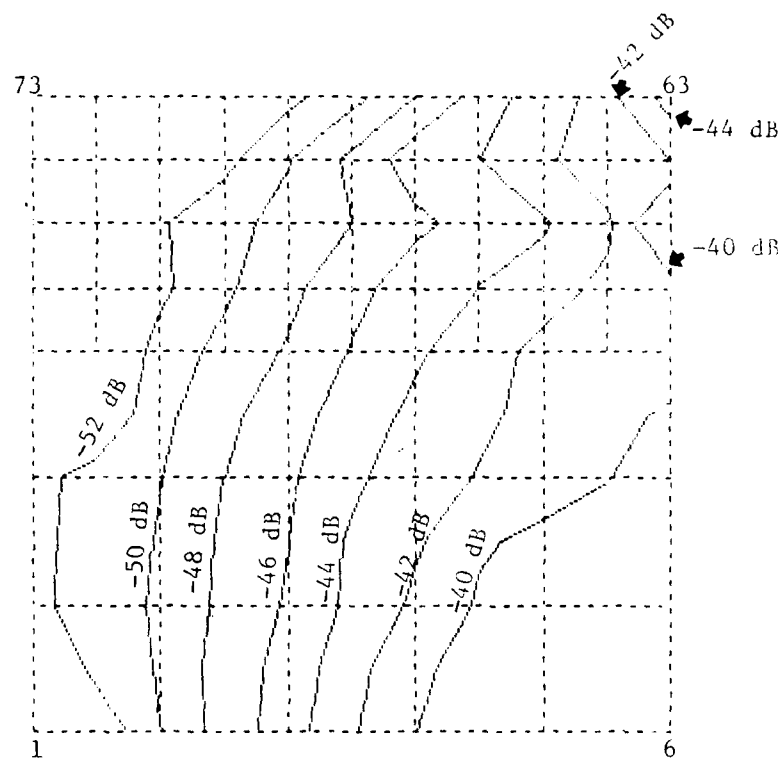


Figure B-32
NOSECONE MAP Ey

AD-A104 312

BELL NORTHERN RESEARCH LTD OTTAWA (ONTARIO)

F/G 16/3

ELECTROMAGNETIC FIELD MAPPING OF CYLINDER AND MISSILE NOSECONE. (U)

JUL 81 R R GOULETTE, K E FELSK

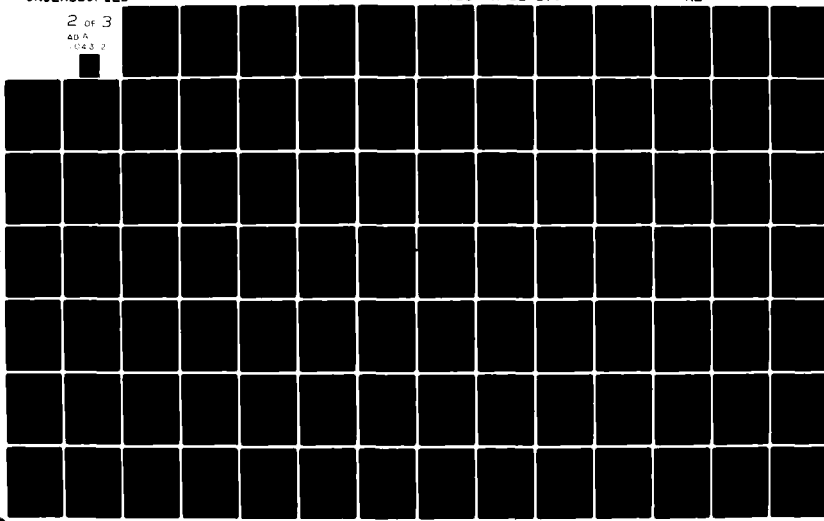
F30602-79-C-0197

UNCLASSIFIED

RADC-TR-81-179

NL

2 of 3
40 A
043 2



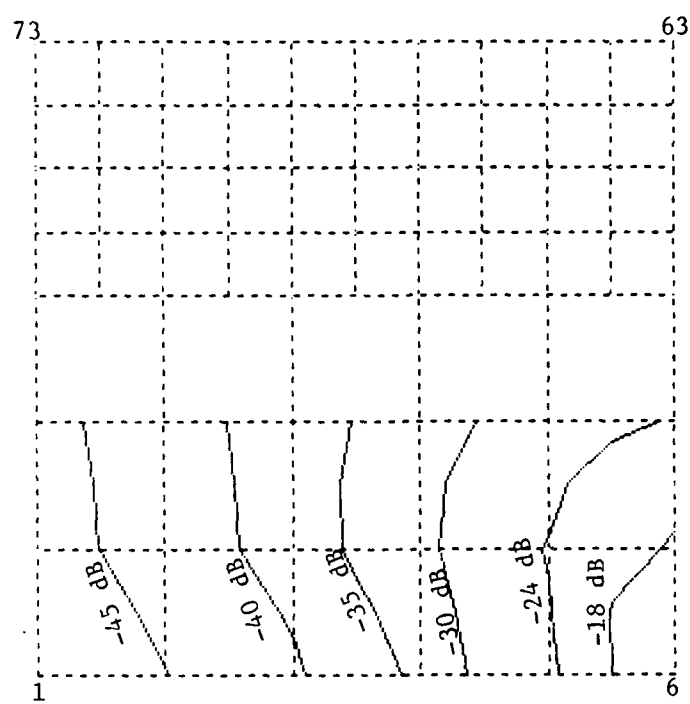


Figure B-33
NOSECONE MAP Ez

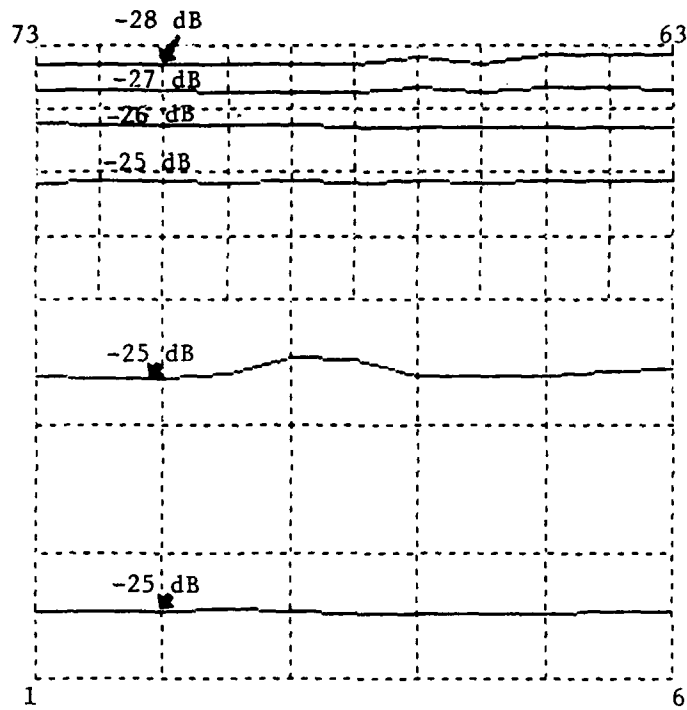


Figure B-34
NOSECONE MAP Hx

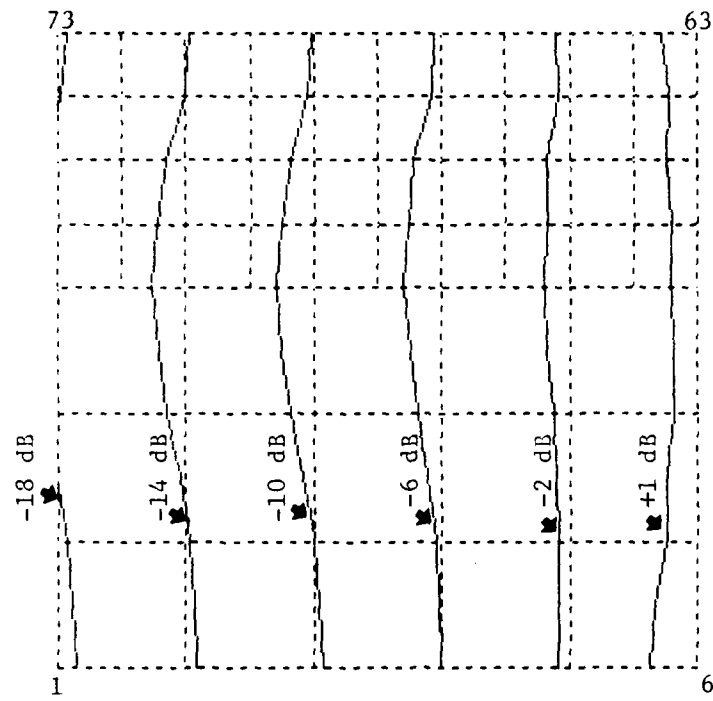


Figure B-35
NOSECONE MAP Hy

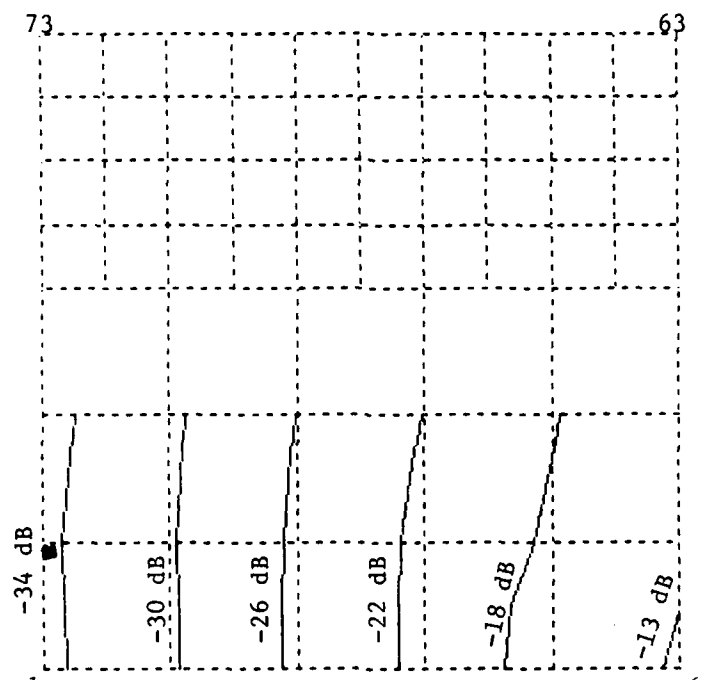


Figure B-36

NOSECONE Hz

APPENDIX C

TABULATION OF E-FIELD AND H-FIELD MEASUREMENT DATA

C.1 INTRODUCTION

This appendix contains a tabulation of all E-Field and H-Field measurements made during field mapping of the cylinder and missile nosecone.

This comprises the source data from which the final field contour maps shown Appendix "B" were derived.

The tabulation shows field strength levels in dB relative to the incident plane wave field strength used during the mapping procedure.

The 73 measurement points correspond to the scanning grid locations as defined in Appendix A.

The numerical suffixes of the figure numbers correspond to the test numbers defined in Table A-1 of Appendix A.

TABLE C-1
CYLINDER MAP Ex

POINT	LEVEL dB	POINT	LEVEL dB
1	-8.95356	51	-10.6574
2	-8.37354	52	-10.8918
3	-7.67411	53	-10.7898
4	-6.77432	54	-10.6324
5	-5.89276	55	-10.3963
6	-4.96334	56	-10.0605
7	-5.00654	57	-9.50165
8	-5.97309	58	-8.61034
9	-6.98987	59	-7.61381
10	-7.90585	60	-6.57132
11	-8.64349	61	-5.73125
12	-9.29812	62	-4.95229
13	-9.66781	63	-4.81432
14	-9.08389	64	-5.6214
15	-8.28482	65	-6.53705
16	-7.31005	66	-7.74517
17	-6.14392	67	-9.04434
18	-5.06681	68	-10.0374
19	-5.07709	69	-10.5348
20	-5.6971	70	-10.7945
21	-6.31966	71	-10.9274
22	-7.028	72	-11.0208
23	-7.69016	73	-11.0965
24	-8.27486		
25	-8.80018		
26	-9.29046		
27	-9.63903		
28	-9.92547		
29	-10.1488		
30	-10.3865		
31	-10.2097		
32	-9.96774		
33	-9.64241		
34	-9.22006		
35	-8.62376		
36	-7.57176		
37	-7.25107		
38	-6.44659		
39	-5.75612		
40	-5.09113		
41	-5.03968		
42	-5.75546		
43	-6.52417		
44	-7.42521		
45	-8.25353		
46	-9.0038		
47	-9.59916		
48	-10.0169		
49	-10.2947		
50	-10.4988		

TABLE C-2
CYLINDER MAP Ey

POINT	LEVEL dB	POINT	LEVEL dB
1	-9.98569	51	-9.49998
2	-9.94983	52	-9.45129
3	-9.9231	53	-9.15536
4	-9.92491	54	-9.77413
5	-9.99349	55	-9.37991
6	-10.0823	56	-9.11158
7	-10.0483	57	-9.08761
8	-9.93377	58	-9.44395
9	-9.84425	59	-9.99566
10	-9.81217	60	-9.54119
11	-9.80872	61	-9.93321
12	-9.93614	62	-10.1471
13	-9.7734	63	-10.2584
14	-9.59471	64	-10.0963
15	-9.52533	65	-9.71885
16	-9.59417	66	-8.93383
17	-9.76366	67	-7.83921
18	-9.96593	68	-7.1702
19	-9.98689	69	-7.36707
20	-9.839	70	-7.93849
21	-9.67459	71	-8.49868
22	-9.50658	72	-9.01003
23	-9.33732	73	-9.41304
24	-9.23474		
25	-9.20328		
26	-9.25216		
27	-9.36337		
28	-9.50492		
29	-9.65026		
30	-9.54967		
31	-9.36617		
32	-9.18596		
33	-9.01373		
34	-8.93506		
35	-8.96221		
36	-8.14458		
37	-9.39958		
38	-9.64972		
39	-9.87471		
40	-10.0362		
41	-10.1041		
42	-9.91126		
43	-9.63004		
44	-9.26527		
45	-8.84023		
46	-8.60466		
47	-8.57919		
48	-8.7308		
49	-8.96718		
50	-9.24177		

TABLE C-3
CYLINDER MAP -EZ

POINT	LEVEL dB	POINT	LEVEL dB
1	-10.2215	51	-11.4055
2	-10.0314	52	-11.5004
3	-9.83721	53	-11.3629
4	-9.61768	54	-11.1609
5	-10.1354	55	-10.7617
6	-10.0671	56	-10.1634
7	-10.0121	57	-9.55021
8	-9.91126	58	-9.08451
9	-10.041	59	-8.90134
10	-10.032	60	-8.92949
11	-10.6372	61	-9.0763
12	-10.9549	62	-9.28495
13	-10.9798	63	-9.13757
14	-10.7918	64	-8.7498
15	-10.5916	65	-8.44148
16	-10.221	66	-8.24926
17	-10.003	67	-8.33543
18	-9.93021	68	-8.8746
19	-9.74928	69	-9.82554
20	-9.60643	70	-10.6352
21	-9.52479	71	-11.1692
22	-9.53689	72	-11.4462
23	-9.57059	73	-11.5776
24	-9.90005		
25	-10.1687		
26	-10.4408		
27	-10.6965		
28	-10.935		
29	-11.1692		
30	-11.2465		
31	-11.1185		
32	-10.9316		
33	-10.7371		
34	-10.3951		
35	-10.0525		
36	-9.77456		
37	-9.59027		
38	-9.50078		
39	-9.51211		
40	-9.58745		
41	-9.47329		
42	-9.23797		
43	-9.09205		
44	-9.07347		
45	-9.27621		
46	-9.50811		
47	-10.0296		
48	-10.465		
49	-10.864		
50	-11.1687		

TABLE C-4
CYLINDER MAP Hx

POINT	LEVEL dB	POINT	LEVEL dB
1	-19.5943	51	-19.2087
2	-19.5943	52	-19.1194
3	-19.1194	53	-19.3686
4	-18.4269	54	-18.8291
5	-17.7311	55	-17.7861
6	-16.8784	56	-16.6451
7	-16.7874	57	-15.9641
8	-17.8	58	-15.6821
9	-18.5274	59	-15.5267
10	-19.1305	60	-15.3671
11	-19.51	61	-15.185
12	-19.2943	62	-14.9701
13	-19.3421	63	-14.4913
14	-19.4495	64	-14.663
15	-18.851	65	-14.8459
16	-18.1075	66	-14.9025
17	-17.3857	67	-14.8973
18	-16.5064	68	-15.0281
19	-15.8892	69	-15.7396
20	-16.2715	70	-17.3207
21	-16.6897	71	-18.7682
22	-17.2059	72	-19.321
23	-17.5776	73	-18.6732
24	-17.8761		
25	-18.2254		
26	-18.7596		
27	-19.1918		
28	-19.4007		
29	-19.3053		
30	-19.2943		
31	-19.4061		
32	-19.1139		
33	-18.549		
34	-17.9432		
35	-17.4108		
36	-16.8877		
37	-16.5501		
38	-16.2304		
39	-15.942		
40	-15.6621		
41	-15.3426		
42	-15.6311		
43	-15.9486		
44	-16.2407		
45	-16.5695		
46	-16.857		
47	-17.4171		
48	-18.1678		
49	-18.9224		
50	-19.3474		

TABLE C-5

CYLINDER MAP Hy

POINT	LEVEL dB	POINT	LEVEL dB
1	-2.10219	51	-5.53147
2	-1.612744	52	-7.20569
3	.590987	53	-4.25204
4	1.68363	54	-2.45013
5	2.44741	55	-1.000577112
6	2.05748	56	2.30854
7	3.45853	57	4.28685
8	2.77648	58	5.41972
9	1.92094	59	5.99972
10	.727342	60	6.22095
11	-1.721696	61	6.14981
12	-2.44534	62	5.9502
13	-2.88994	63	6.56774
14	-1.796441	64	6.94318
15	1.02905	65	7.22332
16	2.44532	66	7.2376
17	3.46306	67	6.74261
18	3.9566	68	5.32442
19	4.68956	69	2.69366
20	4.56033	70	-1.486291
21	4.30839	71	-3.82195
22	3.88913	72	-6.92899
23	3.27314	73	-9.84174
24	2.39573		
25	1.41349		
26	.219646		
27	-1.10739		
28	-2.40682		
29	-3.77986		
30	-4.47913		
31	-2.90193		
32	-1.33438		
33	.247031		
34	1.67714		
35	2.85422		
36	3.8718		
37	4.50937		
38	4.89359		
39	5.15345		
40	5.20733		
41	5.46826		
42	5.49647		
43	5.44817		
44	5.2709		
45	4.57788		
46	3.51592		
47	1.99769		
48	.217524		
49	-1.7319		
50	-3.65558		

TABLE C-6
CYLINDER MAP Hz

POINT	LEVEL dB	POINT	LEVEL dB
1	-14.6669	51	-1.37042
2	-14.9571	52	-0.0885712
3	-14.8793	53	.1138602
4	-14.6689	54	.344622
5	-13.9901	55	.215766
6	-13.2516	56	-1.230525
7	-15.282	57	-1.33642
8	-14.661	58	-2.51032
9	-12.4413	59	-4.19844
10	-10.9517	60	-6.33377
11	-10.3833	61	-8.55731
12	-10.6828	62	-11.3628
13	-7.03312	63	-11.5899
14	-7.13617	64	-8.2763
15	-7.75555	65	-5.57357
16	-9.20944	66	-3.15582
17	-11.8761	67	-1.98113
18	-15.1115	68	.577029
19	-13.0812	69	1.70103
20	-10.3051	70	2.17141
21	-8.38842	71	2.16071
22	-6.97888	72	1.70492
23	-5.77857	73	1.69356
24	-4.7918		
25	-4.11284		
26	-3.72743		
27	-3.56323		
28	-3.68972		
29	-3.91498		
30	-2.56514		
31	-2.56775		
32	-2.47151		
33	-2.67506		
34	-3.13999		
35	-3.88746		
36	-4.8868		
37	-6.20517		
38	-7.89968		
39	-9.81892		
40	-12.1538		
41	-11.6154		
42	-8.7582		
43	-6.60152		
44	-4.76765		
45	-3.32114		
46	-2.13704		
47	-1.36231		
48	-0.833023		
49	-0.686563		
50	-0.965223		

TABLE C-7
CYLINDER MAP Ex

POINT	LEVEL dB	POINT	LEVEL dB
1	-11.0326	51	-6.66524
2	-10.3073	52	-6.21386
3	-9.71207	53	-4.88331
4	-9.11225	54	-3.65501
5	-8.37939	55	-2.19843
6	-7.57379	56	-1.21
7	-7.63856	57	-1.18779
8	-8.33299	58	-2.5782
9	-8.77042	59	-5.65761
10	-9.10339	60	-6.16454
11	-9.50824	61	-8.33923
12	-10.208	62	-7.34428
13	-9.1949	63	-6.58428
14	-8.26439	64	-7.91239
15	-7.90491	65	-8.25294
16	-8.04229	66	-8.6343
17	-8.13886	67	-8.0306342
18	-7.57336	68	-2.43747
19	-7.6532	69	-1.40952
20	-8.01817	70	-1.527074
21	-7.96519	71	-2.45679
22	-7.47245	72	-4.19537
23	-6.74269	73	-5.75716
24	-6.23902		
25	-6.03936		
26	-6.16502		
27	-6.55357		
28	-7.19718		
29	-7.89607		
30	-7.283		
31	-6.34255		
32	-5.58912		
33	-4.94726		
34	-4.69512		
35	-4.93889		
36	-5.73996		
37	-6.8311		
38	-7.93921		
39	-8.07843		
40	-7.65363		
41	-7.59619		
42	-8.21773		
43	-7.88817		
44	-6.2775		
45	-4.43668		
46	-3.4126		
47	-3.21964		
48	-3.69533		
49	-4.53996		
50	-5.62437		

TABLE C-8
CYLINDER MAP Ey

POINT	LEVEL dB	POINT	LEVEL dB
1	-17.2271	51	-16.3449
2	-17.3002	52	-16.7003
3	-17.2325	53	-16.727
4	-17.2362	54	-16.316
5	-17.2947	55	-15.7997
6	-17.5383	56	-15.1999
7	-17.5731	57	-14.5131
8	-17.5249	58	-14.3196
9	-17.416	59	-14.9933
10	-17.2544	60	-16.1306
11	-17.129	61	-17.0732
12	-17.1911	62	-17.4597
13	-17.3094	63	-17.4981
14	-17.0557	64	-17.4254
15	-16.7737	65	-17.5134
16	-16.6878	66	-17.3671
17	-16.8815	67	-16.1879
18	-17.3039	68	-13.8729
19	-17.5191	69	-12.6579
20	-17.521	70	-13.5063
21	-17.3839	71	-14.6724
22	-17.1143	72	-15.6738
23	-16.7058	73	-16.3126
24	-16.3968		
25	-16.1879		
26	-16.126		
27	-16.1942		
28	-16.3659		
29	-16.5762		
30	-16.8082		
31	-16.7449		
32	-16.4608		
33	-16.1724		
34	-15.9148		
35	-15.7602		
36	-15.787		
37	-16.0436		
38	-16.4575		
39	-16.9		
40	-17.3205		
41	-17.454		
42	-17.4827		
43	-17.3638		
44	-16.9		
45	-16.2777		
46	-15.6463		
47	-15.2521		
48	-15.2572		
49	-15.5395		
50	-15.9425		

TABLE C-9

CYLINDER MAP Ez

POINT	LEVEL dB	POINT	LEVEL dB
1	-12.5546	51	-14.125
2	-11.3171	52	-17.4712
3	-10.2494	53	-17.4712
4	-9.36617	54	-17.4597
5	-8.51669	55	-17.4654
6	-7.88772	56	-17.4654
7	-6.14243	57	-17.4654
8	-7.98113	58	-17.4693
9	-10.302	59	-16.8722
10	-11.8146	60	-14.6796
11	-11.7919	61	-12.8145
12	-11.8092	62	-10.8979
13	-11.3564	63	-15.9837
14	-11.3485	64	-20.8411
15	-10.7717	65	-21.816
16	-9.39958	66	-21.816
17	-7.78292	67	-21.8241
18	-6.21538	68	-60.7588
19	-5.01981	69	-60.7588
20	-6.79962	70	-60.7588
21	-8.8279	71	-60.7588
22	-10.9363	72	-60.7588
23	-11.7565	73	-60.7588
24	-11.7423		
25	-11.743		
26	-11.7535		
27	-11.7603		
28	-11.7483		
29	-11.7438		
30	-12.5565		
31	-12.5733		
32	-12.5584		
33	-12.5798		
34	-12.5639		
35	-12.578		
36	-12.3462		
37	-11.0417		
38	-9.79421		
39	-8.51521		
40	-7.24076		
41	-7.73974		
42	-10.5765		
43	-13.5033		
44	-14.137		
45	-14.1359		
46	-14.1249		
47	-14.1184		
48	-14.1403		
49	-14.1304		
50	-14.1194		

TABLE C-10
CYLINDER MAP Hx

POINT	LEVEL dB	POINT	LEVEL dB
1	-17.4014	51	-15.4
2	-15.4334	52	-15.6979
3	-13.916	53	-13.6036
4	-12.7972	54	-11.5539
5	-12.0145	55	-9.6058
6	-11.4563	56	-8.03745
7	-10.8047	57	-7.38979
8	-11.3576	58	-7.75555
9	-12.0898	59	-8.7429
10	-13.2136	60	-9.97226
11	-14.8357	61	-11.377
12	-16.6721	62	-12.9314
13	-15.8372	63	-14.8715
14	-13.5851	64	-16.3235
15	-11.9087	65	-29.3466
16	-10.8295	66	-30.6173
17	-10.229	67	-32.1401
18	-9.94885	68	-59.232
19	-9.22835	69	-69.232
20	-9.22689	70	-69.232
21	-9.30104	71	-69.232
22	-9.54345	72	-69.232
23	-9.79357	73	-69.232
24	-10.2104		
25	-10.8257		
26	-11.7492		
27	-12.8495		
28	-14.0887		
29	-15.5851		
30	-15.3671		
31	-13.7215		
32	-12.2476		
33	-10.9507		
34	-9.97384		
35	-9.33292		
36	-8.90773		
37	-8.82348		
38	-8.78478		
39	-8.85085		
40	-8.93103		
41	-8.59379		
42	-8.47761		
43	-8.3131		
44	-8.12955		
45	-8.07515		
46	-8.33612		
47	-9.12212		
48	-10.2631		
49	-11.6354		
50	-13.56		

TABLE C-11
CYLINDER MAP 'Hy

POINT	LEVEL dB	POINT	LEVEL dB
1	-1.81964	51	-2.73101
2	-.561617	52	-2.91059
3	.452172	53	-2.14306
4	1.37735	54	-1.36833
5	2.09194	55	-.571466
6	2.6312	56	.117329
7	2.49324	57	.730446
8	2.00787	58	1.28337
9	1.29048	59	1.64591
10	.347145	60	1.38786
11	-.67106	61	2.04038
12	-1.96046	62	2.12872
13	-2.17792	63	2.19108
14	-.862301	64	2.06904
15	.254756	65	1.99202
16	1.20373	66	1.81214
17	1.89558	67	1.44658
18	2.37541	68	.835259
19	2.25774	69	.103304
20	2.07075	70	-.624586
21	1.83166	71	-1.51585
22	1.51969	72	-2.32287
23	1.131	73	-3.1924
24	.63907		
25	.142799		
26	-.385122		
27	-1.10057		
28	-1.76039		
29	-2.42477		
30	-2.56491		
31	-1.88071		
32	-1.19268		
33	-.460652		
34	.133496		
35	.658076		
36	1.15947		
37	1.52321		
38	1.81689		
39	2.03925		
40	2.20075		
41	2.15948		
42	2.02399		
43	1.83998		
44	1.56573		
45	1.17416		
46	.646663		
47	.0929195		
48	-.499975		
49	-1.28234		
50	-2.00429		

TABLE C-12
CYLINDER MAP Hz

POINT	LEVEL dB	POINT	LEVEL dB
1	-22.3958	51	-14.8407
2	-21.5264	52	-14.1507
3	-19.8891	53	-13.9966
4	-18.3596	54	-14.5798
5	-17.2871	55	-15.6443
6	-16.2126	56	-16.4124
7	-14.9728	57	-14.5511
8	-15.9664	58	-11.431
9	-17.3763	59	-9.45411
10	-18.5577	60	-8.51358
11	-19.39	61	-8.20379
12	-19.8037	62	-8.1765
13	-18.8072	63	-7.15925
14	-18.1187	64	-6.89376
15	-18.1451	65	-7.13617
16	-16.1746	66	-7.67372
17	-14.3237	67	-9.55187
18	-13.1144	68	-10.5277
19	-11.4174	69	-13.2574
20	-11.8648	70	-11.6301
21	-12.71	71	-11.4592
22	-13.6401	72	-11.8692
23	-14.7201	73	-12.5506
24	-15.9353		
25	-16.7102		
26	-17.0615		
27	-16.052		
28	-16.8326		
29	-16.8784		
30	-16.3833		
31	-15.8157		
32	-15.8979		
33	-16.0949		
34	-16.722		
35	-15.6933		
36	-13.908		
37	-12.3984		
38	-11.4116		
39	-10.6395		
40	-10.3267		
41	-9.32179		
42	-9.54728		
43	-10.2469		
44	-11.3607		
45	-12.9636		
46	-14.8306		
47	-15.7711		
48	-15.4208		
49	-14.8844		
50	-14.6689		

TABLE C-13
NOSECONE MAP Ex

POINT	LEVEL dB	POINT	LEVEL dB
1	-38.5069	51	-39.6936
2	-43.3792	52	-41.9571
3	-44.1581	53	-49.1563
4	-36.9423	54	-47.2915
5	-34.5633	55	-41.6128
6	-34.2827	56	-38.6343
7	-34.3283	57	-37.0216
8	-34.7082	58	-36.258
9	-37.225	59	-35.9927
10	-44.0228	60	-36.0354
11	-42.1193	61	-36.3644
12	-37.3976	62	-36.7665
13	-36.6599	63	-37.3587
14	-41.4196	64	-36.7231
15	-43.8799	65	-36.1027
16	-37.3521	66	-35.4961
17	-34.9374	67	-35.3255
18	-34.5467	68	-35.5924
19	-35.0677	69	-36.5115
20	-34.9942	70	-38.1742
21	-35.179	71	-41.2632
22	-35.8122	72	-49.36
23	-37.0175	73	-44.9048
24	-39.08		
25	-42.5469		
26	-46.0528		
27	-43.515		
28	-39.5525		
29	-37.0798		
30	-38.0692		
31	-40.9997		
32	-45.5707		
33	-46.0765		
34	-41.6505		
35	-38.6538		
36	-36.896		
37	-35.9771		
38	-35.4734		
39	-35.3936		
40	-35.5591		
41	-36.1616		
42	-35.8293		
43	-35.6762		
44	-35.8886		
45	-36.5028		
46	-37.7356		
47	-40.1168		
48	-44.3631		
49	-49.0811		
50	-44.3265		

TABLE C-14
NOSECONE MAP E_y

POINT	LEVEL dB	POINT	LEVEL dB
1	-47.5948	51	-42.1042
2	-46.8489	52	-40.6714
3	-46.9898	53	-44.6552
4	-48.0724	54	-47.4574
5	-49.3648	55	-46.263
6	-50.7511	56	-44.9632
7	-51.4004	57	-44.3711
8	-50.9	58	-44.3643
9	-50.1995	59	-44.38
10	-49.1238	60	-45.7637
11	-46.9548	61	-46.743
12	-43.6636	62	-47.7761
13	-42.1865	63	-46.2975
14	-44.8555	64	-45.0906
15	-48.4062	65	-43.886
16	-51.6325	66	-42.7218
17	-52.4689	67	-41.6335
18	-52.4844	68	-40.9874
19	-52.5303	69	-41.0213
20	-52.6774	70	-41.9806
21	-52.9899	71	-43.4484
22	-53.2282	72	-43.8279
23	-53	73	-38.6794
24	-52.2726		
25	-50.5787		
26	-48.4197		
27	-46.2227		
28	-44.1566		
29	-42.5318		
30	-42.6649		
31	-44.9848		
32	-48.4971		
33	-51.7411		
34	-52.8272		
35	-52.4226		
36	-51.6		
37	-51.4106		
38	-51.4004		
39	-51.4621		
40	-51.504		
41	-49.3536		
42	-49.2945		
43	-48.7839		
44	-48.3838		
45	-48.4062		
46	-48.9868		
47	-50.7		
48	-52.6344		
49	-50.4499		
50	-45.4272		

SEE APPENDIX C

C.1 INTRODUCTION FOR EXPLANATION
FOR TABLE C-15

TABLE C-16
NOSECONE MAP Hx

POINT	LEVEL dB	POINT	LEVEL dB
1	-30.0179	51	-33.5431
2	-30.2874	52	-34.7707
3	-31.3261	53	-36.5399
4	-33.1793	54	-41.7491
5	-35.249	55	-43.0114
6	-37.1144	56	-39.4153
7	-35.8317	57	-37.205
8	-35.3022	58	-36.1581
9	-33.5334	59	-35.6768
10	-32.8041	60	-35.7038
11	-40.935	61	-36.2575
12	-34.5441	62	-36.9725
13	-35.6396	63	-37.109
14	-41.1213	64	-36.2046
15	-50.1662	65	-35.3911
16	-41.2245	66	-34.8951
17	-38.8246	67	-34.7932
18	-39.1511	68	-34.9958
19	-38.0408	69	-35.7573
20	-37.6528	70	-37.607
21	-37.7599	71	-41.7689
22	-38.4925	72	-42.7031
23	-40.2729	73	-36.7017
24	-43		
25	-46.0345		
26	-42.0187		
27	-37.2497		
28	-34.0388		
29	-32.7334		
30	-32.7429		
31	-33.8927		
32	-37.2266		
33	-42.2529		
34	-44.8597		
35	-41.5516		
36	-39.025		
37	-37.637		
38	-37.1035		
39	-37.1958		
40	-37.5254		
41	-37.1965		
42	-36.5945		
43	-36.3121		
44	-36.4955		
45	-37.2359		
46	-38.9655		
47	-42.5313		
48	-44.4544		
49	-39.6049		
50	-35.294		

TABLE C-17
NOSECONE MAP ' Hy

POINT	LEVEL dB	POINT	LEVEL dB
1	-7.09672	51	-5.76143
2	-7.38437	52	-5.02729
3	-8.22183	53	-4.53486
4	-9.65016	54	-4.75369
5	-11.5221	55	-5.53064
6	-13.5365	56	-6.5181
7	-13.3558	57	-7.77522
8	-11.3846	58	-9.06632
9	-9.65953	59	-10.345
10	-8.34602	60	-11.7193
11	-7.58781	61	-13.0389
12	-7.34128	62	-14.3539
13	-7.25014	63	-14.0015
14	-7.41863	64	-12.6938
15	-8.26045	65	-11.43
16	-9.51826	66	-10.0759
17	-11.2088	67	-8.7845
18	-13.2185	68	-7.57461
19	-13.5146	69	-6.35479
20	-12.3685	70	-5.40333
21	-11.3369	71	-4.66619
22	-10.2597	72	-4.51297
23	-9.38426	73	-5.10966
24	-8.47558		
25	-7.76721		
26	-7.21153		
27	-6.75249		
28	-6.59485		
29	-6.70081		
30	-6.29924		
31	-6.10896		
32	-6.25778		
33	-6.69291		
34	-7.44785		
35	-8.28307		
36	-9.29734		
37	-10.3		
38	-11.4789		
39	-12.6018		
40	-13.8163		
41	-14.1864		
42	-12.9314		
43	-11.7045		
44	-10.4236		
45	-9.27743		
46	-8.10852		
47	-7.11088		
48	-6.18875		
49	-5.64322		
50	-5.46741		

SEE APPENDIX C

C.1 INTRODUCTION FOR EXPLANATION

FOR TABLE C-18

TABLE C-19
NOSECONE MAP 'EX

POINT	LEVEL dB	POINT	LEVEL dB
1	-44.6443	51	-35.0366
2	-42.1304	52	-31.8713
3	-34.2685	53	-34.0152
4	-31.482	54	-37.7
5	-30.9523	55	-24.5448
6	-31.6349	56	-23.9639
7	-32.4598	57	-23.8672
8	-31.9341	58	-24.3145
9	-32.7502	59	-25.197
10	-35.4812	60	-26.0829
11	-40.9184	61	-27.7374
12	-43.2134	62	-29.2182
13	-42.3141	63	-28.1508
14	-39.0967	64	-26.4881
15	-34.6293	65	-24.9723
16	-31.9362	66	-23.6141
17	-31.5344	67	-22.3634
18	-32.2712	68	-21.5383
19	-30.9941	69	-21.2787
20	-30.3306	70	-21.0282
21	-29.7401	71	-23.4161
22	-29.4423	72	-29.5897
23	-29.4675	73	-27.5391
24	-29.9713		
25	-31.033		
26	-33.0526		
27	-36.2552		
28	-39.9322		
29	-40.098		
30	-37.6776		
31	-38.7917		
32	-34.0627		
33	-30.6843		
34	-28.8771		
35	-28.5776		
36	-28.6247		
37	-28.9198		
38	-28.8072		
39	-29.2181		
40	-30.1934		
41	-29.263		
42	-28.8115		
43	-28.065		
44	-27.3391		
45	-26.7567		
46	-26.6451		
47	-27.2946		
48	-28.9819		
49	-31.1818		
50	-37.3573		

TABLE C-20
NOSECONE MAP E_y

POINT	LEVEL dB	POINT	LEVEL dB
1	-41.5183	51	-34.1156
2	-43.8255	52	-32.9964
3	-45.1049	53	-33.2785
4	-47.4923	54	-33.5802
5	-49.36	55	-34.2707
6	-50.4062	56	-35.4204
7	-52.2873	57	-37.2274
8	-49.8229	58	-39.4831
9	-45.6092	59	-42.1761
10	-42.6346	60	-45.144
11	-41.4295	61	-48.207
12	-42.8357	62	-50.9987
13	-39.0133	63	-52.6991
14	-37.6812	64	-51.0376
15	-38.8143	65	-48.3395
16	-42.1762	66	-45.8483
17	-47.0413	67	-43.4243
18	-51.8017	68	-41.3455
19	-51.6162	69	-39.7285
20	-49.1078	70	-38.5741
21	-45.8645	71	-37.7114
22	-43.1639	72	-36.4523
23	-40.5828	73	-33.5904
24	-38.3896		
25	-36.7459		
26	-35.5113		
27	-35.0766		
28	-35.2179		
29	-35.8179		
30	-34.9859		
31	-34.5252		
32	-34.4509		
33	-34.9393		
34	-36.2331		
35	-38.0751		
36	-40.4088		
37	-43.1307		
38	-46.3827		
39	-49.5383		
40	-52.5817		
41	-52.3921		
42	-49.6474		
43	-45.9858		
44	-43.0915		
45	-40.2873		
46	-37.8571		
47	-35.9879		
48	-34.5365		
49	-33.8983		
50	-33.7983		

SEE APPENDIX C

C.1 INTRODUCTION FOR EXPLANATION

FOR TABLE C-21

TABLE C-22
NOSECONE MAP Hx

POINT	LEVEL dB	POINT	LEVEL dB
1	-20.6751	51	-19.3737
2	-22.5369	52	-19.3729
3	-23.8444	53	-19.3730
4	-25.1841	54	-19.3730
5	-26.7393	55	-19.7359
6	-27.6013	56	-20.1368
7	-27.4409	57	-21.1421
8	-25.7779	58	-22.2623
9	-24.1414	59	-23.2959
10	-22.8862	60	-24.3351
11	-21.5188	61	-25.5559
12	-20.4271	62	-26.6025
13	-19.4495	63	-27.4468
14	-20.3305	64	-28.2175
15	-21.7752	65	-24.7465
16	-23.324	66	-23.8749
17	-24.4613	67	-22.8724
18	-26.429	68	-21.9768
19	-26.0732	69	-21.1279
20	-24.7231	70	-20.46
21	-24.0328	71	-20.1097
22	-23.1849	72	-19.924
23	-22.3763	73	-20.5686
24	-21.6918		
25	-20.9421		
26	-20.2245		
27	-19.6647		
28	-18.9134		
29	-18.9542		
30	-18.5621		
31	-19.0214		
32	-19.4605		
33	-19.9848		
34	-20.6393		
35	-21.4439		
36	-22.2507		
37	-23.1255		
38	-24.0494		
39	-25.1841		
40	-26.3167		
41	-26.3456		
42	-24.92		
43	-24.1414		
44	-23.155		
45	-22.1643		
46	-21.3464		
47	-20.4403		
48	-19.8461		
49	-19.4605		
50	-18.9679		

TABLE C-23
NOSECONE MAP Hy

POINT	LEVEL dB	POINT	LEVEL dB
1	-9.8068	51	-8.9874
2	-8.62131	52	-8.63558
3	-8.8873	53	-8.13481
4	-10.0767	54	-8.04783
5	-11.8441	55	-8.30131
6	-13.8382	56	-8.44526
7	-13.7614	57	-8.21815
8	-11.6426	58	-9.99738
9	-10.0274	59	-10.9194
10	-8.89626	60	-11.9426
11	-8.53812	61	-12.9946
12	-9.56723	62	-14.1104
13	-9.29218	63	-14.3237
14	-8.36121	64	-13.2347
15	-8.76987	65	-12.0234
16	-9.9966	66	-11.0857
17	-11.6541	67	-10.124
18	-13.5926	68	-9.54958
19	-13.839	69	-8.75746
20	-13.6416	70	-8.16522
21	-11.6104	71	-7.82157
22	-10.7525	72	-7.81661
23	-9.96288	73	-8.279
24	-9.28186		
25	-8.65988		
26	-8.25405		
27	-8.10655		
28	-8.26213		
29	-8.94658		
30	-8.75019		
31	-8.0941		
32	-7.97062		
33	-8.15285		
34	-8.56348		
35	-9.2087		
36	-9.92474		
37	-10.7507		
38	-11.7534		
39	-12.7208		
40	-13.7917		
41	-13.9207		
42	-12.8692		
43	-11.7374		
44	-10.8525		
45	-9.99188		
46	-9.22253		
47	-8.56206		
48	-8.12823		
49	-7.83646		
50	-8.15919		

SEE APPENDIX C

C.1 INTRODUCTION FOR EXPLANATION

FOR TABLE C-24

TABLE C-25
NOSECONE MAP Ex

POINT	LEVEL dB	POINT	LEVEL dB
1	-40.7694	51	-37.3089
2	-37.3604	52	-38.3944
3	-34.0531	53	-36.6264
4	-30.507	54	-34.9312
5	-26.4528	55	-33.0606
6	-19.0602	56	-31.2
7	-16.6825	57	-29.3236
8	-22.5213	58	-27.7563
9	-27.4701	59	-25.6694
10	-30.7505	60	-23.0647
11	-34.4114	61	-20.3608
12	-37.99	62	-17.3933
13	-36.6353	63	-18.5751
14	-32.9811	64	-21.9615
15	-29.2125	65	-24.7507
16	-25.7301	66	-27.4845
17	-21.0301	67	-26.946
18	-15.8655	68	-30.8855
19	-15.8397	69	-32.7537
20	-18.3672	70	-34.4941
21	-20.8257	71	-36.2344
22	-23.3094	72	-37.9058
23	-25.5593	73	-39.64
24	-27.7186		
25	-29.0121		
26	-30.8872		
27	-32.7759		
28	-34.5838		
29	-36.4299		
30	-36.7875		
31	-34.9507		
32	-33.158		
33	-31.2724		
34	-29.4073		
35	-28		
36	-25.9806		
37	-23.653		
38	-21.2589		
39	-18.7172		
40	-16.0816		
41	-16.5006		
42	-19.2879		
43	-21.361		
44	-24.3531		
45	-26.6451		
46	-28.94		
47	-30.1115		
48	-31.8659		
49	-33.7154		
50	-35.4984		

TABLE C-26
NOSECONE MAP Ey

POINT	LEVEL dB	POINT	LEVEL dB
1	-47.8576	51	-53.2567
2	-43.1806	52	-50.6794
3	-36.989	53	-47.4613
4	-30.581	54	-44.7726
5	-24.4912	55	-42.8532
6	-20.7359	56	-39.2001
7	-27.5433	57	-36.4586
8	-28.7832	58	-33.7363
9	-33.2031	59	-31.3704
10	-38.7313	60	-29.51
11	-44.1345	61	-26.2049
12	-48.9971	62	-28.3179
13	-54.6556	63	-24.7422
14	-49.6003	64	-25.8728
15	-44.6405	65	-26.4583
16	-39.8481	66	-29.1229
17	-36.6726	67	-31.8801
18	-35.4842	68	-34.7478
19	-41.942	69	-37.7505
20	-43.9265	70	-40.6827
21	-47.1461	71	-43.6372
22	-49.9948	72	-46.4454
23	-53.0128	73	-49.7591
24	-56.2327		
25	-57.0096		
26	-57.0096		
27	-57.0096		
28	-57.0096		
29	-57.0096		
30	-57.0096		
31	-55.3642		
32	-52.6344		
33	-49.7431		
34	-46.9454		
35	-44.353		
36	-41.9944		
37	-40.0575		
38	-38.6153		
39	-37.1105		
40	-36.803		
41	-32.3771		
42	-32.2348		
43	-33.3319		
44	-34.8558		
45	-36.8754		
46	-39.2227		
47	-41.8683		
48	-44.5388		
49	-47.4152		
50	-50.3095		

TABLE C-27
NOSECONE MAP Ez

POINT	LEVEL dB	POINT	LEVEL dB
1	-54.1701	51	-60.7588
2	-55.2276	52	-60.7588
3	-53.4749	53	-60.7588
4	-45.1257	54	-60.7588
5	-34.7197	55	-60.7588
6	-44.5314	56	-60.7588
7	-40.8134	57	-60.7588
8	-48.5811	58	-60.7588
9	-54.1701	59	-60.7588
10	-56.6	60	-60.7588
11	-54.5432	61	-60.7588
12	-54.5432	62	-60.7588
13	-48.6284	63	-60.7588
14	-48.6332	64	-60.7588
15	-48.6189	65	-60.7588
16	-48.6189	66	-60.7588
17	-48.6237	67	-60.7588
18	-48.5811	68	-60.7588
19	-60.7588	69	-60.7588
20	-60.7588	70	-60.7588
21	-60.7588	71	-60.7588
22	-60.7588	72	-60.7588
23	-60.7588	73	-60.7588
24	-60.7588		
25	-60.7588		
26	-60.7588		
27	-60.7588		
28	-60.7588		
29	-60.7588		
30	-60.7588		
31	-60.7588		
32	-60.7588		
33	-60.7588		
34	-60.7588		
35	-60.7588		
36	-60.7588		
37	-60.7588		
38	-60.7588		
39	-60.7588		
40	-60.7588		
41	-60.7588		
42	-60.7588		
43	-60.7588		
44	-60.7588		
45	-60.7588		
46	-60.7588		
47	-60.7588		
48	-60.7588		
49	-60.7588		
50	-60.7588		

TABLE C-28
NOSECONE MAP Hx

POINT	LEVEL dB	POINT	LEVEL dB
1	-46.0172	51	-30.1621
2	-44.4739	52	-29.5339
3	-41.145	53	-27.4292
4	-34.1774	54	-25.2702
5	-22.4056	55	-23.3668
6	-11.7791	56	-21.354
7	-13.1334	57	-19.3954
8	-18.682	58	-17.6269
9	-25.5559	59	-15.9508
10	-31.6371	60	-14.6455
11	-36.4082	61	-13.6083
12	-41.4564	62	-12.8705
13	-35.0168	63	-12.6925
14	-30.5826	64	-13.2185
15	-26.1391	65	-14.0788
16	-21.5571	66	-15.4628
17	-17.2	67	-17.2179
18	-13.3069	68	-19.8268
19	-14.254	69	-21.0785
20	-15.3671	70	-23.1108
21	-16.4874	71	-25.2702
22	-18.1451	72	-27.2213
23	-19.8783	73	-29.3411
24	-21.7752		
25	-23.773		
26	-25.6706		
27	-27.7927		
28	-29.9386		
29	-32.1657		
30	-31.3783		
31	-29.2619		
32	-27.1649		
33	-24.9462		
34	-23.2681		
35	-21.4073		
36	-19.5943		
37	-17.9575		
38	-16.2844		
39	-15.0546		
40	-13.9416		
41	-13.487		
42	-14.2705		
43	-15.3758		
44	-16.6172		
45	-18.2487		
46	-19.9909		
47	-21.9082		
48	-23.8898		
49	-25.8814		
50	-28.0184		

TABLE C-29
NOSECONE MAP Hy

POINT	LEVEL dB	POINT	LEVEL dB
1	-15.0228	51	-10.1474
2	-15.0466	52	-11.534
3	-15.0626	53	-11.537
4	-15.0626	54	-11.539
5	-15.052	55	-11.532
6	-15.0573	56	-11.53
7	-10.5899	57	-11.532
8	-10.5861	58	-11.533
9	-10.5899	59	-11.531
10	-10.5899	60	-11.53
11	-10.5852	61	-11.533
12	-10.5908	62	-11.53
13	-8.96391	63	-13.5703
14	-8.95958	64	-13.5703
15	-8.95785	65	-13.5689
16	-8.96044	66	-13.5689
17	-8.95611	67	-13.5689
18	-8.96044	68	-13.5718
19	-8.89327	69	-13.563
20	-8.89402	70	-13.56
21	-8.89028	71	-13.5644
22	-8.88878	72	-13.5659
23	-8.88878	73	-13.563
24	-8.89028		
25	-8.88507		
26	-8.88133		
27	-8.88356		
28	-8.8858		
29	-8.88208		
30	-9.40258		
31	-9.40107		
32	-9.40484		
33	-9.40258		
34	-9.39957		
35	-9.39957		
36	-9.40107		
37	-9.40258		
38	-9.40333		
39	-9.3958		
40	-9.39731		
41	-10.1566		
42	-10.1557		
43	-10.149		
44	-10.1474		
45	-10.1541		
46	-10.1524		
47	-10.1499		
48	-10.1465		
49	-10.1465		
50	-10.149		

TABLE C-30

NOSECONE MAP Hz

POINT	LEVEL dB	POINT	LEVEL dB
1	-18.9405	51	-69.232
2	-14.7739	52	-69.232
3	-10.4628	53	-69.232
4	-6.05529	54	-69.232
5	-1.45109	55	-69.232
6	2.01614	56	-69.232
7	-4.85401	57	-69.232
8	-5.85684	58	-69.232
9	-9.15066	59	-69.232
10	-12.9987	60	-69.232
11	-17.2119	61	-69.232
12	-21.3846	62	-69.232
13	-69.232	63	-69.232
14	-69.232	64	-69.232
15	-69.232	65	-69.232
16	-69.232	66	-69.232
17	-69.232	67	-69.232
18	-69.232	68	-69.232
19	-69.232	69	-69.232
20	-69.232	70	-69.232
21	-69.232	71	-69.232
22	-69.232	72	-69.232
23	-69.232	73	-69.232
24	-69.232		
25	-69.232		
26	-69.232		
27	-69.232		
28	-69.232		
29	-69.232		
30	-69.232		
31	-69.232		
32	-69.232		
33	-69.232		
34	-69.232		
35	-69.232		
36	-69.232		
37	-69.232		
38	-69.232		
39	-69.232		
40	-69.232		
41	-69.232		
42	-69.232		
43	-69.232		
44	-69.232		
45	-69.232		
46	-69.232		
47	-69.232		
48	-69.232		
49	-69.232		
50	-69.232		

TABLE C-31
NOSECONE MAP Ex

POINT	LEVEL dB	POINT	LEVEL dB
1	-33.9815	51	-37.896
2	-29.5212	52	-38.8756
3	-25.21	53	-37.6869
4	-20.3268	54	-36.4359
5	-15.7	55	-35.1298
6	-11.6029	56	-33.8864
7	-14.3919	57	-32.7127
8	-17.8816	58	-31.4152
9	-21.8487	59	-30.2658
10	-26.1125	60	-28.9
11	-30.2317		
12	-34.5882		
13	-35.1477		
14	-31.1889		
15	-27.4845		
16	-23.4739		
17	-19.2848		
18	-14.7747		
19	-15.569		
20	-18.2045		
21	-20.8285		
22	-23.3494		
23	-25.8098		
24	-27.6356		
25	-29.2594		
26	-31.0724		
27	-32.8814		
28	-34.5855		
29	-36.3054		
30	-37.049		
31	-35.5356		
32	-34.0033		
33	-32.4539		
34	-30.764		
35	-29.0722		
36	-27.2946		
37	-25.1221		
38	-22.4936		
39	-19.552		
40	-16.4509		
41	-17.9873		
42	-21.7039		
43	-25.0484		
44	-27.7		
45	-29.2493		
46	-30.9223		
47	-32.4272		
48	-33.7951		
49	-35.1578		
50	-36.5891		

TABLE C-32

NOSECONE MAP Ey

POINT	LEVEL dB	POINT	LEVEL dB
1	-60.7588	51	-60.7588
2	-50.0255	52	-60.7588
3	-44.9813	53	-60.7588
4	-40.0903	54	-60.7588
5	-35.5217	55	-52.628
6	-31.5333	56	-50.1292
7	-37.4125	57	-47.5036
8	-38.2329	58	-44.911
9	-41.6739	59	-44.0133
10	-45.7563	60	-42.3251
11	-49.6933	61	-40.8461
12	-52.5433	62	-41.9684
13	-52.628	63	-44.876
14	-50.0656	64	-41.4595
15	-46.3144	65	-42.7242
16	-42.8614	66	-45.232
17	-41.001	67	-47.989
18	-39.1933	68	-50.7239
19	-40.5655	69	-52.5264
20	-40.6295	70	-60.7588
21	-41.5067	71	-60.7588
22	-42.7738	72	-60.7588
23	-44.3024	73	-60.7588
24	-46.0309		
25	-47.7916		
26	-49.4537		
27	-51.2164		
28	-60.7588		
29	-60.7588		
30	-60.7588		
31	-60.7588		
32	-52.4677		
33	-50.3885		
34	-48.5031		
35	-46.6501		
36	-44.8412		
37	-43.9818		
38	-42.7242		
39	-41.578		
40	-40.8242		
41	-36.515		
42	-42.3772		
43	-44.2373		
44	-45.1958		
45	-46.4806		
46	-47.989		
47	-49.3948		
48	-50.5882		
49	-52.2123		
50	-60.7588		

TABLE C-33
NOSECONE MAP EZ

POINT	LEVEL dB	POINT	LEVEL dB
1	-47.788	51	-60.7588
2	-45.1398	52	-60.7588
3	-40.8139	53	-60.7588
4	-34.1419	54	-60.7588
5	-24.9815	55	-60.7588
6	-14.1491	56	-60.7588
7	-17.4122	57	-60.7588
8	-23.7123	58	-60.7588
9	-31.3864	59	-60.7588
10	-38.2297	60	-60.7588
11	-43.2457	61	-60.7588
12	-47.664	62	-60.7588
13	-46.6262	63	-60.7588
14	-42.6582	64	-60.7588
15	-37.8627	65	-60.7588
16	-32.5347	66	-60.7588
17	-27.4138	67	-60.7588
18	-23.6335	68	-60.7588
19	-60.7588	69	-60.7588
20	-60.7588	70	-60.7588
21	-60.7588	71	-60.7588
22	-60.7588	72	-60.7588
23	-60.7588	73	-60.7588
24	-60.7588		
25	-60.7588		
26	-60.7588		
27	-60.7588		
28	-60.7588		
29	-60.7588		
30	-60.7588		
31	-60.7588		
32	-60.7588		
33	-60.7588		
34	-60.7588		
35	-60.7588		
36	-60.7588		
37	-60.7588		
38	-60.7588		
39	-60.7588		
40	-60.7588		
41	-60.7588		
42	-60.7588		
43	-60.7588		
44	-60.7588		
45	-60.7588		
46	-60.7588		
47	-60.7588		
48	-60.7588		
49	-60.7588		
50	-60.7588		

TABLE C-34
NOSECONE MAP Hx

POINT	LEVEL dB	POINT	LEVEL dB
1	-24.493	51	-25.1026
2	-24.493	52	-25.2735
3	-24.4457	53	-26.3088
4	-24.4771	54	-26.3249
5	-24.4771	55	-26.3368
6	-24.4457	56	-26.3419
7	-25.5141	57	-26.35
8	-25.5141	58	-26.3597
9	-25.5141	59	-26.3774
10	-25.5141	60	-26.3729
11	-25.455	61	-26.4008
12	-25.455	62	-26.3954
13	-25.241	63	-28.3318
14	-25.2123	64	-28.2996
15	-25.241	65	-28.3002
16	-25.241	66	-28.7544
17	-25.241	67	-28.3774
18	-25.2702	68	-28.7559
19	-24.6815	69	-28.7578
20	-24.6633	70	-28.7544
21	-24.6453	71	-28.7556
22	-24.6275	72	-28.7759
23	-24.6275	73	-28.7543
24	-24.6453		
25	-24.7943		
26	-24.6815		
27	-24.6633		
28	-24.6633		
29	-24.6275		
30	-24.4771		
31	-24.5091		
32	-24.493		
33	-24.493		
34	-24.5091		
35	-24.5091		
36	-24.4771		
37	-24.5091		
38	-24.5091		
39	-24.493		
40	-24.4771		
41	-25.0763		
42	-25.0763		
43	-25.0763		
44	-25.1026		
45	-25.0763		
46	-25.1026		
47	-25.0763		
48	-25.1026		
49	-25.0763		
50	-25.0763		

TABLE C-35
NOSECONE MAP - Hy

POINT	LEVEL dB	POINT	LEVEL dB
1	-18.7127	51	-17.5613
2	-14.4255	52	-18.1112
3	-10.3938	53	-16.0386
4	-6.01558	54	-13.969
5	-1.67675	55	-11.9163
6	2.28926	56	-9.81818
7	1.78348	57	-7.73961
8	-1.71663	58	-5.67595
9	-5.82262	59	-3.61537
10	-10.025	60	-1.52744
11	-14.1864	61	.148922
12	-18.3196	62	1.73127
13	-17.5906	63	1.91751
14	-13.4596	64	.314866
15	-9.34187	65	-1.60741
16	-5.33361	66	-3.63081
17	-1.56878	67	-5.73296
18	1.50096	68	-7.85642
19	1.53724	69	-9.95117
20	.249728	70	-12.0683
21	-1.33715	71	-14.144
22	-3.05145	72	-16.2126
23	-4.66818	73	-18.3156
24	-6.8095		
25	-8.8198		
26	-10.8295		
27	-12.9115		
28	-15.0096		
29	-17.0773		
30	-17.2358		
31	-15.15		
32	-13.0545		
33	-10.9664		
34	-8.94572		
35	-6.94022		
36	-4.96025		
37	-3.12814		
38	-1.38885		
39	.212475		
40	1.58819		
41	1.65974		
42	.304297		
43	-1.32125		
44	-3.14642		
45	-5.07845		
46	-7.18068		
47	-9.23273		
48	-11.3104		
49	-13.3685		
50	-15.4607		

TABLE C-36

POINT	NOSECONE LEVEL dB	Hz	POINT	LEVEL dB
1	-34.9216	51		-69.232
2	-30.3935	52		-69.232
3	-25.5082	53		-69.232
4	-21.2059	54		-69.232
5	-16.4684	55		-69.232
6	-12.5729	56		-69.232
7	-13.5483	57		-69.232
8	-17.5128	58		-69.232
9	-21.3312	59		-69.232
10	-25.5491	60		-69.232
11	-30.2959	61		-69.232
12	-34.8064	62		-69.232
13	-35.3813	63		-69.232
14	-30.6736	64		-69.232
15	-25.936	65		-69.232
16	-21.9082	66		-69.232
17	-18.2879	67		-69.232
18	-13.9593	68		-69.232
19	-69.232	69		-69.232
20	-69.232	70		-69.232
21	-69.232	71		-69.232
22	-69.232	72		-69.232
23	-69.232	73		-69.232
24	-69.232			
25	-69.232			
26	-69.232			
27	-69.232			
28	-69.232			
29	-69.232			
30	-69.232			
31	-69.232			
32	-69.232			
33	-69.232			
34	-69.232			
35	-69.232			
36	-69.232			
37	-69.232			
38	-69.232			
39	-69.232			
40	-69.232			
41	-69.232			
42	-69.232			
43	-69.232			
44	-69.232			
45	-69.232			
46	-69.232			
47	-69.232			
48	-69.232			
49	-69.232			
50	-69.232			

APPENDIX D

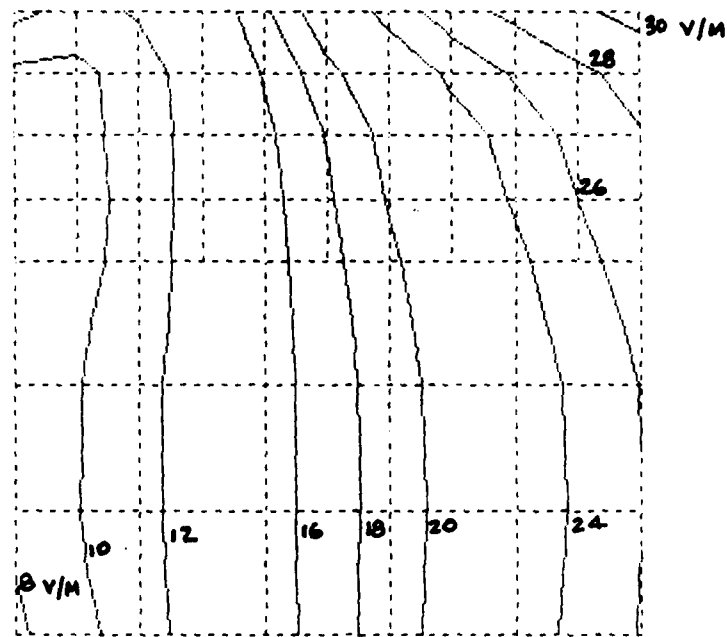
RESULTS OF E-FIELD PERTURBATION TEST CONDUCTED IN MISSILE (NOSECONE REMOVED)

D.1 INTRODUCTION

A test was conducted in the missile nosecone area, with the nosecone removed to assess the effects of E-field perturbations due to the presence of another E-field probe, located at the grid centre, 1 cm away from the plane of the grid.

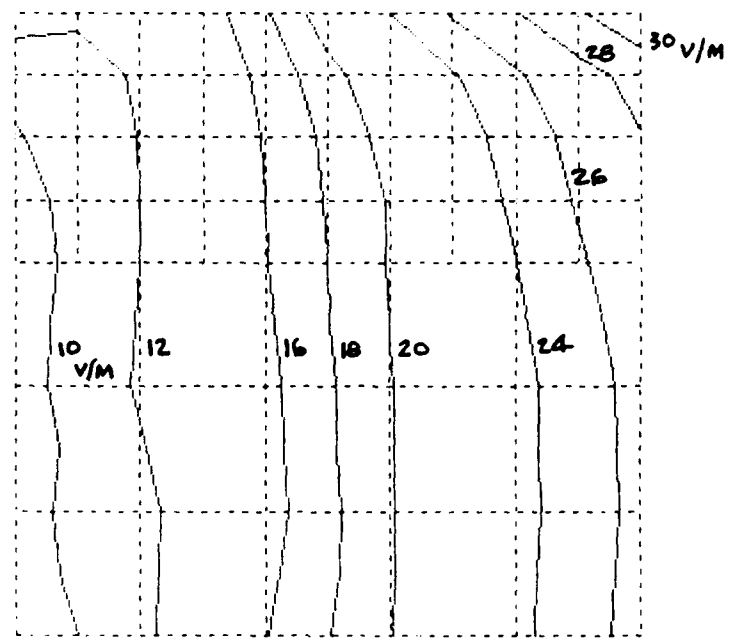
The resulting contours are shown in Figs. D-1, D-2. The perturbations caused are negligible when referred to the incident carrier level of 43.65 v/m.

No similar test was conducted for the H-field probe due to its smaller size and the absence of any significant amount of metallic material.



Probe and Grid Orientation per Test No. 19
of Table A-1, Appendix A

FIG. D-1 NO PERTURBING PROBE IN PLACE



Probe and Grid Orientation per Test No. 19
of Table A-1, Appendix A

FIG. D-2 PERTURBING PROBE INSTALLED

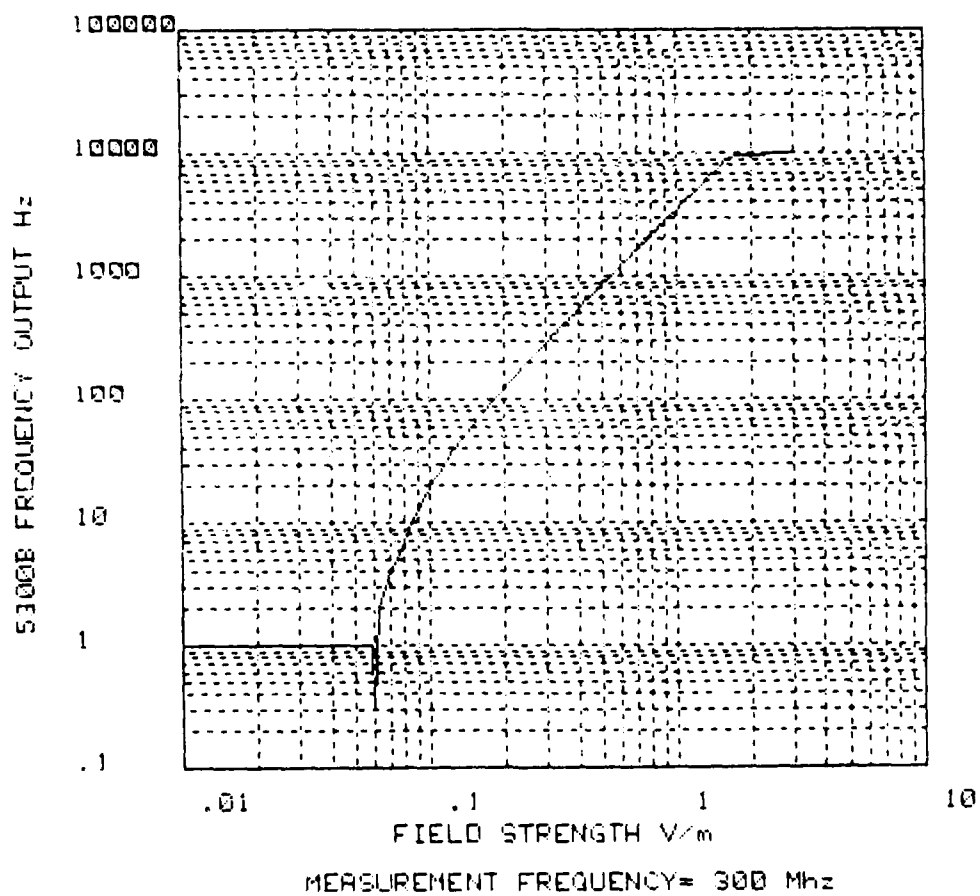
APPENDIX E

PROBE CALIBRATION CURVES AND LOOKUP TABLE

E.1 INTRODUCTION

This appendix contains E-field and H-field probe calibration data obtained at 300 MHz. All data is based upon the use of 100% amplitude modulation, except pages E-23 to E-27, which show the effect of using 50% A.M. for the E-field probe.

E-Field Probe Calibration, low range,
100% Modulation
Run 1 of 2: 0.01 v/m to 3 v/m



E-Field 100% A.M.

FREQUENCY= 300 Mhz

LEVEL	v/m	READING	Hz	STD DEV	Hz
.01		1		1.05409255343	
1.03514216669E-02		1		1.05409255343	
1.07151330525E-02		1		1.05409255343	
1.10917481526E-02		1		1.05409255343	
1.14815362157E-02		1		1.05409255343	
1.18850222744E-02		1		1.05409255343	
1.23026877084E-02		1		1.05409255343	
.01273583081		1		1.05409255343	
1.31825673857E-02		1		1.05409255343	
1.36458313661E-02		1		1.05409255343	
1.41153754465E-02		1		1.05409255343	
1.46217717445E-02		1		1.05409255343	
1.51156124851E-02		1		1.05409255343	
1.56675107015E-02		1		1.05409255343	
.015213100974		1		1.05409255343	
1.67980401614E-02		1		1.05409255343	
1.73730082884E-02		1		1.05409255343	
1.799827091516E-02		1		1.05409255343	
.013620871367		1		1.05409255343	
1.82752481321E-02		1		1.05409255343	
1.88516131506E-02		1		1.05409255343	
2.06538015583E-02		1		1.05409255343	
2.13796208955E-02		1		1.05409255343	
2.21309470964E-02		1		1.05409255343	
2.29086765277E-02		1		1.05409255343	
2.37137370571E-02		1		1.05409255343	
2.45470891581E-02		1		1.05409255343	
.025409727056		1		1.05409255343	
2.63026799191E-02		1		1.05409255343	
2.72270130814E-02		1		1.05409255343	
2.81838293125E-02		1		1.05409255343	
2.91742701399E-02		1		1.05409255343	
.01995172046E-02		1		1.05409255343	
.031260793671		1		1.05409255343	
3.23593656927E-02		1		1.05409255343	
3.34965439171E-02		1		1.05409255343	
3.46736850456E-02		1		1.05409255343	
3.58921934644E-02		1		1.05409255343	
3.71535229101E-02		1		1.05409255343	
3.84591782046E-02		1		1.05409255343	
3.98107170558E-02		1		1.05409255343	
4.12097519094E-02		1		1.05409255343	
4.26579518787E-02		1		1.05409255343	
.044157044736		1		1.05409255343	
4.57088189609E-02		1		1.05409255343	
4.73151258965E-02		1		1.05409255343	
4.89778619352E-02		1		1.05409255343	

E-Field 100% A.M.

v/m	Hz	Hz
5.06990708279E-02	1	1.05409255343
5.24807460259E-02	1	1.05409255343
5.43250331504E-02	1	1.05409255343
5.62341325187E-02	1	1.05409255343
5.82103217767E-02	1	1.05409255343
6.02559586081E-02	.3	.67494855771
6.23734835482E-02	2	.666666666666
6.45654229044E-02	2.6	.966091783079
6.68343917557E-02	3	.942809041582
6.91830970931E-02	4	.47140452079
7.16143410216E-02	4.3	.67494855771
7.41310241296E-02	5.3	.67494855771
7.67361489387E-02	6.2	1.22927259434
7.94328234702E-02	7.6	.966091783079
8.22242649958E-02	8.9	.87559503577
8.51138033188E-02	9.9	.737864787372
8.81048872987E-02	12.1	1.19721899976
9.12010939367E-02	13.4	.69920589878
9.44060876301E-02	15.4	.516397779493
9.77237220966E-02	17.6	.516397779493
.1	19.7	.94868329805
.103514216669	22.5	.849836585598
.107151930525	24.5	.527046276694
.110917481526	26.5	.971625315807
.114815362157	30	1.56347191992
.118850222744	32.9	1.28668393772
.123026877084	36.7	.94868329805
.1273503081	40.1	.737864787372
.131825673857	44.7	.823272602348
.136458313661	48.8	.788810637746
.141253754465	52.6	1.42984078595
.146217717445	56.4	1.57762127546
.151356124851	62.8	1.13529242435
.156675107015	68.5	1.50923085636
.16218100974	74.6	1.34989711541
.1673800401814	81.2	1.6865480854
.173780082884	89.2	1.03279555895
.179887091516	95.2	1.31656117723
.18620871367	102.8	1.39841179757
.192177141321	111.6	.955551792073
.199526231506	121.1	1.19721899976
.206538015583	132	1.49071198499
.213796208955	142.2	1.13529242435
.221309470964	151.1	1.10050493465
.229086765277	163.7	1.41813649244
.237137370571	176.4	1.07496769979
.245470891581	190.9	1.10050493465
.25409727056	208.1	1.10050493465
.263026799191	224.2	1.81352940114
.272270130814	242.7	1.49443411811
.281838293125	257.4	1.34989711541
.291742701399	276.7	1.56702123648
.301995172046	298.3	1.94630684273
.31260793671	322.4	2.27058484879

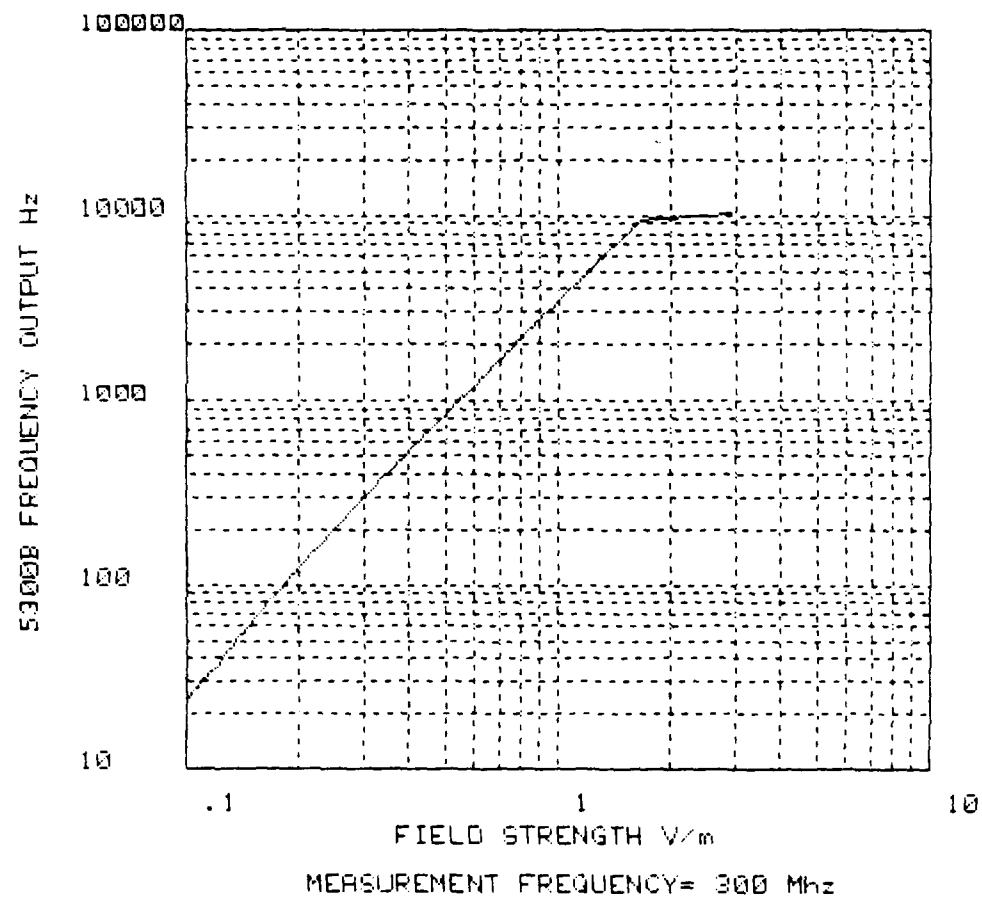
E-Field 100% A.M.

.323593656927	348.4	1.50554530539
.334965439171	375.2	2.57336787541
.346736850456	404.7	1.56702123648
.358921934644	426.9	1.96920739837
.371535229101	459.4	2.54732975658
.384591782046	493.4	2.41292814277
.396107170558	533	2.53659103527
.412097519094	574.6	2.8751811537
.426579518787	617.8	2.52982212813
.44157044736	655	3.59010987143
.457088189609	704.4	3.09838667696
.473151258965	755.8	3.64539283054
.489778819352	812.4	3.43834585552
.506990708279	875.5	4.47834294751
.524807460259	943.2	4.44222166639
.543250331504	1014.8	5.02680591085
.562341325187	1077.9	4.97661196664
.582103217767	1156	5.03322295685
.602559586081	1243	5.73488351137
.623734835482	1337.9	6.50555318341
.645654229044	1440	6.37704215656
.668343917557	1548.2	7.14608450445
.691830970931	1666.3	7.55792446527
.716143410216	1755	7.87400787401
.741310241296	1880.1	7.83794190673
.767361489387	2021.7	9.40508136689
.794328234702	2174.2	9.65861733836
.822242649956	2341.2	10.3042601762
.851138038188	2516.2	10.6854002161
.881048872987	2673.9	11.589746426
.912010839367	2870.6	12.5715728705
.944060876301	3077.6	13.2438275156
.977237220966	3303.5	13.6075959177
1	3469.9	10.5561988111
1.03514216667	3733.5	15.7266009629
1.07151930523	4011.4	17.0632809142
1.10917481529	4196.1	15.9195896096
1.14815362146	4503.3	18.4152714403
1.1885022274	4825.6	19.5913813249
1.23026877079	5178.7	20.6991679919
1.27350308102	5574.5	23.0855635405
1.31325673851	5991.1	25.0308698238
1.36456313659	6439.7	26.9775626314
1.41253754462	6791.4	30.3980993557
1.46217717443	7270.6	28.3556774639
1.5135612484	7807.4	32.541255866
1.56675107006	8386.9	35.1329221987
1.62181009733	9014.8	37.5878230872
1.67880401811	9474	26.3818119165
1.73780082871	9526.2	2.52982212813
1.79997091509	9562.1	5.66568618963
1.85100717111	9591.1	1.11111111111

E-Field 100% A.M.

1.92752491316	9659.3	2.9458068127
1.99526231494	9712.6	3.06231575409
2.06536015578	9768.2	3.25917508308
2.1379620895	9816.7	2.75075747142
2.21309470956	9850.6	6.20394139954
2.29086765276	9898	2.49443825784
2.37137370562	9942.8	2.4404006957
2.4547089156	9987.2	2.57336787541
2.54097270546	10027	2.49443825784
2.6302679919	10062	2.16024689945
2.722270130804	10098.3	2.21359436211
2.81338293116	10129.1	2.88482620311
2.91742701384	10166.2	2.20100986921

E-Field Probe Calibration, low range
100% Modulation
Run 2 of 2: 0.1 v/m to 3 v/m



E-Field 100% A.M.

FREQUENCY= 300 Mhz

LEVEL	v/m	READING	Hz	STD DEV	Hz
.1		23.9		1.44913767461	
.102329299228		24.7		1.63639169449	
.104712854805		27.1		.994428926012	
.107151930525		28.1		.994428926012	
.109647819613		29.9		1.10050493465	
.112201845432		31		.47148452079	
.114815362157		32.6		1.26491106406	
.117489755495		34		.942809041582	
.120226443466		36.4		.69920589878	
.123026877084		38.5		.707106781186	
.125882541181		41.2		1.13529242435	
.128824955169		43.6		1.07496769979	
.131825673857		46		.816496580927	
.134896288259		48.3		1.251665557	
.136038426462		52.1		.87559503577	
.141253754465		54.1		1.19721899976	
.1445443977081		57.6		.69920589878	
.147910858815		59.9		1.19721899976	
.151256124851		64.1		1.37032031941	
.154321561889		67.2		1.03279555895	
.157453318246		71.4		.966091783078	
.16218100974		74.8		.788810637746	
.165958690737		79.9		.87559503577	
.16982436525		84.5		1.50923085636	
.173780082884		88.6		.84327404271	
.177827941011		93.2		.788810637746	
.181970085862		98.2		1.39841179757	
.18620871367		103.4		1.71269767717	
.190546071803		109.9		1.52388392674	
.19498445998		115.8		.632455532033	
.199526231506		121.6		.966091783079	
.204173794472		128.1		.994428926012	
.208929613065		135.9		1.52388392674	
.213796208955		143.4		.84327404271	
.216776162396		151.5		1.0801234497	
.223872113864		155.4		1.17378779078	
.229086765277		164.4		.966091783079	
.234422681537		173		1.63299316183	
.239883291908		182.1		1.37032031941	
.245470891581		190.9		1.28668393772	
.251188643153		201.1		1.19721899976	
.257039578277		212.5		1.17851130193	
.263026799191		223.5		1.17851130193	
.269153480395		235.1		1.28668393772	
.275422870329		248.2		1.75119007152	
.281638293125		258		1.1547005384	
.288403150315		270.4		1.26491106406	
.295120922671		283.8		1.22927259434	

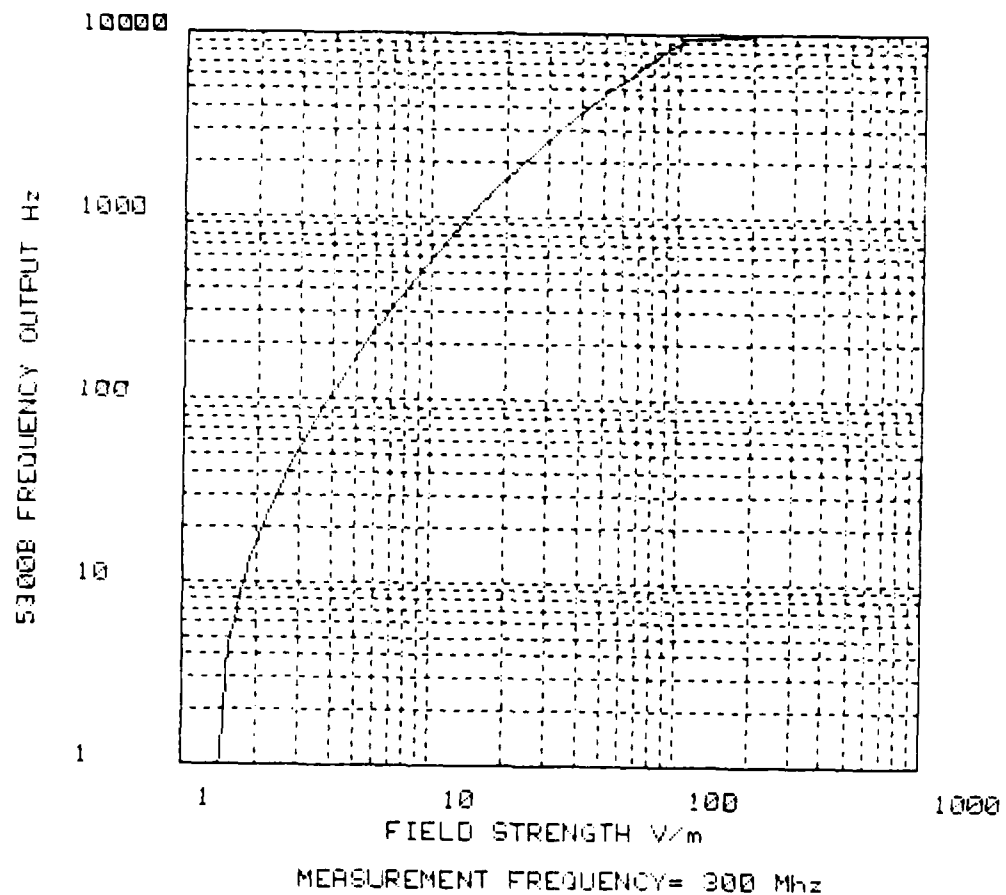
E-Field 100% A.M.

.301995172046	298.3	.87559503577
.309029543255	313.9	1.37032031941
.31622776603	329.5	1.17851130193
.323593656927	347.2	1.31656117723
.331131121481	364.7	1.33749350981
.33884415614	384.3	.94868329805
.346736850456	403.9	2.02484567313
.354813889247	415.7	1.88856206321
.363078054775	436.7	1.33749350981
.371535229101	458.7	1.88856206321
.38013939632	481.4	1.26491106406
.389045145011	504.8	1.68654806854
.398107170558	531.4	1.83787316695
.407380277818	557.7	1.8287822299
.416669383484	587.4	1.71269767717
.426579518787	616.7	1.94650684273
.436515852242	648.6	2.27058484879
.446683592157	669.7	2.26323269289
.457088169609	702.6	2.50333111405
.467735141288	735.6	1.9550504398
.476660692335	772.1	2.80673792467
.488778818952	811.2	2.93636207273
.501187283635	851.6	2.59868123038
.512861384609	896.7	2.86937856221
.524807460259	941.1	4.0674862562
.537031796388	987.6	2.75680975041
.54954087387	1037.3	3.40098825983
.562341325187	1076	4.82768199118
.57543993735	1128.2	4.04969104626
.588643655339	1180.3	3.40098825981
.602559586081	1239.1	3.98469293194
.615595001872	1300.4	3.77712412644
.630957344465	1365.9	3.98469293364
.645654229844	1434.9	4.37661196664
.660693446023	1507	5.43650214293
.676062975409	1580.9	4.62961481473
.691336970931	1660.8	5.65292451251
.707945764386	1739.2	5.09465951321
.714475550111	1792.9	4.92261541464
.741310241296	1874.3	5.1218486246
.758577575056	1967.1	5.44569146716
.776247116631	2063.8	5.59364719025
.794326234702	2166.3	6.1653151672
.812830516179	2275.2	6.52856969191
.831763771142	2390.5	6.57013444813
.851138838188	2506.2	6.95701085237
.870963589984	2632.7	7.67463354173
.891250938151	2729	7.87400787401
.912010839367	2861.1	8.23879710745
.933254300804	2991.9	7.80953832751
.95499258604	3139.9	8.41229259278
.977237220966	3292.3	9.34582497398

E-Field 100% A.M.

1	3455.6	9.78888258292
1	3458.9	1.19721899976
1.01329299227	3628.8	10.5388171376
1.04712854803	3809.5	10.7832174131
1.07151930523	3995.7	10.8735152246
1.09647819613	4194.6	12.1856017036
1.12201845428	4282.3	10.6879995013
1.14815362146	4488.1	12.7405738575
1.17489755496	4692.5	12.545472844
1.20226443456	4922.6	14.3465055752
1.23026877079	5160.6	14.6757547601
1.25892541183	5415.6	16.4330290707
1.28824955169	5687	15.8605030046
1.31825673851	5968.1	16.5827889355
1.3489628826	6258.2	17.6811261581
1.38038426453	6568.6	18.88679727
1.41253754462	6770.9	19.677680532
1.44543977072	7095.7	19.2587642386
1.47910838813	7417.4	19.8561493411
1.5135612484	7780	22.528993665
1.54881661889	8154	21.7970436325
1.5848931925	8554.1	23.6268430148
1.62181089733	8980.5	24.8517828559
1.65958690742	9420.4	26.1839645584
1.69824365251	9498.7	4.11096095821
1.73780082871	9530.1	1.52388392674
1.77827941005	9551.5	6.5192024052
1.81970085857	9583.5	1.53113883006
1.8620671366	9613.3	1.88856206321
1.90546071793	9647.2	1.87379590969
1.94984459969	9681.4	1.8973665961
1.99526231494	9717.8	2.09761769634
2.04173794474	9755.9	2.13177026069
2.0892961308	9791.8	2.09761769634
2.1379620895	9824.4	1.8973665961
2.18776162398	9857.2	1.87379590969
2.23872113854	9875.2	5.00666222813
2.29036765276	9907.4	1.8973665961
2.3442288154	9936.6	1.64654520472
2.39883291894	9967.8	1.75113007152
2.4547069156	9997.9	1.79195734078
2.51166643148	10027.7	1.70293863659
2.57039578266	10052.1	1.53388392674
2.6302679919	10075.6	1.26491106406
2.6915346039	10099	1.49071198499
2.7542287033	10120.9	1.44913767461
2.81838293116	10143.4	1.8973665961
2.8840315031	10168.7	1.33749350981
2.95120922666	10193.4	1.57762127546

E-Field Probe Calibration, High Range
100% Modulation
Run 1 of 1: 1 v/m to 200 v/m



E-Field 100% A.M.

FREQUENCY = 300 MHz

LEVEL v/m	READING Hz	STD DEV Hz
1	1	1.05409255343
1.03514216667	1	1.05409255343
1.07151930523	1	1.05409255343
1.10917481529	1	1.05409255343
1.14815362146	1	1.05409255343
1.1685022274	1	1.05409255343
1.23026877079	1	1.05409255343
1.27050308102	1	1.05409255343
1.31825673851	1	1.05409255343
1.36459313659	1	1.05409255343
1.41253754462	1	1.05409255343
1.46217717443	1.1	.994426926012
1.5135612484	3.2	.421637021356
1.56675107006	4.5	.527046276694
1.62191609723	5.6	.516397779493
1.67886401911	7.1	.316227766016
1.73760082871	8.8	.421637021356
1.79397021509	10.3	.48304589154
1.8620871366	12.3	.48304589154
1.91775149114	14.4	.516397779493
1.99526231494	15.7	.48304589154
2.06538015578	17.9	.316227766016
2.1379620895	20.6	.516397779493
2.21309470956	23.1	.316227766016
2.29086765276	26	0
2.37137370562	29.1	.567646212197
2.4547089156	31.5	.527046276694
2.54097270546	34.9	.316227766016
2.6302679919	38.4	.516397779493
2.72270130304	42.4	.516397779493
2.81038293116	46.7	.48304589154
2.91742701384	51.3	.48304589154
3.01995172042	56.1	.567646212197
3.12607936698	60.4	.69920589878
3.26593656926	65.7	.48304589154
3.34965439152	71.2	.632455532033
3.4673635045	77.4	.69920589878
3.5892193463	84.7	.67494855771
3.71535219994	91.5	.707106781186
3.8459178204	99.1	.87559503577
3.9810717055	104.8	.632455532033
4.12097519984	113	.47140452079
4.26579518792	121.8	.632455532033
4.4157044734	130.9	.737864787372
4.57088189612	141.7	.67494855771
4.70151258956	152	.816496580927
4.89778819356	162.2	.918936583472

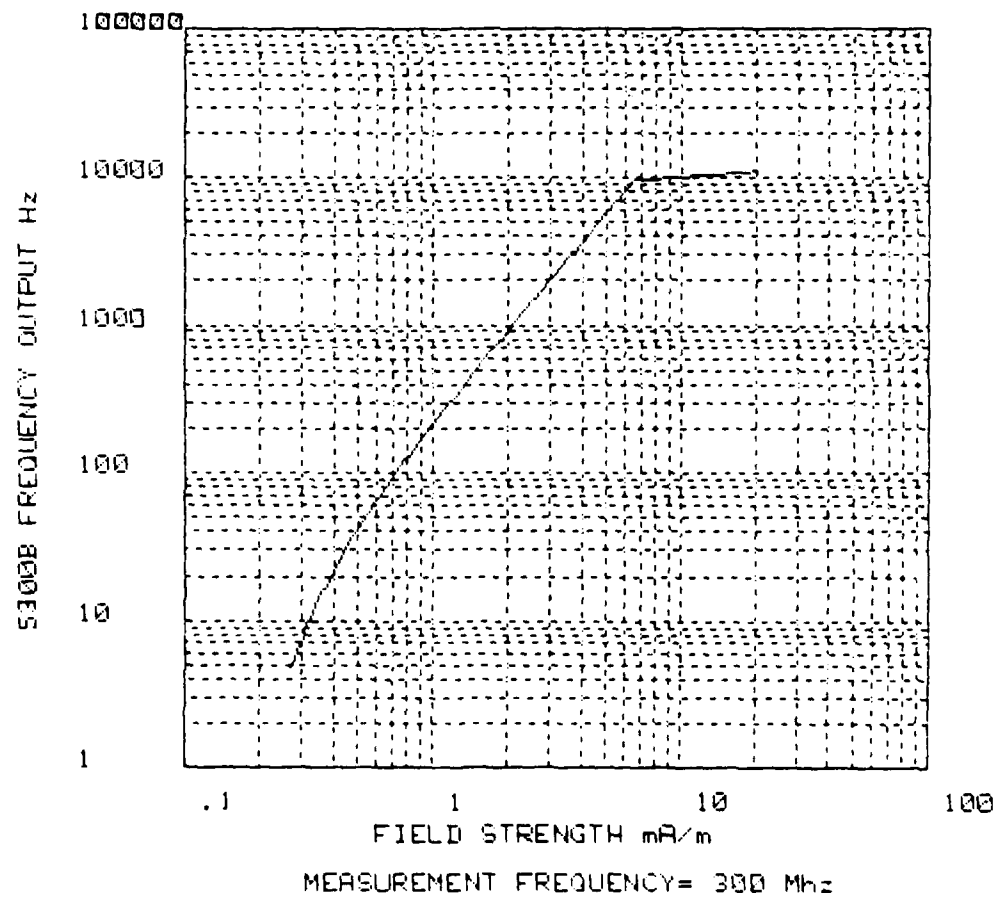
E-Field 100% A.M.

5.06990708268	174	.816496580927
5.24807460232	186.5	.971825315807
5.43250331472	199.7	.94868329805
5.62341325168	214.4	.966091783079
5.82103217776	229.6	.966091783079
6.025595861	245.7	.94868329805
6.23734835472	256	1.1547005384
6.45654229044	272.7	1.41813649244
6.6634391756	290.9	1.44913767461
6.81830970888	310.3	1.251665557
7.16143410192	331.2	1.22927259434
7.413102413	353.6	1.71269767717
7.67361469364	377.1	1.52388392674
7.94328234716	394.8	1.75119007152
8.22242649952	419.2	1.54919333848
8.51138038192	445.8	1.39841179757
8.81048873032	473.6	1.64654520472
9.12010839368	503.2	1.87379590969
9.44060876264	533.6	2.01108041718
9.77237220952	560.3	1.88856206221
10	583.3	1.33749350981
10.3514216667	615	2.16024689945
10.715130523	650.8	2.4404006957
11.0917481528	688.1	2.18326971915
11.4815362146	728.2	2.57336787541
11.885022274	769.3	3.02030167734
12.3026877079	801.8	3.11982905515
12.7350308102	846.1	2.84604989415
13.1825673851	890	2.66666666666
13.6458313659	940.5	3.06412938512
14.1253754462	990.9	3.17804971641
14.6217717443	1044.1	3.24722163411
15.125612484	1098.2	3.61478445645
15.6675107006	1146.1	4.30632609591
16.2181009723	1202.9	3.47850542619
16.7980401811	1263.4	3.68781778291
17.3780082871	1328	4.37162568265
17.9887091509	1393.1	3.95671019351
18.620671386	1461.8	4.15799096788
19.2752491316	1534.4	4.78887539895
19.9526231494	1586.7	5.57872944515
20.6538015578	1666.8	3.92390143991
21.379620895	1745.2	4.73286382647
22.1309470956	1827.5	5.54276304943
22.9086765276	1916.6	5.87272414548
23.7137370562	2004	5.29150262212
24.547089156	2076.2	7.81451640644
25.4097270546	2167.1	5.38413306754
26.302679919	2261.2	6.23253114267
27.2270130804	2359.8	6.71317113342
28.1838293116	2466.3	6.79950978625
29.1742701384	2575.6	6.96339636161
30.1995172042	2686.4	6.535873831

E-Field 100% A.M.

31.2687936698	2780	7.48331477354
32.3593656926	2888.9	6.70737570805
33.4985439152	3009.8	8.00277729568
34.673685045	3134.6	7.26024180802
35.892193463	3274.3	11.4022414954
37.1535229094	3404.1	7.12507309903
38.459178204	3543.6	8.66923039004
39.810717055	3642.7	10.832564075
41.1097519084	3781	8.58939915115
42.6579518792	3927.8	7.81451640644
44.157044734	4080.7	9.09273214044
45.7088189612	4240.6	10.3085724841
47.3151253956	4400.9	11.327939893
48.9778819356	4541.4	12.5273035143
50.6990708288	4707.3	10.4035250439
52.4807460232	4873.2	9.58934593992
54.3250331472	5043.7	10.4035250439
56.2341325168	5229.4	10.7103273115
58.2102217776	5409.8	10.8504992207
60.25595861	5598.8	11.3019172417
62.3734835472	5717.6	12.9460418661
64.5654229044	5898	10.9036181554
66.834391756	6094.4	12.7393934096
68.1830970888	6298.9	12.0041659435
71.6143410192	6505	13.4164078649
74.13102413	6715	12.6666666664
76.7361489364	6927	13.4329611195
79.4328234716	7078.3	16.7335325356
82.2242649952	7504.4	25.8936002015
85.1128038192	7737.3	14.5910931735
88.1049873032	7965.9	14.0669036315
91.2010839368	8195.4	14.2610580876
94.4060876264	8393.3	19.5564709382
97.7237220952	8632.6	12.9868841368
100	8785.6	10.221980673
103.514216667	9466.3	40.5710624842
107.151930523	9498.4	1.26431106406
110.917481528	9508.3	6.92001494766
114.815362146	9527.4	.966091783079
118.85022274	9543.6	.69920589878
123.026877079	9559.2	.918936583472
127.350308102	9575.6	.966091783079
131.825673651	9591.7	1.05934990546
136.456313659	9609	1.1547005384
141.253754462	9622	2.82842712474
146.817717442	9639.3	.94868329805
151.35612484	9653.8	3.11982905515
156.675107006	9700.5	.527046276694
161.161009733	9761.1	3.212831536
167.830401811	9762.6	.516387773433
171.730231171	9781.1	.49201513154
179.887091509	9698.2	.421637021356
186.20871366	9693.8	.632455532033
192.752491316	9687.8	.632455532033
199.526231494	9681.1	.316227766016

H-Field Probe Calibration, Low Range
100% Modulation
Run 1 of 1: .26 ma/m to 20 ma/m



H-Field, 100% A.M.

FREQUENCY= 300 Mhz

LEVEL ma/m	READING Hz	STD DEV Hz
.26525138939	4.6	1.22927259434
.271430501931	5	1.33333333334
.277752930517	5.8	.632455532033
.284222627367	6.2	1.03279555895
.290843022846	6.9	.994428926012
.297617627141	6.6	.966091783079
.304550032247	8.3	.823272602348
.31164391378	9.6	.84327404271
.318903033066	10	1.05408255343
.32633123895	9.9	.737864787372
.333932469976	11.9	.737864787372
.341710756416	12.5	.849836585598
.349670222432	14.6	1.26491106406
.35781508822	15.8	.788810637746
.365149672313	16.4	1.07496769979
.374678393606	17.6	.966091783079
.383405774751	18.5	1.58113883008
.39233644248	20.7	1.1595018087
.401475132231	21.9	.994428926012
.410926689361	23.9	.823272602348
.420396072271	25	1.41421356237
.430138354748	27.4	1.34989711541
.440208728745	28.1	1.10050493465
.450462507294	31.4	.69920589878
.460955127013	33.8	1.13529242435
.471692151223	35.8	1.31656117723
.482679272844	37.3	.94668329805
.493922317427	39.7	1.1595018087
.505427246162	42	1.1547005384
.517209159098	45.7	1.1595018087
.523247298424	47	.666666666666
.54157505165	51.9	1.10050493465
.554189955133	54.5	1.17851130193
.567098697493	58.5	1.26929551767
.580308123066	61.9	.87559503577
.593825235714	64.1	1.10050493465
.607657202326	67.9	1.37032031941
.621811356862	72.1	.994428926012
.636295204	77.2	1.13529242435
.651116423292	80.9	.994428926012
.666282873085	85.5	.527046276694
.681802594999	90.4	1.17378779078
.697683817483	96.5	.971825315807
.71393496126	101	1.49071198499
.730564642782	107	1.1547005384
.747581679377	112.3	1.56702123648
.764995093674	118.1	.567646212197
.782814118491	123.6	1.42984070595
.801048201714	130.2	1.22927259434
.919707011296	138.7	1.05934990546

H-Field, 100% A.M.

.833800440398	145.4	1.50554530539
.858338612538	154.2	1.31656117723
.878331887218	162.5	1.17851130193
.898790865093	171.4	1.42984070595
.919726393782	180.8	1.31656117723
.941149573521	186.8	1.31656117723
.963071783329	196	.942809041582
.985504536475	206.1	1.19721899976
1.00845993719	216.5	1.26929551767
1.03194998677	227.6	1.57762127546
1.05598718981	239.5	.707106781186
1.08058429129	252.8	1.13523242425
1.10575433285	265.7	1.63639169443
1.13151065991	280	1.7638342074
1.15786692902	295.1	.737854787372
1.18483711447	305.1	1.19721899976
1.2124255162	320.9	1.59513148185
1.24067676734	336.3	.94868329905
1.26957584174	353.5	.971825315607
1.29914806194	372.3	1.63639169443
1.32940910779	390.6	1.8973665961
1.3603750239	411.4	2.17050941283
1.3920622208	432.1	1.59513148185
1.42448752358	454.2	1.47572957475
1.45766810045	478.2	1.98885785203
1.49162155222	495.9	1.59513148185
1.52636588156	520.8	2.09761769634
1.56191951018	545	1.94365063162
1.59830128934	572.3	2.162817093
1.63553050894	601.7	1.494434111811
1.6736269064	631.4	2.065531111795
1.71261066712	665	2.40370065031
1.75250251465	698.5	3.02765635406
1.7733235422	732.4	2.36643131223
1.83509541361	770.9	2.96085573214
1.87734627686	792.7	1.55917156242
1.92158079606	832.3	2.71006354958
1.96634016259	870.1	2.33095116495
2.0121421089	913.8	2.93636207273
2.05901091945	959.3	2.58413965911
2.10697144483	1007.7	3.19895816374
2.15604911453	1059.2	3.48966728755
2.20626394998	1112	4
2.25766057875	1167.4	4.52646538561
2.31024824929	1227	3.77123616632
2.3640608439	1272.3	4.4484703988
2.41312689487	1334.5	4.52769256906
2.47547559895	1397	4.34613493681
2.533136833	1465.6	4.2998707991
2.59214116967	1537.4	5.01553143301
2.6525198939	1613	4.9888765157
2.6525198939	1615.8	.918936583472
2.71430501928	1694.5	5.10446427704
2.77752930512	1780.6	5.18973345494

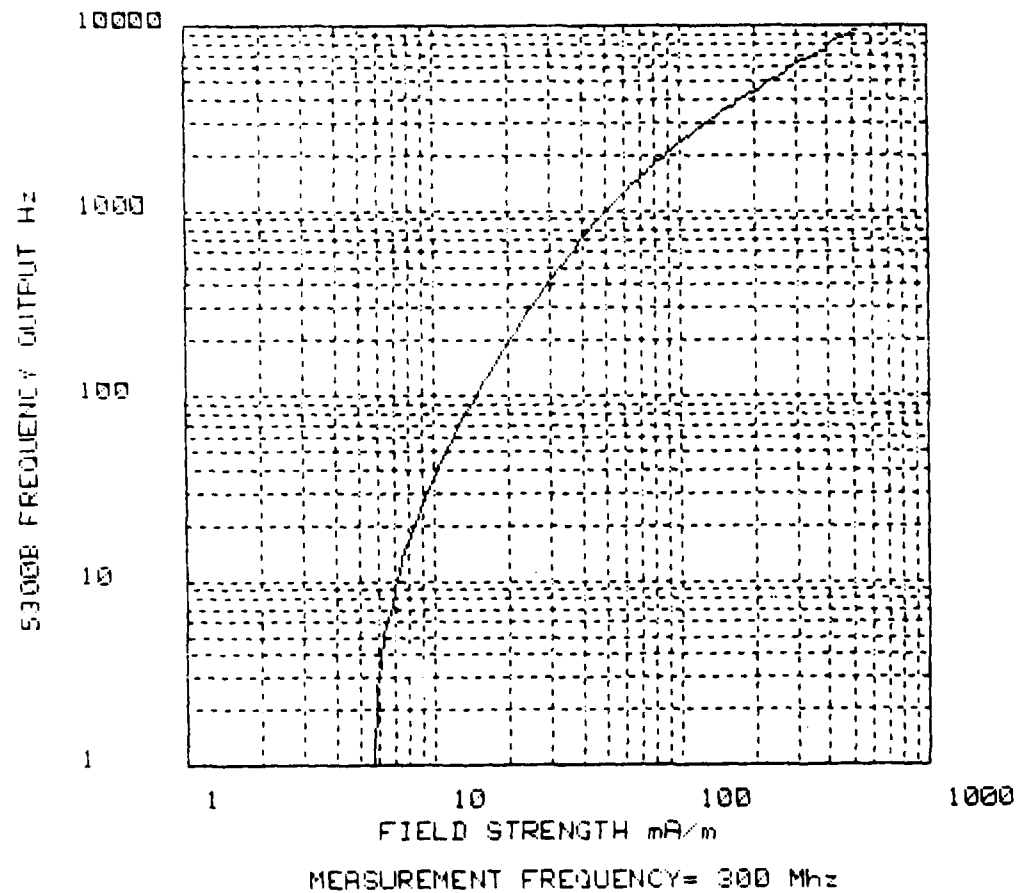
H-Field, 100% A.M.

2.84222627382	1867.6	5.23237783209
2.90843022846	1961.1	5.72421755933
2.9761762713	2002.4	5.54176065082
3.04550032218	2099.6	6.61983551322
3.11643913782	2195.7	6.36046818682
3.1890303304	2305.9	6.36745195854
3.26331238936	2417.4	6.9153613226
3.33932469981	2537.8	7.43564986326
3.41710756416	2665.9	8.464960458
3.49670222416	2798.9	8.87505868524
3.57815088223	2935.3	8.31397752115
3.66149672289	3083	8.13770374382
3.74678393798	3179.1	9.68905453477
3.83405774727	3332.7	10.1330043807
3.92336442475	3485.7	8.76926450735
4.01475132202	3658	10.5934990546
4.10826689361	3836.4	10.8135717198
4.20396072281	4025.3	12.1202310209
4.30168354729	4228.9	12.635487943
4.40208728759	4439.5	13.5912553585
4.50462507297	4656.4	13.5662981111
4.60355126979	4888.9	14.0431873561
4.71692151207	5088.8	16.4775942151
4.8267827283	5314.1	15.2275335422
4.93922917401	5556.4	14.5922353784
5.05427246135	5830.5	16.0225535486
5.17200159069	6113.7	16.7865687047
5.29247298393	6416	18.281745601
5.41575051655	6739.6	19.2307623931
5.54189955119	7074.3	20.1937834216
5.6709869748	7420.2	20.4982384067
5.80308123072	7790	22.5141930541
5.93825235687	8019.4	24.4322191652
6.07657202324	8407.4	24.1117767445
6.2181135687	8789.9	23.5770604143
6.36295203963	9224	26.7664798664
6.51116423236	9483.4	15.980543726
6.65292873972	9517.9	1.79195734078
6.8180259487	9547.7	1.70293863659
6.9768381748	9577.2	1.54919333848
7.13934961247	9606.9	1.79195734078
7.30564642785	9637.8	2.09761769634
7.47581679353	9660.9	4.55704582669
7.6499509366	9693.4	1.8973665961
7.82814118477	9723.8	1.75119007152
8.01048101703	9757.7	1.70293863659
8.18787011284	9792	2.16024689945
8.35538144015	9824.2	1.391582004711

H-Field, 100% A.M.

8.58336612536	9856.3	1.88856206321
8.78331887204	9887.3	1.88856206321
8.98790865077	9917.5	1.58113883008
9.19726393767	9948.4	1.57762127546
9.4114957357	9966.2	4.66190232988
9.62071763332	9997.2	1.54919333848
9.85504586456	10025.6	1.64654520472
10.08459937118	10056.8	2.09761769634
10.3194998672	10086.8	2.09761769634
10.5598718979	10117.2	1.87379590969
10.805842912	10143.3	1.56702123648
11.0575433279	10169.9	1.44913767461
11.3151065993	10196.1	1.52388392674
11.5786692992	10224	1.49071198499
11.8483711442	10242	3.88730126321
12.1243551621	10271.2	1.54919333848
12.4067676731	10298.3	1.56702123648
12.6957584171	10328.7	1.70293863659
12.9914806195	10359.1	1.85292561464
13.294091077	10375.6	.966091783079
13.6037502382	10407.9	2.13177026069
13.9206222873	10441.1	2.18326971915
14.244875235	10474.4	1.8973665961
14.5766810041	10509.2	1.87379590969
14.9162155217	10537.1	3.212821536
15.2636508145	10572.7	2.05750658161
15.619195102	10606.5	1.95789002076
15.9830128939	10643.9	2.46981780704
16.3553050887	10680.9	2.13177026069
16.7362690844	10719.7	2.40601099099
17.1261068712	10759.4	2.27058484879
17.5250351453	10799.4	2.27058484879
17.9332354218	10839.6	2.36643191323
18.350954135	10880.9	2.46981780704
18.7784027685	10907.5	4.74341649025
19.2158079593	10949.9	2.46981780704
19.663401626	10989.4	2.27058484879

H-Field Probe Calibration, High Range
100% Modulation
Run 1 of 1: 5.6 ma/m to 520 ma/m



H-Field, 100% A.M.

FREQUENCY = 300 MHz

LEVEL ma/m	READING Hz	STD DEV Hz
2.6525198939	1	1.05409255343
2.74573519011	1	1.05409255343
2.84222627382	1	1.05409255343
2.94210826337	1	1.05409255343
3.04550032219	1	1.05409255343
3.15252580212	1	1.05409255343
3.26331236936	1	1.05409255343
3.37799225735	1	1.05409255343
3.49570222416	1	1.05409255343
3.61958391668	1	1.05409255343
3.74678393798	1	1.05409255343
3.87845404358	1	1.05409255343
4.01475132202	1	1.05409255343
4.15583838212	1	1.05409255343
4.30138354729	1	1.05409255343
4.45366105599	1	1.05409255343
4.60955126379	1	1.05409255343
4.771540688883	1	1.05409255343
4.93922317401	1	1.05409255343
5.11279817814	1	1.05409255343
5.26247282181	1	1.05409255343
5.47846195167	1	1.05409255343
5.6709869748	1	1.05409255343
5.87027774419	2.6	.516397779493
6.07657202324	3.6	.516397779493
6.29011593003	5.2	.421637021356
6.51116423236	6.3	.48304589154
6.73998065109	7.5	.527046276694
6.9768381748	9.3	.48304589154
7.22201938472	11.3	.48304589154
7.47581679353	13.2	.421637021356
7.73853319321	15.6	.516397779493
8.01048201703	17.7	.48304589154
8.29198771082	19.8	.421637021356
8.58338612536	22.1	.316227766016
8.88502491119	25.1	.567646212197
9.19726393767	28.3	.48304589154
9.52047571963	31	0
9.85504586456	34.9	.316227766016
10.2013735289	39	0
10.5598718979	41.9	.316227766016
10.930968676	46.1	.316227766016
11.3151065993	50.8	.421637021356
11.7127439613	55.6	.69920589878
12.1243551621	61.4	.69920589878
12.550431272	66.9	.737864787372
12.9914806195	72.3	.67494855771
13.448029397	79.1	.567646212197
13.9206222873	86	.816496580927

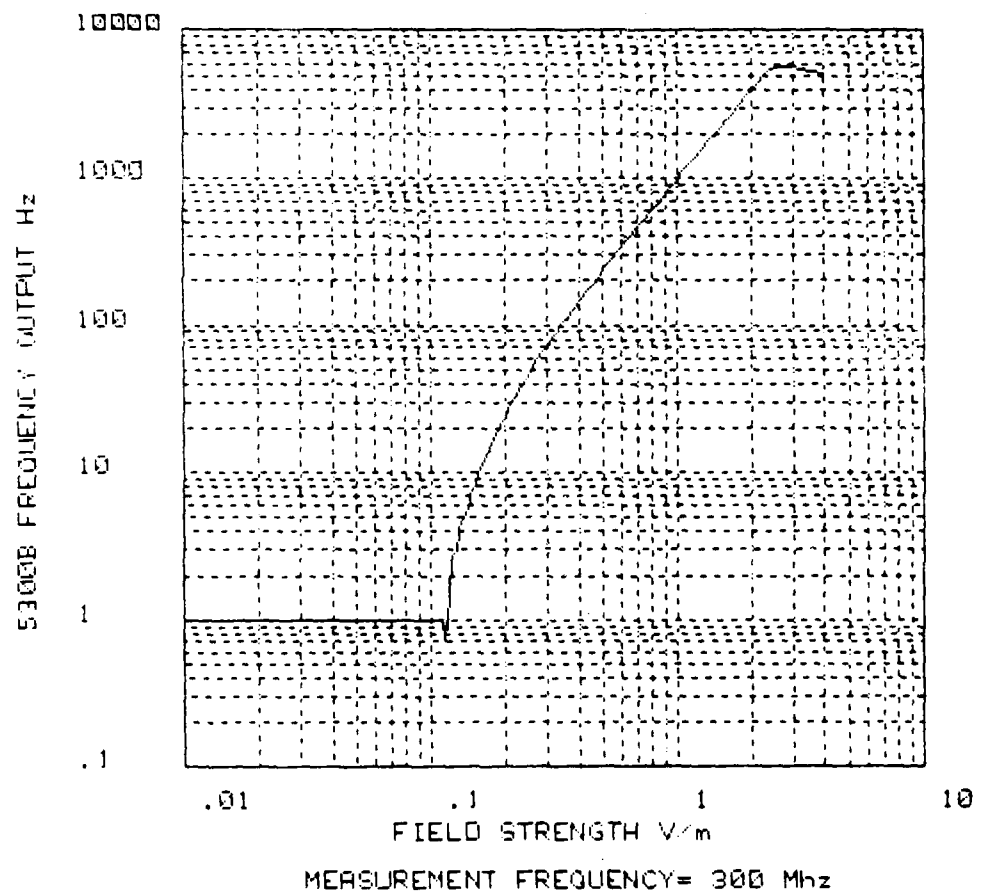
H-Field, 100% A.M.

14.409823116	93.7	.67494855771
14.9162155217	102.1	.567646212197
15.4404036545	111.1	.87559503577
15.9830128939	120.8	.632455532033
16.5446905961	126.5	.707106781186
17.1261068712	136.6	.69920589878
17.7279553729	147.8	1.03279555895
18.350954135	159.8	1.31656117723
18.9958464242	173.7	.94868329805
19.663401626	187.6	.966091783079
20.3544161635	202.7	.94868329805
21.0697144487	214.2	.918936583472
21.8101498661	229.6	.966091783079
22.5766057876	247.4	1.26491106406
23.3699966321	265.6	1.07496769979
24.1912689488	286.6	1.26491106406
25.0414025534	307.5	1.58113883008
25.9214116963	326.3	1.56702123648
26.525198939	341.4	.966091783079
27.4573519011	363.9	1.44913767461
28.4222627382	390.2	1.87379590969
29.4210026334	416.9	1.79195734078
30.4550032218	445	1.49071198499
31.5252580212	475.8	2.82055944018
32.6331238936	498.2	1.93218356617
33.7799225735	529.4	2.27058484879
34.9670222416	561.6	2.41292814277
36.1958391668	596.8	2.14993539954
37.4676393798	635.3	2.31180545124
38.7845404358	673.7	2.4517567398
40.1475132202	713.9	2.46981780704
41.5583838212	748	2.82842712474
42.0138354729	789.2	2.93636207273
44.5306105599	833.8	2.78088714862
46.0955126379	879.2	2.97396106975
47.7154088863	927.3	3.33499958353
49.3912317401	977.6	3.06231575409
51.1273117314	1028.7	3.4657043246
52.9247298393	1066	3.88730126321
54.7846195167	1119.5	4.06201920231
56.709869748	1176	3.97212509594
58.7027774419	1233.3	4.59589188539
60.7657202324	1296.5	3.71931893407
62.9011593003	1357.7	3.77270901785
65.1116423236	1406.4	4.83505716386
67.3998065109	1467.9	3.7549966711
69.768381748	1532.1	3.212821536
72.2201936472	1598.5	4.14326763154
74.7581679353	1672.1	3.92852813829
77.3853319321	1743.5	5.16935413975
80.1048201703	1821	4.05517502019
82.9198771082	1882.3	6.56675126848
95.8338612536	1958.3	5.14349643293

H-Field, 100% A.M.

88.8502491119	2039.8	4.87168690839
91.9726393767	2122.1	5.10681590977
95.2047571963	2207.1	4.97661196664
98.5504586456	2289.8	4.80277697448
102.013735289	2377.5	5.12618549974
105.536718979	2443	7.4087035903
109.30968676	2529.6	4.88080139139
113.151065993	2625.9	7.09381577306
117.127439613	2722	7.22649446289
121.243551621	2822.9	7.09381577306
125.50431272	2921.7	5.88878406615
129.914806195	3006.2	8.5738620884
134.48029397	3108	6.34209919681
139.206222873	3208.1	6.77331364826
144.09823116	3314.4	6.50128192486
149.162155217	3422.1	7.26406681319
154.404036545	3533.6	6.931409998963
159.830128939	3649.4	9.37135114176
165.446905961	3720.8	7.714344583
171.261068712	3832.2	6.76264248156
177.279553729	3945.8	6.64663657632
183.50954135	4063.2	6.76264248156
189.358464242	4180.5	7.23033732116
196.63401626	4303.7	8.01457006541
203.544161635	4428.2	7.46547609556
210.697144487	4515.8	10.485969462
218.101498661	4758.9	15.4736334886
225.766057876	4891.3	8.60297106301
233.699966321	5024	8.19213715162
241.312689488	5155.5	8.47545475673
250.414025534	5263.7	9.01911550233
259.214116963	5398	10.0443461151
265.25198939	5482.2	4.80277697448
274.573519011	5903.3	26.1790841023
284.222627382	6056.9	9.66609193694
294.210826334	6165.3	14.3994598662
304.550032218	6309.8	9.42573309851
315.252580212	6459	10.3922048454
326.331238936	6614.8	9.40212741683
337.733265735	6775.9	11.327939893
349.670222416	6940.7	10.7888831674
361.958391668	7108.5	11.530153704
374.670393793	7250.6	12.5361698919
387.345404356	7418	10.2523709999
401.475132202	8093.6	42.5341692706
415.563038212	8310.8	11.7265131697
430.166354729	8448.7	16.1455188142
445.306105599	8651.9	14.7531540885
460.955126979	8862.3	12.4130713557
477.154098951	9060.7	14.5129295711
511.279817814	9470.7	10.0890479669
529.247298393	9491.6	1.26491106406

E-Field Probe Calibration, Low Range
50% Modulation (for reference only)
Run 1 of 1: .01 v/m to 1.5 v/m



E-Field, 50% A.M.

FREQUENCY= 300 Mhz

LEVEL	v/m	READING Hz	STD DEV Hz
.01		1	1.05409255343
1.03514216669E-02		1	1.05409255343
1.07151939525E-02		1	1.05409255343
1.10317481526E-02		1	1.05409255343
1.14315262157E-02		1	1.05409255343
1.18850222744E-02		1	1.05409255343
1.23028877084E-02		1	1.05409255343
.01273503081		1	1.05409255343
1.01625673857E-02		1	1.05409255343
1.06458313661E-02		1	1.05409255343
1.41253754465E-02		1	1.05409255343
1.48217717445E-02		1	1.05409255343
1.51356124851E-02		1	1.05409255343
1.56675107015E-02		1	1.05409255343
.016218100974		1	1.05409255343
1.67990401814E-02		1	1.05409255343
1.73780082884E-02		1	1.05409255343
1.798870891516E-02		1	1.05409255343
.019620971367		1	1.05409255343
1.81751491221E-02		1	1.05409255343
1.88526231506E-02		1	1.05409255343
2.06538015583E-02		1	1.05409255343
2.13796208955E-02		1	1.05409255343
2.21309470964E-02		1	1.05409255343
2.29086765277E-02		1	1.05409255343
2.37137370571E-02		1	1.05409255343
2.45470891581E-02		1	1.05409255343
.025409727056		1	1.05409255343
2.63026799191E-02		1	1.05409255343
2.72270130814E-02		1	1.05409255343
2.81838293125E-02		1	1.05409255343
2.91742701399E-02		1	1.05409255343
3.01995172046E-02		1	1.05409255343
.031260793671		1	1.05409255343
3.23593656927E-02		1	1.05409255343
3.34965439171E-02		1	1.05409255343
3.46736850456E-02		1	1.05409255343
3.58921934644E-02		1	1.05409255343
3.71535229101E-02		1	1.05409255343
3.84591782046E-02		1	1.05409255343
3.98107170558E-02		1	1.05409255343
4.12097519094E-02		1	1.05409255343
4.26579518787E-02		1	1.05409255343
.044157044736		1	1.05409255343
4.57088189609E-02		1	1.05409255343
4.73151258965E-02		1	1.05409255343
4.89778819352E-02		1	1.05409255343

E-Field, 50% A.M.

5.06990708279E-02	1	1.05409255343
5.24807460259E-02	1	1.05409255343
5.43250331504E-02	1	1.05409255343
5.62341325187E-02	1	1.05409255343
5.82103217767E-02	1	1.05409255343
6.02559586081E-02	1	1.05409255343
6.23734835482E-02	1	1.05409255343
6.45654229044E-02	1	1.05409255343
6.68343917557E-02	1	1.05409255343
6.91830970931E-02	1	1.05409255343
7.16143410216E-02	1	1.05409255343
7.41310241296E-02	1	1.05409255343
7.67361489387E-02	1	1.05409255343
7.94326234702E-02	1	1.05409255343
8.22242649958E-02	1	1.05409255343
8.511389381688E-02	1	1.05409255343
8.81048872987E-02	1	1.05409255343
9.12010839367E-02	1	1.05409255343
9.44060876301E-02	1	1.05409255343
9.77237220966E-02	1	1.05409255343
.1	1	1.05409255343
.103514216669	1	1.05409255343
.107151330525	1	1.05409255343
.110917481526	1	1.05409255343
.114815362157	.7	.823272602348
.118850322744	1.4	.69920589878
.122026877084	2.7	.94868329805
.1273503081	2.9	.316227766016
.131825673857	4.0	.788810637746
.136458813661	5	.942809041582
.141253754465	5.7	1.05934990546
.146217717445	7.1	1.10050493465
.151356124851	8.5	.971825315807
.156675107015	9.7	1.05934990546
.16218100974	11.6	.84327404271
.167880401814	12.7	1.1595018087
.173780082884	15	1.41421356237
.173887031516	16.4	.966091783079
.18620971167	18.1	1.251665557
.192752491321	21.7	1.05934990546
.199526231506	23	.666666666666
.206528015583	27.5	.849836585598
.213796208955	30.3	1.05934990546
.221309470964	32.2	1.13529242435
.229086765277	36.4	.966091783079
.237137370571	39.3	1.251665557
.245470831581	43.4	.84327404271
.25409727056	47.7	.94868329805
.263026799191	52.9	1.37032031941
.272270130814	58.2	1.03279555895
.281836293125	63.5	.849836585598
.291742701399	68.5	1.0801234497
.301995172046	74.4	1.8973665961

E-Field, 50% A.M.

.31260793671	80.6	1.17378779078
.323593656927	88.1	1.37032031941
.334965439171	95.8	.918936583472
.346736850456	104.2	1.13529242435
.358921934644	111.2	1.75119007152
.371535229101	120.3	1.05934990546
.384591782046	129.9	1.28668393772
.398107170558	140.9	1.66332999329
.412097519094	153.1	.87559503577
.426579518787	165.2	1.03279555895
.44157044736	176.4	1.50554530539
.457088189609	191.1	1.28668393772
.473151258965	204.7	.823272602348
.489778819352	221.5	1.43372087785
.506990708279	239.7	1.70293863659
.524807460259	257.5	1.26929551767
.543250331504	277.3	1.49443411811
.562341325187	298.1	2.4244128728
.582103217767	319.3	1.62639169449
.602559586081	345.5	1.90029237518
.623734835482	371.5	2.068278941
.645654229044	400.1	2.13177026069
.668343917557	430.5	1.77951304198
.691830970931	465.4	2.36643191323
.716143410216	492.4	2.11869981092
.741310241296	527.4	2.50330111405
.767361469387	568.2	1.75119007152
.794328234702	610.1	2.7668674626
.822242649958	657.9	3.41402336775
.8511380038188	707.5	3.4399612401
.8810488872987	756.4	4.32563418598
.912010839367	812.3	4.02906109824
.944060876301	869.9	4.33205109233
.977237220966	934.6	4.37670601658
1	981.9	3.51020229783
1.03514216667	1055.6	4.90351347957
1.07151930523	1134.7	4.54728246074
1.10917481529	1193.2	5.07280330127
1.14815362146	1280.3	4.73872931866
1.1885022274	1372.2	6.44291169511
1.23026877079	1473.1	6.488451279
1.27350308102	1584.7	7.36432843736
1.31825673851	1701.9	7.43041796341
1.36458313659	1829.3	7.55792446523
1.41253754462	1939.2	9.97552560575
1.4621717443	2074.8	8.44327477279
1.5135612484	2226	8.88194172965
1.56675107006	2392.3	9.68446637089
1.62181003733	2570.5	10.4695325167
1.67880401811	2759.9	11.249197502
1.73790092871	2963.1	13.0677720618
1.77687091509	3158.1	14.1378137553

E-Field, 50% A.M.

1.8620871366	3376.5	13.2182533725
1.92752491316	3623.2	15.3101273672
1.99526231494	3886.5	15.6507010846
2.06538015578	4176.4	17.7275679849
2.1379620895	4475.9	17.5654332266
2.21309470956	4733.1	21.5223398151
2.29086765276	5050	18.3666364187
2.37137370562	5274	43.1740662898
2.4547089156	5433.4	44.9967900088
2.54097270546	5639.2	24.7691564474
2.6302679919	5648.6	7.77746031098
2.72270130804	5668.7	5.88878406615
2.81838293116	5661.8	10.870960297
2.91742701384	5639.5	15.3202843028
3.01995172042	5606.2	19.1357722023
3.12607936698	5561.3	22.4551404658
3.23593656926	5521.5	10.6379822645
3.34965439152	5444.3	28.7326759397
3.4673685045	5370.2	31.5305847992
3.5892193463	5279.9	33.2714425431
3.71535229094	5191.8	35.143515286
3.8459176204	5103.6	34.345305356
3.9910717055	5009	38.2157617278

APPENDIX F

COMPUTER PROGRAMS

F.1 INTRODUCTION

This appendix contains listings of computer programs used during field mapping to acquire and process data from the field measurement system.

The programs are written in Hewlett-Packard Compatable BASIC, level 1, and were excuted on the H.P. model 9845B desktop computer.

The programs are designated as file number 1, 2, and 3. File No. 1 is a brief utility program which upon manual command allows a series of 10 probe readings to be acquired and printed. File No. 2 provides for complete automatic control of probe scanning operations, and results in a printout and a magnetic tape file of all 73 measurement grid data points in engineering units. (ie., in volts/m or Amps/m.)

File 3 provides for contour plotting of the data obtained from File No. 2.

```

10      REM THIS PROGRAM IS A UTILITY PROGRAM TO ACQUIRE AND PROCESS DATA FROM THE
      hp5300B FREQUENCY COUNTER.REF TEST PLAN:FILE NO.1
20      ON KEY #0 GOTO 140
30      OPTION BASE 1
40      DIM Freq(50),Mean(100),Std(100),Error(100),Label$(70)
50      PRINTER IS 16
60      J=0
70      PRINT "THIS PROGRAM WILL TAKE N NUMBER OF MEASURMENTS AND THEN"
80      PRINT "FIND THE MEAN STANDARD DEVIATION AND STANDARD ERROR."
90      INPUT "WHAT IS N THE NUMBER OF MEASURMENTS?",K
100     PRINT "TO START PROGRAM PRESS KEY #K0"
110     DISP "WAITING TO START"
120     GOTO 110
130     STOP
140     INPUT "TEST LABEL?",Label$
150     PRINTER IS 0
160     FOR I=1 TO K STEP 1
170     OUTPUT 717;"I"
180     ENTER 717;Freq(I)
190     NEXT I
200     Z=0          !START OF THE MEAN CALCULATION
210     J=J+1
220     FOR I=1 TO K STEP 1
230     Z=Z+Freq(I)
240     NEXT I
250     Mean(J)=Z/K
260     T=0          !START OF THE STD DEV. CALCULATION
270     FOR I=1 TO K STEP 1
280     T=T+(Freq(I)-Mean(J))^2
290     NEXT I
300     Std(J)=SQR(T/(K-1))
310     Error(J)=Std(J)/SQR(K)
320     PRINT
330     PRINT
340     PRINT
350     PRINT Label$
360     PRINT
370     FOR I=1 TO K STEP 1
380     PRINT Freq(I);
390     NEXT I
400     PRINT
410     PRINT
420     PPINT "MEAN           STD DEV           STD ERROR"
430     PRINT
440     PRINT Mean(J),Std(J),Error(J)
450     PRINTER IS 16
460     DISP "READY FOR NEXT READING"
470     GOTO 460
480     END

```

```

10 REM THIS IS THE MAIN PROGRAM FOR EM FIELD MAPPING.REF TEST PLAN:FILE NO.2
20 REM IT IS CALLED "MAP" AND IS FOR LOW RANGE INITIAL SCANS
30 PRINTER IS 16
40 PRINT " THIS PROGRAM IS AN AUTOMATIC SCANNING PROGRAM FOR EM FIELD MAPPING
"
50 PRINT "CONSULT BNR REPORT NUMBER           BEFORE USING. "
60 OPTION BASE 1
70 SHORT Reading(80),Std(80),Stderr(80),F2(20),F(200),R(200),S(200),Range(80),
, R1(200),F1(200),S1(200)
80 DIM Label1$(80),Label2$(80),Label3$(80),Name$(50)
90 ASSIGN #1 TO "DATA"
100 ASSIGN #2 TO "LOW"
110 ASSIGN #3 TO "HIGH"
120 ASSIGN #4 TO "HLOW"
130 ASSIGN #5 TO "HHIGH"
140 Count=0
150 PRINT "YOU ARE ALLOWED 3 LINES OF COMMENT (SO CHARACTERS) WHICH WILL APPER
P ON ALL DATA OUTPUT."
160 INPUT "PLEASE ENTER EACH LINE OF COMMENT AND PUSH <CONT> AFTER EACH LINE. ,
Label1$,Label2$,Label3$
170 INPUT "WHAT IS THE RECORD NUMBER IN WHICH THIS DATA IS TO BE STORED",Record
d
180 INPUT "WHAT IS THE RECORD NAME FOR THIS RECORD",Name$
190 INPUT "IS THIS A E FIELD OR H FIELD SCAN?(TYPE E OR H)",Ident$
200 IF Ident$="E" THEN Limit=9420
210 IF Ident$="H" THEN Limit=9224
220 INPUT "WHAT IS THE RADIANTING FIELD FREQUENCY (MHz)?",Freq
230 INPUT "WHAT IS THE GENERATOR POWER OUTPUT(dbm)?",Power
240 PRINT "SETUP INSTRUMENTATION AND SET PROBE AT IT START POSITION"
250 PRINT "TO START SCANNING PRESS <CONT> KEY"
260 REMOTE 710
270 LOCAL LOCKOUT 7
280 OUTPUT 710;"B123456"    ! RESETS RELAYS TO THE B-C POSITION
290 PAUSE
300 PRINT "NOW DOUBLE CHECK EVERYTHING SO YOU DON T DESTROY THE POSITIONER"
310 PRINT "IF YOU ARE SURE THEN PRESS THE <CONT> KEY TO START SCANNING"
320 PAUSE
330 OUTPUT 728;"R";Freq;"L,B50.0,Y1,S";Power;,""
340 WAIT 10000
350 GOSUB Scan
360 GOSUB Store
370 GOSUB Plotco
380 END
390 Scan:OUTPUT 710;"R6"                                ! set positionner remote relay on.
400 FOR J=1 TO 3 STEP 1
410 FOR I=1 TO 5 STEP 1
420 GOSUB Measure
430 OUTPUT 710;"R2"
440 WAIT 500
450 OUTPUT 710;"B2"
460 WAIT 23500
470 NEXT I
480 GOSUB Measure
490 OUTPUT 710;"R4"
500 WAIT 500
510 OUTPUT 710;"B4"
520 WAIT 23500
530 NEXT J

```

```

540 FOR J=1 TO 5 STEP 1
550 FOR I=1 TO 10 STEP 1
560 GOSUB Measure
570 OUTPUT 710;"A1"
580 WAIT 500
590 OUTPUT 710;"B1"
600 WAIT 11500
610 NEXT I
620 GOSUB Measure
630 IF J=5 THEN GOTO Local
640 OUTPUT 710;"A3"
650 WAIT 500
660 OUTPUT 710;"B3"
670 WAIT 11500
680 NEXT J
690 Local: LOCAL 7
700 RETURN
710 STOP
720 Measure: REM THIS SECTION READS THE 5300B AND DOES SOME STATISTICS
730 Count=Count+1
740 Range(Count)=1
750 K=10
760 FOR N=1 TO 10 STEP 1
770 OUTPUT 717;"I"
780 ENTER 717;F2(N)
790 NEXT N
800 C=0      ! START OF MEAN CALCULATION
810 FOR N=1 TO 10 STEP 1
820 C=C+F2(N)
830 NEXT N
840 Reading(Count)=Z/K
850 IF Reading(Count)>Limit THEN GOTO Switch
860 IF Reading(Count)=0 THEN Reading(Count)=1
870 T=0      ! START OF STANDARD DEV
880 FOR N=1 TO K STEP 1
890 T=T+(F2(N)-Reading(Count))^2
900 NEXT N
910 Std(Count)=SQRT(T/(K-1))
920 OUTPUT 710;"B5"
930 GOTO 990
940 Switch: IF Range(Count)=2 THEN GOTO 860   ! IF ALREADY ON HIGH RANGE RETURN
950 OUTPUT 710;"A5"
960 Range(Count)=2
970 WAIT 10000
980 GOTO 750
990 RETURN
1000 Store: REM THIS ROUTINE STORES THE DATA ON TO MAG TAPE
1010 PRINT #1,Record;Name$,Reading(*),Std(*),Range(*),END
1020 RETURN
1030 Plot: REM THIS IS THE CONTOUR SECTION
1040 SHOPT X(11,11),Y(11,11),Data(11,11),Xline(2),Yline(2),Contour(10),Y(80)
1050 GOSUB Grid
1060 GOSUB Data
1070 GOSUB Print
1080 GOSUB Sort
1090 GOSUB Fill
1100 PRINTER IS 16
1110 PRINT "WHAT ARE THE VALUES OF THE CONTOURS YOU WANT TO SEE? ENTER 0 AS LAST VALUE"
1120 FOR I=1 TO 10 STEP 1
1130 INPUT "CONTOUR VALUE=",Contour(I)
1140 IF Contour(I)=0 THEN GOTO 1160
1150 NEXT I
1160 Contour=I-1
1170 GOSUB Draw
1180 GOSUB Contour

```

```

1190 GOSUB Label
1200 PRINTER IS 16
1210 INPUT "DO YOU WANT A HARD COPY",A$
1220 IF A$="YES" THEN DUMP GRAPHICS
1230 PRINTER IS 0
1240 PRINT LIN(5),"CONTOUR VALUES=";
1250 FOR I=1 TO Conmax STEP 1
1260 PRINT Contour(I);
1270 NEXT I
1280 INPUT "DO YOU WANT TO PLOT MORE CONTOURS?(TYPE YES OR NO)",B$
1290 IF B$="YES" THEN GOTO 1100
1300 RETURN
1310 STOP
1320 END
1330 Draw: REM THIS SUBROUTINE DRAWS THE GRID
1340 GCLEAR
1350 PRINTER IS 0
1360 PRINT PAGE
1370 GRAPHICS
1380 LINE TYPE 3,8
1390 DEG
1400 LOCATE 20,80,20,80
1410 SCALE 0,5,0,5
1420 M=1
1430 FOR N=1 TO 11 STEP 2
1440 MOVE X(N,M),Y(N,M)
1450 DRAW X(N,11),Y(N,11)
1460 NEXT N
1470 N=1
1480 FOR M=1 TO 11 STEP 2
1490 MOVE X(N,M),Y(N,M)
1500 DRAW X(11,M),Y(11,M)
1510 NEXT M
1520 M=7
1530 FOR N=1 TO 11 STEP 1
1540 MOVE X(N,M),Y(N,M)
1550 DRAW X(N,11),Y(N,11)
1560 NEXT N
1570 N=1
1580 FOR M=7 TO 11 STEP 1
1590 MOVE X(N,M),Y(N,M)
1600 DRAW X(11,M),Y(11,M)
1610 NEXT M
1620 RETURN
1630 STOP
1640 Contour: REM THIS SUBROUTINE PLOTS THE CONTOURS
1650 GRAPHICS
1660 LINE TYPE 1
1670 FOR I=1 TO Conmax STEP 1
1680 FOR M=1 TO 10 STEP 1
1690 FOR N=1 TO 10 STEP 1
1700 L=1
1710 IF <Contour(I)>=Data(N,M) AND <Contour(I)><Data(N+1,M) THEN GOTO P1
1720 IF <Contour(I)>=Data(N,M) AND <Contour(I)>Data(N+1,M) THEN GOTO P1
1730 IF <Contour(I)>=Data(N,M) AND <Contour(I)>>Data(N+1,M) THEN GOTO P1
1740 IF <Contour(I)>=Data(N+1,M) AND <Contour(I)><Data(N+1,M+1) THEN GOTO P2
1750 IF <Contour(I)>=Data(N+1,M) AND <Contour(I)>Data(N+1,M+1) THEN GOTO P2
1760 IF <Contour(I)>=Data(N+1,M) AND <Contour(I)>>Data(N+1,M+1) THEN GOTO P2
1770 IF L=3 THEN GOTO Plot
1780 IF <Contour(I)>=Data(N+1,M+1) AND <Contour(I)><Data(N,M+1) THEN GOTO P3
1790 IF <Contour(I)>=Data(N+1,M+1) AND <Contour(I)>Data(N,M+1) THEN GOTO P3
1800 IF <Contour(I)>=Data(N+1,M+1) AND <Contour(I)>>Data(N,M+1) THEN GOTO P3
1810 IF L=3 THEN GOTO Plot
1820 IF <Contour(I)>=Data(N,M+1) AND <Contour(I)><Data(N,M) THEN GOTO P4
1830 IF <Contour(I)>=Data(N,M+1) AND <Contour(I)>Data(N,M) THEN GOTO P4
1840 IF <Contour(I)>=Data(N,M+1) AND <Contour(I)>>Data(N,M) THEN GOTO P4

```

```

1850 IF L=3 THEN GOTO Plot
1860 NEXT N
1870 NEXT M
1880 NEXT I
1890 RETURN
1900 STOP
1910 P1: Xline(L)=ABS((Contour(I)-Data(N,M))/(Data(N,M)-Data(N+1,M)))+(X(N+1,M)-
X(N,M))+X(N,M)
1920 Yline(L)=Y(N,M)
1930 L=L+1
1940 GOTO 1740
1950 P2: Yline(L)=ABS((Contour(I)-Data(N+1,M))/(Data(N+1,M)-Data(N+1,M+1)))+Y(N
+1,M+1)-Y(N+1,M))+Y(N+1,M)
1960 Xline(L)=X(N+1,M)
1970 L=L+1
1980 GOTO 1770
1990 P3: Xline(L)=-ABS((Contour(I)-Data(N+1,M+1))/(Data(N,M+1)-Data(N+1,M+1)))+
(X(N+1,M+1)-X(N,M+1))+X(N+1,M+1)
2000 Yline(L)=Y(N,M+1)
2010 L=L+1
2020 GOTO 1810
2030 P4: Yline(L)=-ABS((Contour(I)-Data(N,M+1))/(Data(N,M+1)-Data(N,M)))*(Y(N,M+
1)-Y(N,M))+Y(N,M+1)
2040 Xline(L)=X(N,M+1)
2050 PRINTER IS 0
2060 L=L+1
2070 GOTO 1850
2080 Plot: REM THIS SUBROUTINE DRAWS THE CONTOUR
2090 MOVE Xline(1),Yline(1)
2100 DRAW Xline(2),Yline(2)
2110 GOTO 1860
2120 STOP
2130 Grid: REM PROGRAM TO LOAD VALUES IN X,Y MATRIX
2140 Y1=0
2150 FOR J=1 TO 11 STEP 1
2160 X1=0
2170 FOR I=1 TO 11 STEP 1
2180 X(I,J)=X1
2190 X1=X1+.5
2200 Y(I,J)=Y1
2210 NEXT I
2220 Y1=Y(I-1,J)+.5
2230 NEXT J
2240 RETURN
2250 STOP
2260 Sort: REM THIS SECTION SORTS THE MEASURED DATA ARRAY INTO THE MATRIX
2270 READ N,M,L,S,J
2280 GOSUB Load
2290 IF J<11 THEN GOTO 2270
2300 RETURN
2310 Load: I=1
2320 FOR K=N TO M STEP L
2330 Data(I,J)=V(K)
2340 I=I+S
2350 NEXT K
2360 RETURN
2370 STOP
2380 Data: REM THIS SUBROUTINE LOADS THE RAW DATA INTO V
2390 GOTO 2420 ! THIS JUMPS OVER THE NEXT LINE DEL IT IF YOU WANT DATA FROM
TAPE
2400 READ #1,Record;Name$,Reading(*),Std(*),Range(*)
2410 IF Ident$="H" THEN GOTO 2450
2420 READ #2;R(*),S(*),F(*)
2430 READ #3;R1(*),S1(*),F1(*)
2440 GOTO 2490
2450 READ #4;R(*),S(*),F(*)

```

```

2460 FEND #5;R1++,$1(*),F1++
2470 PRINTER IS 0
2480 PRINT PAGE
2490 FOR I=1 TO 70 STEP 1
2500 IF Range(I)=1 THEN GOTO Low
2510 IF Range(I)=2 THEN GOTO High
2520 Low: FOR J=1 TO 199 STEP 1
2530 IF (Reading(I)=F(J)) AND (Reading(I)<F(J+1)) THEN GOTO Value
2540 NEXT J
2550 PRINT "VALUE OF DATA IN 5300B FREQ. NOT FOUND ON LOW LOOK UP TABLE"
2560 PRINT "VALUE IS=",Reading(I)
2570 V(I)=0
2580 GOTO 2740 ! GO TO NEXT I
2590 Value: M=LGT(R(J+1)-R(J))/LGT(F(J+1)-F(J)) ! LINEAR EXTRAP.
2600 B=LGT(R(J))-M*LGT(F(J))
2610 V(I)=10*(M*LGT(Reading(I))+B)
2620 GOTO 2740
2630 High: FOR J=1 TO 199 STEP 1
2640 IF (Reading(I)=F1(J)) AND (Reading(I)<F1(J+1)) THEN GOTO Value2
2650 NEXT J
2660 PRINT "VALUE OF DATA IN 5300B FREQ NOT FOUND IN HIGH LOOK UP TABLE"
2670 PRINT "VALUE IS=",Reading(I)
2680 V(I)=1.5
2690 GOTO 2740 ! GO TO NEXT I
2700 Value2: M=LGT(R1(J+1)-R1(J))/LGT(F1(J+1)-F1(J))
2710 B=LGT(R1(J))-M*LGT(F1(J))
2720 V(I)=10*(M*LGT(Reading(I))+B)
2730 GOTO 2740
2740 NEXT I
2750 RETURN
2760 STOP
2770 REM THE FOLLOWING DATA STATEMENTS ARE USED IN 'Sort'
2780 DATA 1,6,1,2,1,12,7,-1,2,3,13,18,1,2,5,29,19,-1,1,7,30,40,1,1,6
2790 DATA 51,41,-1,1,9,52,62,1,1,10,73,63,-1,1,11
2800 END
2810 F111: REM THIS SUBROUTINE FILLS THE DATA MATRIX
2820 SHORT B(3),A(3,3),R1(3,3),C(3),E(3)
2830 MAT B=CON
2840 MAT A=CON
2850 U=2
2860 FOR J=1 TO 5 STEP 2
2870 FOR I=1 TO 9 STEP 2
2880 GOSUB Mat
2890 B(2)=X(I+1,J)
2900 B(3)=Y(I+1,J)
2910 Data(I+1,J)=DOT(C,B)
2920 B(2)=X(I,J+1)
2930 B(3)=Y(I,J+1)
2940 Data(I,J+1)=DOT(C,B)
2950 B(2)=X(I+1,J+1)
2960 B(3)=Y(I+1,J+1)
2970 Data(I+1,J+1)=DOT(C,B)
2980 NEXT I
2990 NEXT J
3000 U=-2
3010 I=11
3020 FOR J=3 TO 7 STEP 2
3030 GOSUB Mat
3040 B(2)=X(I,J-1)
3050 B(3)=Y(I,J-1)
3060 Data(I,J-1)=DOT(C,B)
3070 NEXT J
3080 RETURN
3090 STOP
3100 Mat: A(1,2)=X(I,J)
3110 A(1,3)=Y(I,J)

```

```
3120  A(2,2)=X(I+U,J)
3130  A(2,3)=Y(I+U,J)
3140  A(3,2)=X(I,J+U)
3150  A(3,3)=Y(I,J+U)
3160  E(1)=Data(I,J)
3170  E(2)=Data(I+U,J)
3180  E(3)=Data(I,J+U)
3190  MAT A1=INV(A)
3200  MAT C=A1*E
3210  RETURN
3220  STOP
3230 Label: REM THIS SECTION PRINTS THE LABELS ON THE GRAPHS
3240  PRINT LIN(S),Label1$
3250  PRINT Label2$
3260  PRINT Label3$
3270  RETURN
3280 Print: REM THIS SECTION PRINTS THE DATA
3290  FFINGER IS 0
3300  PRINT PAGE
3310  PRINT "POINT"           FIELD STRENGTH"
3320  FOR I=1 TO 73 STEP 1
3330  PRINT I,V(I)
3340  NEXT I
3350  RETURN
```

```

10      REM THIS IS THE MAIN PROGRAM FOR EM FIELD DATA ANALYSIS
20      REM REF TEST PLAN:FILE NO.3
30      PRINTER IS 16
40      OPTION BASE 1
50      SHORT Reading(80),Std(80),Stderr(80),F2(20),F(2000),R(2000),S(2000),Range(30)
60      DIM Label1$(80),Label2$(80),Label3$(80),Name$(50)
70      ASSIGN #1 TO "DATA"
80      ASSIGN #2 TO "ULOW"
90      ASSIGN #3 TO "HIGH"
100     ASSIGN #4 TO "HLOW"
110     ASSIGN #5 TO "HHIGH"
111     GCLEAR
120     Signal=152.8
130     Count=0
140     PRINT "YOU ARE ALLOWED 3 LINES OF COMMENT (80 CHARACTERS) WHICH WILL AFFECT
R ON ALL DATA OUTPUT."
150     INPUT "PLEASE ENTER EACH LINE OF COMMENT AND PUSH 'CONT' AFTER EACH LINE",
Label1$,Label2$,Label3$
160     INPUT "DO YOU WANT TO ENTER DATA FROM THE KEYBOARD?(TYPE YES OR NO)",B$
170     IF B$="YES" THEN GOTO Enter
180     INPUT "WHAT IS THE RECORD NUMBER OF THE DATA YOU WANT TO SEE?",Record
190     READ #1,Record;Name$,Reading(*),Std(*),Range(*)
200     PRINT "THE RECORD NAME FOUND IS";Name$
210     INPUT " IS THIS A E FIELD OR H FIELD SCAN?(TYPE E OR H)",Ident$
220     IF Ident$="E" THEN Limit=3
230     IF Ident$="H" THEN Limit=3.5
240     GOSUB Plotco
250     END
260 Enter: PRINTER IS 16
270     INPUT "DO YOU WANT TO ENTER Reading(FREQ) OR V(V/m)?(TYPE Read OR V)",B$
280     IF B$="V" THEN GOTO Pass1
290     PRINT "ENTER DATA FROM THE KEYBOARD IN THE FOLLOWING ORDER"
300     PRINT "Reading ,Range"
310     PRINT "TYPE ANY NUMBER GREATER THAN 2 FOR Range TO EXIT AND BEGIN CALCULAT
IONS"
320     FOR I=1 TO 73 STEP 1
330     INPUT Reading(I),Range(I)
340     IF Range(I)>2 THEN GOTO Pass
350     NEXT I
360 Pass: Range(I)=0
370     Reading(I)=0
380     GOTO 210
390 Pass1: PRINT "ENTER VALUES OF V IN V/m OR mR/m;TYPE A NUMBER >200 TO EXIT"
400     FOR I=1 TO 73 STEP 1
410     INPUT V(I)
420     IF V(I)>200 THEN GOTO Pass2
430     NEXT I
440 Pass2: V(I)=0
450     GOTO 430
460 Plotco: REM THIS IS THE CONTOUR SECTION
470     SHORT X(11,11),Y(11,11),Data(11,11),Xline(2),Yline(2),Contour(30),V(80),Nd
b(80)
480     GOSUB Data
490     GOSUB Grid
500     GOSUB Convt1
510     GOSUB Print

```

```

520 GOSUB Sort
530 GOSUB F111
540 GOSUB Contour2
550 PRINTER IS 16
560 PRINT "WHAT ARE THE VALUES OF THE CONTOURS YOU WANT TO SEE?ENTER 100 AS L
AST VALUE"
570 FOR I=1 TO 30 STEP 1
580 INPUT "CONTOUR VALUE=",Contour(I)
590 IF Contour(I)=100 THEN GOTO 610
600 NEXT I
610 Conmax=I-1
620 GOSUB Draw
630 GOSUB Contour
640 GOSUB Label
650 PRINTER IS 16
660 INPUT "DO YOU WANT A HARD COPY?",R$
670 IF R$="YES" THEN DUMP GRAPHICS
680 PRINTER IS 0
690 PRINT LIN(3),"CONTOUR VALUES(dB)="
700 FOR I=1 TO Conmax STEP 1
710 PRINT Contour(I);
720 NEXT I
730 PRINT
740 INPUT "DO YOU WANT TO PLOT MORE CONTOURS?(TYPE YES OR NO)",B$
750 IF B$="YES" THEN GOTO 550
760 RETURN
770 STOP
780 END
790 Draw: REM THIS SUBROUTINE DRAWS THE GRID
800 CLS
810 PRINTER IS 0
820 PRINT PAGE
830 GRAPHICS
840 LINE TYPE 3,8
850 DEG
860 LOCATE 20,80,20,80
870 SCALE 0,5,0,5
880 M=1
890 FOR N=1 TO 11 STEP 2
900 MOVE X(N,M),Y(N,M)
910 DRAW X(N,11),Y(N,11)
920 NEXT N
930 N=1
940 FOR M=1 TO 11 STEP 2
950 MOVE X(N,M),Y(N,M)
960 DRAW X(11,M),Y(11,M)
970 NEXT M
980 M=7
990 FOR N=1 TO 11 STEP 1
1000 MOVE X(N,M),Y(N,M)
1010 DRAW X(N,11),Y(N,11)
1020 NEXT N
1030 N=1
1040 FOR M=7 TO 11 STEP 1
1050 MOVE X(N,M),Y(N,M)
1060 DRAW X(11,M),Y(11,M)
1070 NEXT M
1080 RETURN
1090 STOP
1100 Contour: REM THIS SUBROUTINE PLOTS THE CONTOURS
1110 GRAPHICS
1120 LINE TYPE 1
1130 FOR I=1 TO Conmax STEP 1
1140 FOR M=1 TO 10 STEP 1
1150 FOR N=1 TO 10 STEP 1
1160 L=1

```

```

1170 IF (Contour(I)=Data(N,M)) AND (Contour(I)<Data(N+1,M)) THEN GOTO F1
1180 IF (Contour(I)=Data(N,M)) AND (Contour(I)>Data(N+1,M)) THEN GOTO F1
1190 IF (Contour(I)=Data(N,M)) AND (Contour(I)<>Data(N+1,M)) THEN GOTO F1
1200 IF (Contour(I)=Data(N+1,M)) AND (Contour(I)<Data(N+1,M+1)) THEN GOTO F2
1210 IF (Contour(I)=Data(N+1,M)) AND (Contour(I)>Data(N+1,M+1)) THEN GOTO F2
1220 IF (Contour(I)=Data(N+1,M)) AND (Contour(I)<>Data(N+1,M+1)) THEN GOTO F2
1230 IF L=3 THEN GOTO Plot
1240 IF (Contour(I)=Data(N+1,M+1)) AND (Contour(I)<Data(N,M+1)) THEN GOTO F3
1250 IF (Contour(I)=Data(N+1,M+1)) AND (Contour(I)>Data(N,M+1)) THEN GOTO F3
1260 IF (Contour(I)=Data(N+1,M+1)) AND (Contour(I)<>Data(N,M+1)) THEN GOTO F3
1270 IF L=3 THEN GOTO Plot
1280 IF (Contour(I)=Data(N,M+1)) AND (Contour(I)<Data(N,M)) THEN GOTO F4
1290 IF (Contour(I)=Data(N,M+1)) AND (Contour(I)>Data(N,M)) THEN GOTO F4
1300 IF (Contour(I)=Data(N,M+1)) AND (Contour(I)<>Data(N,M)) THEN GOTO F4
1310 IF L=3 THEN GOTO Plot
1320 NEXT N
1330 NEXT M
1340 NEXT I
1350 RETURN
1360 STOP
1370 F1: Xline(L)=ABS((Contour(I)-Data(N,M))/(Data(N,M)-Data(N+1,M))+X(N+1,M--X(N,M)+X(N,M))
1380 Yline(L)=Y(N,M)
1390 L=L+1
1400 GOTO 1200
1410 F2: Yline(L)=ABS((Contour(I)-Data(N+1,M))/(Data(N+1,M)-Data(N+1,M+1))+Y(N+1,M--Y(N+1,M)+Y(N+1,M))
1420 Xline(L)=X(N+1,M)
1430 L=L+1
1440 GOTO 1200
1450 F3: Xline(L)=-ABS((Contour(I)-Data(N+1,M+1))/(Data(N,M+1)-Data(N+1,M+1))+X(N+1,M+1--X(N,M+1)+X(N,M+1))
1460 Yline(L)=Y(N,M+1)
1470 L=L+1
1480 GOTO 1200
1490 F4: Yline(L)=-ABS((Contour(I)-Data(N,M+1))/(Data(N,M+1)-Data(N,M))+Y(N,M+1--Y(N,M)+Y(N,M+1))
1500 Xline(L)=X(N,M+1)
1510 PRINTER IS 0
1520 L=L+1
1530 GOTO 1310
1540 Plot: REM THIS SUBROUTINE DRAWS THE CONTOUR
1550 MOVE Xline(1),Yline(1)
1560 DRAW Xline(2),Yline(2)
1570 GOTO 1320
1580 STOP
1590 Grid: REM PROGRAM TO LOAD VALUES IN X,Y MATRIX
1600 Y=0
1610 FOR J=1 TO 11 STEP 1
1620 X1=0
1630 FOR I=1 TO 11 STEP 1
1640 X(I,J)=X1
1650 X1=X1+.5
1660 X(I,J)=Y1
1670 NEXT I
1680 Y1=Y(I-1,J)+.5
1690 NEXT J
1700 RETURN
1710 STOP
1720 Sort: REM THIS SECTION SORTS THE MEASURED DATA ARRAY INTO THE MATRIX
1730 READ N,M,L,S,J
1740 SUBR Load
1750 IF T=11 THEN GOTO 1730
1760 RETURN
1770 FOR I=1
1780 TO M STEP L

```

```

1790 Data(I,J)=V(I,J)
1800 I=I+1
1810 NEXT I
1820 RETURN
1830 STOP
1840 REM THIS SUBROUTINE LOADS THE RAW DATA INTO V
1850 IF Ident$="H" THEN GOTO 1890
1860 READ #2;R(+),S(+),F(+)
1870 READ #3;R1(+),S1(+),F1(+)
1880 GOTO 1920
1890 READ #4;R(+),S(+),F(+)
1900 READ #5;R1(+),S1(+),F1(+)
1910 PRINTER IS 0
1920 FOR I=1 TO 73 STEP 1
1930 IF Range(I)=1 THEN GOTO Low
1940 IF Range(I)=2 THEN GOTO High
1950 Low: FOR J=1 TO 199 STEP 1
1960 IF (Reading(I))=F(J) AND (Reading(I)<F1(J+1)) THEN GOTO Value
1970 NEXT J
1980 PRINT "VALUE OF DATA IN 5300B FREQ. NOT FOUND ON LOW LOOK UP TABLE"
1990 PRINT "VALUE IS=",Reading(I)
2000 V(I)=.04
2010 GOTO 2170      ! GO TO NEXT I
2020 value1: M=LGT(R(J)+1)*R(J)/LGT(F(J+1)-F(J))      ! LINEAR EXTRAP.
2030 B=LGT(R(J))-M*LGT(F(J))
2040 V(I)=10*(M*LGT(Reading(I))+B)
2050 GOTO 2170
2060 High: FOR J=1 TO 199 STEP 1
2070 IF (Reading(I))=F1(J) AND (Reading(I)<F1(J+1)) THEN GOTO Value2
2080 NEXT J
2090 PRINT "VALUE OF DATA IN 5300B FREQ. NOT FOUND IN HIGH LOOK UP TABLE"
2100 PRINT "VALUE IS=",Reading(I)
2110 V(I)=1.5
2120 GOTO 2170      ! GO TO NEXT I
2130 value2: M=LGT(R1(J+1)-R1(J))/LGT(F1(J+1)-F1(J))
2140 B=LGT(R1(J))-M*LGT(F1(J))
2150 V(I)=10*(M*LGT(Reading(I))+B)
2160 GOTO 2170
2170 NEXT I
2180 RETURN
2190 STOP
2200 REM THE FOLLOWING DATA STATEMENTS ARE USED IN Sort
2210 DATA 1,6,1,2,1,12,7,-1,2,3,13,18,1,2,5,29,19,-1,1,7,30,40,1,1,8
2220 DATA 51,41,-1,1,9,52,62,1,1,10,73,63,-1,1,11
2230 END
2240 REM THIS SUBROUTINE FILLS THE DATA MATRIX
2250 SUBROUTINE B(3),A(3,3),C(3),E(3)
2260 M=1,I=1,N=1
2270 P=1,B=1,C=1
2280 M=1,I=1,N=1
2290 FOR I=1 TO 5 STEP 2
2300 FOR J=1 TO 9 STEP 2
2310 GOSUB Mat
2320 B(2)=X(I+1,J)
2330 E(3)=Y(I+1,J)
2340 Data(I+1,J)=DOT(C,B)
2350 E(2)=X(I,J+1)
2360 B(3)=Y(I,J+1)
2370 Data(I,J+1)=DOT(C,B)
2380 E(2)=X(I+1,J+1)
2390 B(3)=Y(I+1,J+1)
2400 Data(I+1,J+1)=DOT(C,B)
2410 NEXT I
2420 NEXT J
2430 I=1
2440 N=1

```

```

2450 FOR J=3 TO 7 STEP 2
2460 GOSUB Mat
2470 B(2)=X(I,J-1)
2480 B(3)=Y(I,J-1)
2490 Data(I,J-1)=DOT(C,B)
2500 NEXT J
2510 RETURN
2520 STOP
2530 Mat: A(1,2)=X(I,J)
2540 A(1,3)=Y(I,J)
2550 A(2,2)=X(I+U,J)
2560 A(2,3)=Y(I+U,J)
2570 A(3,2)=X(I,J+U)
2580 A(3,3)=Y(I,J+U)
2590 E(1)=Data(I,J)
2600 E(2)=Data(I+U,J)
2610 E(3)=Data(I,J+U)
2620 MAT A1=INV(A)
2630 MAT C=A1*E
2640 RETURN
2650 STOP
2660 Label1: REM THIS SECTION PRINTS THE LABELS ON THE GRAPHS
2670 PRINT LIN(5),Label1$
2680 PRINT Label12$
2690 PRINT Label13$
2700 RETURN
2710 Print: REM THIS SECTION PRINTS THE DATA
2720 PRINTER IS 0
2730 PRINT "TEST NO.";Record
2740 PRINT LIN(3)
2750 PRINT "POINT" LEVEL (dB DOWN FROM INCIDENT FIELD)"
2760 GOTO 2790
2770 IF Ident$="E" THEN PRINT " CM/m"
2780 IF Ident$="H" THEN PRINT " dB/m"
2790 FOR I=1 TO 73 STEP 1
2800 PRINT I,Vdb(I)
2810 NEXT I
2820 RETURN
2830 Conv1: REM THIS SECTION CONVERTS FIELD STR. TO dB DOWN
2840 FOR I=1 TO 73 STEP 1
2850 IF Ident$="E" THEN Vdb(I)=20+LGT(V(I)/1E-6)-Signal
2860 IF Ident$="H" THEN Vdb(I)=20+LGT(V(I)/1E-3)-Signal+20*LGT(377)
2870 NEXT I
2880 RETURN
2890 Conv2: REM Converts Data TO dB DOWN
2900 IF Ident$="E" THEN GOTO Xx
2910 IF Ident$="H" THEN GOTO Uu
2920 PRINT "ERROR E OR H NOT FOUND"
2930 STOP
2940 Xx: FOR M=1 TO 11 STEP 1
2950 FOR N=1 TO 11 STEP 1
2960 Data(N,M)=20+LGT(Data(N,M)/1E-6)-Signal
2970 NEXT N
2980 NEXT M
2990 GOTO Return
3000 Uu: FOR M=1 TO 11 STEP 1
3010 FOR N=1 TO 11 STEP 1
3020 Data(N,M)=20+LGT(Data(N,M)/1E-3)-Signal+20*LGT(377)
3030 NEXT I
3040 NEXT M
3050 Return: RETURN
3060 END

```

APPENDIX G

OPERATING AND MAINTENANCE DATA FOR EM FIELD MAPPING COMPONENTS

G.1 INTRODUCTION

This section contains a description of the measurement system operating procedure along with schematic diagrams and parts lists for the probe signal conditioner, the optic link receiver unit, and the probe position control unit.

G2. OPERATING PROCEDURE

This section contains a description of the measurement system operating procedure for the probe signal conditioner, the optic link receiver unit , and the probe position control unit.

The probe position controller causes the probe to scan in a fixed scan sequence, therefore, proper setting of the probe starting position is extremely important for correct scanning operation. The setting of the probe start position is as follows:

1. Loosen the two screws on the probe carriage so that it slides freely on the thread. This step need only be done for the initial setting up of the probe positioner or when the thread is replaced.
2. Turn Probe Position Controller ON and push the Axial and Radial RESET buttons.
3. Check that the LED in the lower left hand corner of the position indicator matrix lights.
4. The motion in both axes will now correspond to the settings of the radial and axial direction switches. These should now be set to the positive direction.
5. Move the Axial carriage (using the .5cm or 1 cm buttons) such that the back of the motor is 1/8 inch from the back support plate. Note: The reset switch can be used to stop the actuator motion.
6. Move the Radial carriage to the point where the carriage just touches the brass coupler.
7. Move the Radial carriage off the brass coupler to the point where any system backlash is removed. Note the direction switch must be in the positive or middle position.
8. Check that the Radial carriage is no more than 1/16 inch from the brass coupler.
9. Push the RESET button on both the Radial and Axial channel.

10. Move the probe carriage so that it is 3/32 inch from the side that the scan will start. (The side is determined by how the thread is installed, check this by tracing the thread routing.) Tighten the plexiglass mount to the teflon slide such that the thread is pinched between them.
11. The probe positioner can now scan the 73 positions indicated in Figures 7 and 9 by actuating the 1 cm and 0.5 cm step switches. This must be accomplished in ascending numerical order from position 1 to position 73 in order to obtain the highest possible mechanical positioning accuracy. In this way, the probe carriage is driven by the thread-pulley system in one direction only, minimizing the effects of friction and backlash.
12. The Probe Position Control Unit automatically changes scanning directions at the grid boundaries as manual scanning proceeds. Accordingly, the scanning sequence described in Step 11 above should be followed exactly to prevent the probe from getting out of step with the indicated position on the light-emitting diode display, and to minimize the risk of probe damage. When performing manual measurements observe the frequency counter output to determine over-range conditions and change the range switch on the signal conditioner accordingly.

When a scan is complete, the probe can be moved to its start position by following Steps 2 to 9 in the instructions for setting probe positioner start position.

Automatic Control of the scanning and measurement process may be obtained through the use of the IEEE 488 bus-controlled relay actuator (H.P. 59306A). This allows the Probe Position Control Unit and the Range Switch on the Signal Conditioner to be computer controlled, and completely eliminates Steps 11 and 12 above.

A Measurement system used to automatically map the electric and magnetic fields within a cylinder and missile nosecone is illustrated in Figure 6. The connection of the H.P. 59306A Relay Actuator to the Probe Position Controller is given in Table 3 following.

TABLE 3

LIST OF CONNECTIONS FOR REMOTE CONTROL INTERFACE

H.P. 59306A Relay Actuator Terminal	Connected to Probe Position Control Unit Circuit Designation (Ref. Fig.13)
A1	(Normally Open) N.O. - 1
B1	(Normally Closed) N.C. - 1
C1	(Common) COM
A2	N.O. - 2
B2	N.C. - 2
C2	COM
A3	N.O. - 3
B3	N.C. - 3
C3	COM
A4	N.O. - 4
B4	N.C. - 4
C4	COM
A5	For pneumatic actuator coil
B5	Not used
C5	Pneumatic actuator power supply
A6	Local/Remote coil
B6	Not used
C6	External +20 vdc supply

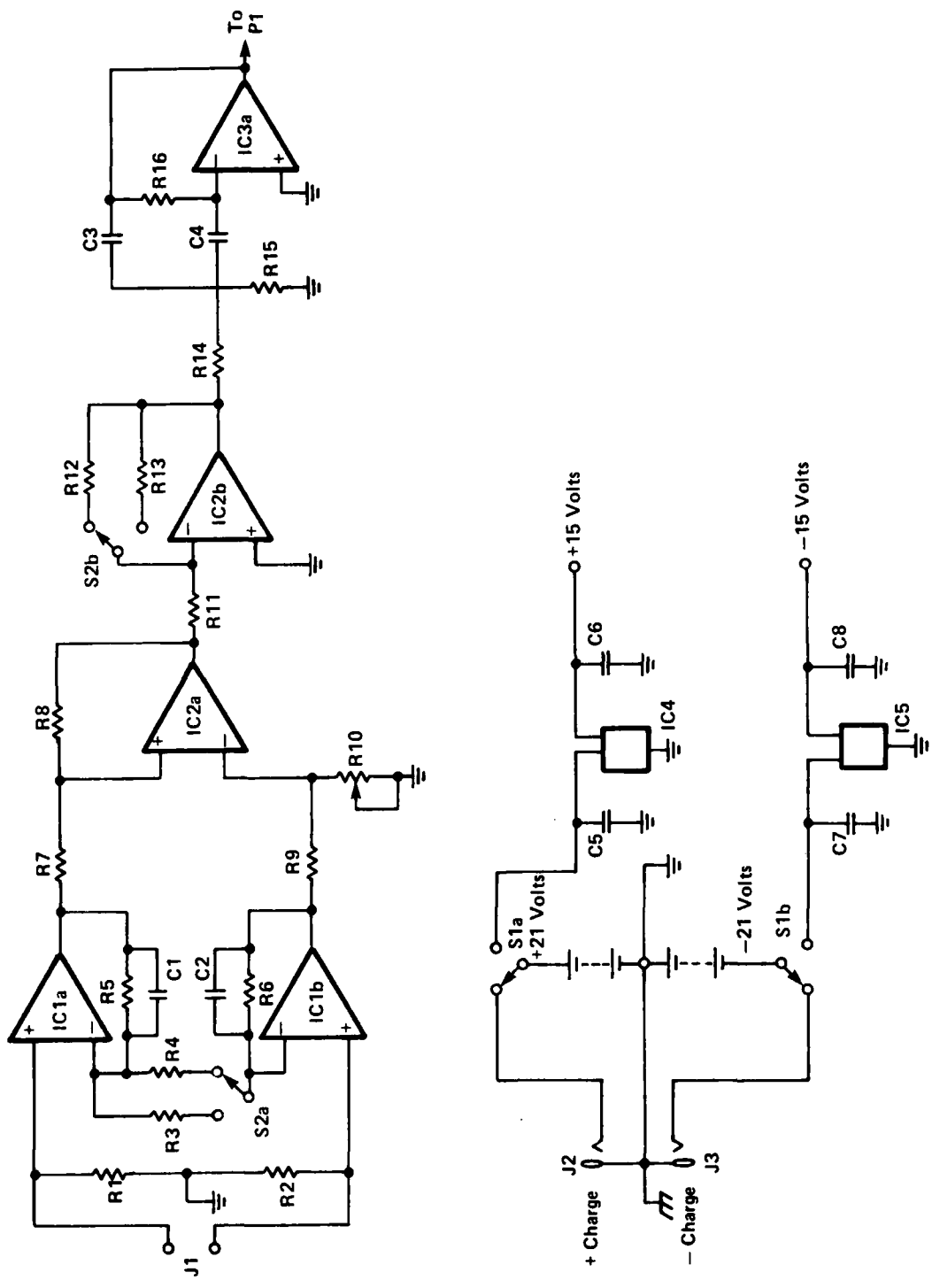


Fig. G-1 Sheet 1 of 2 Schematic Diagram, Signal Conditioner

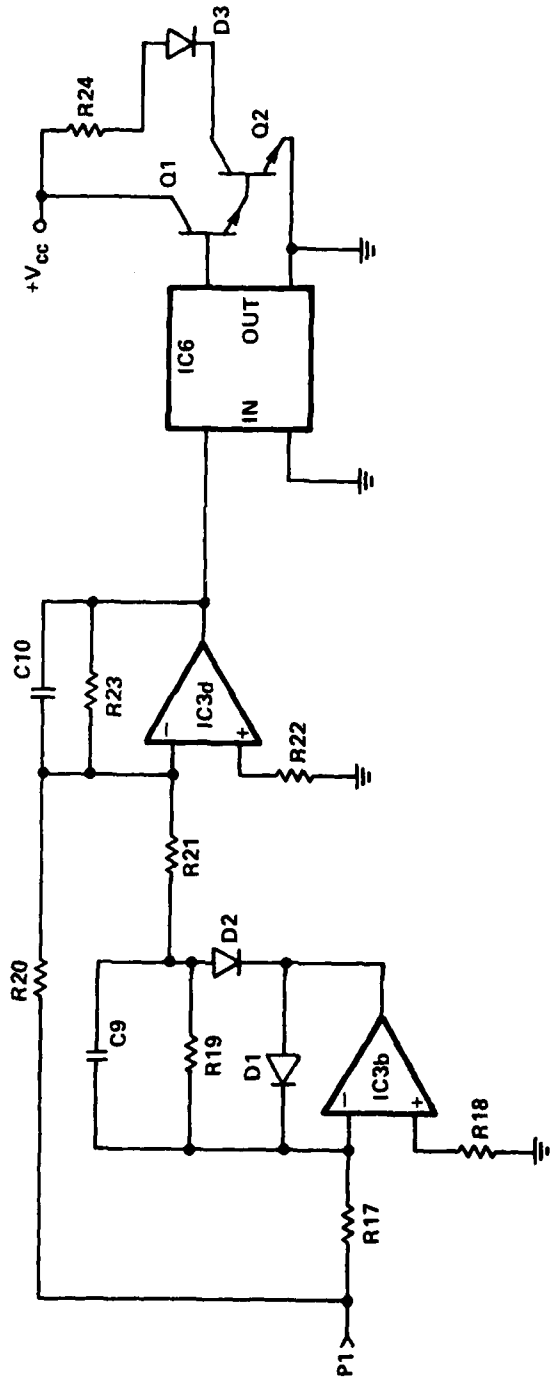


Fig. G-1 Sheet 2 of 2 Schematic Diagram, Signal Conditioner

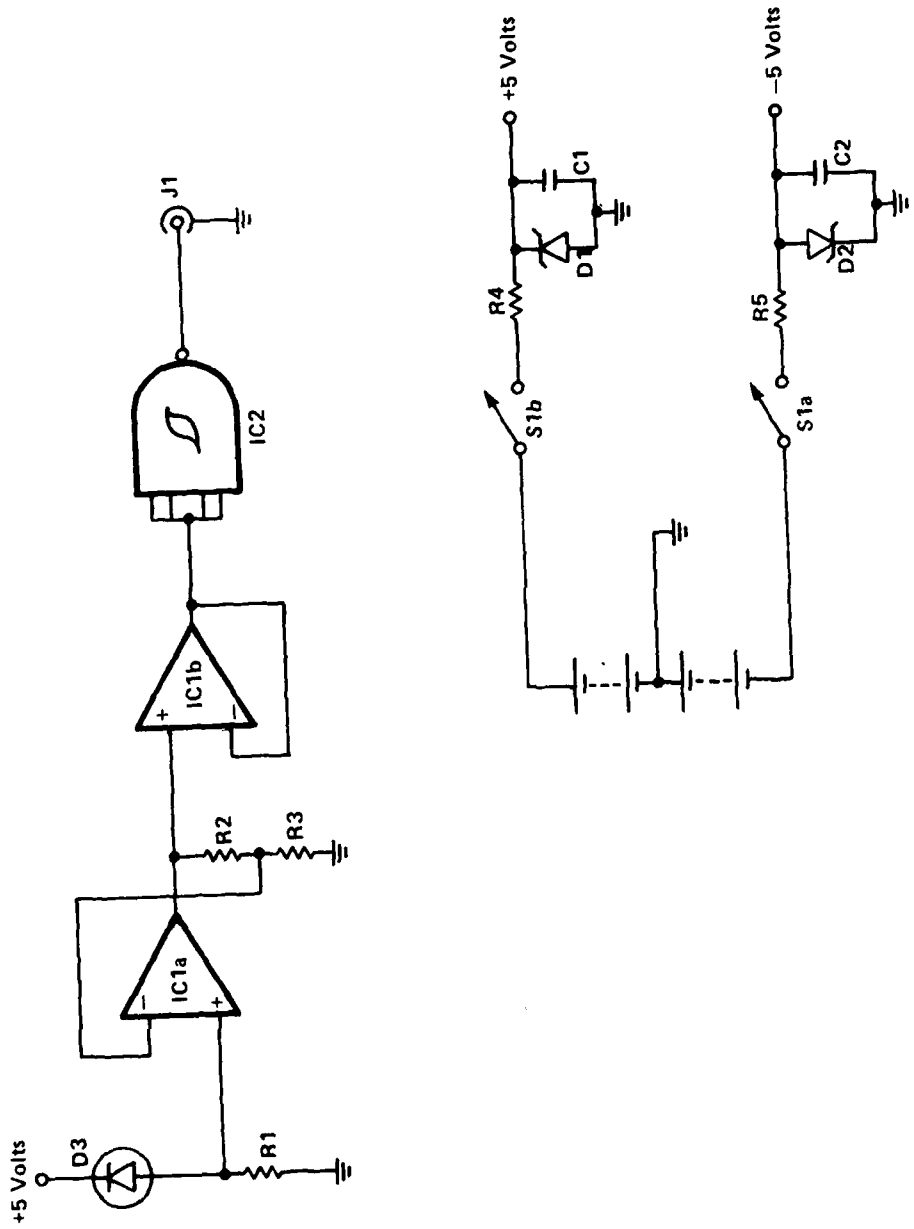
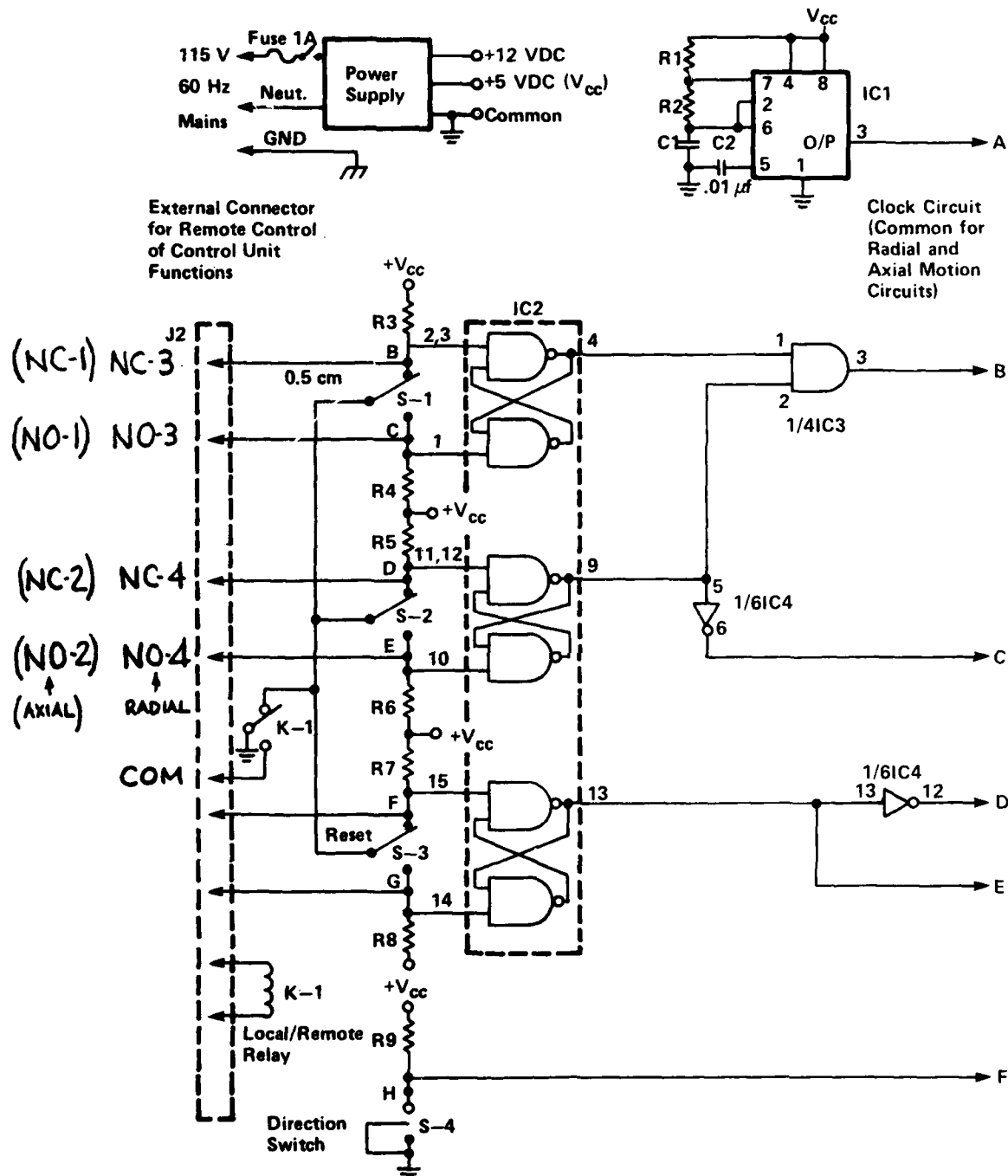


Fig. G-2 Schematic Diagram, Optic Link Receiver Unit



* Note: Circuitry for radial motion is shown, except where indicated. Circuitry for axial motion is identical to that shown for radial motion.

Fig. G-3 Sheet 1 of 4 Probe Position Control Unit

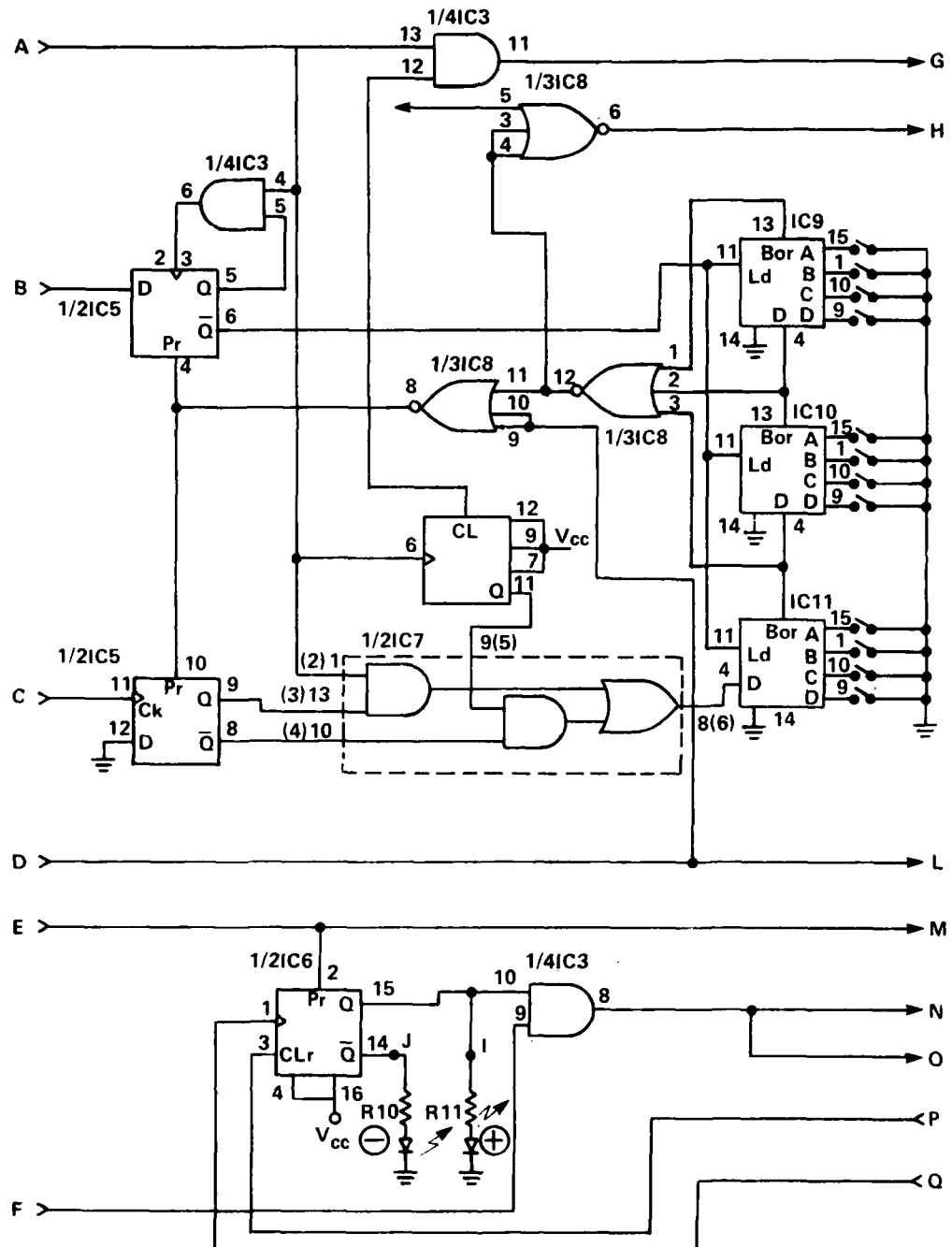


Fig. G-3 Sheet 2 of 4 Probe Position Control Unit

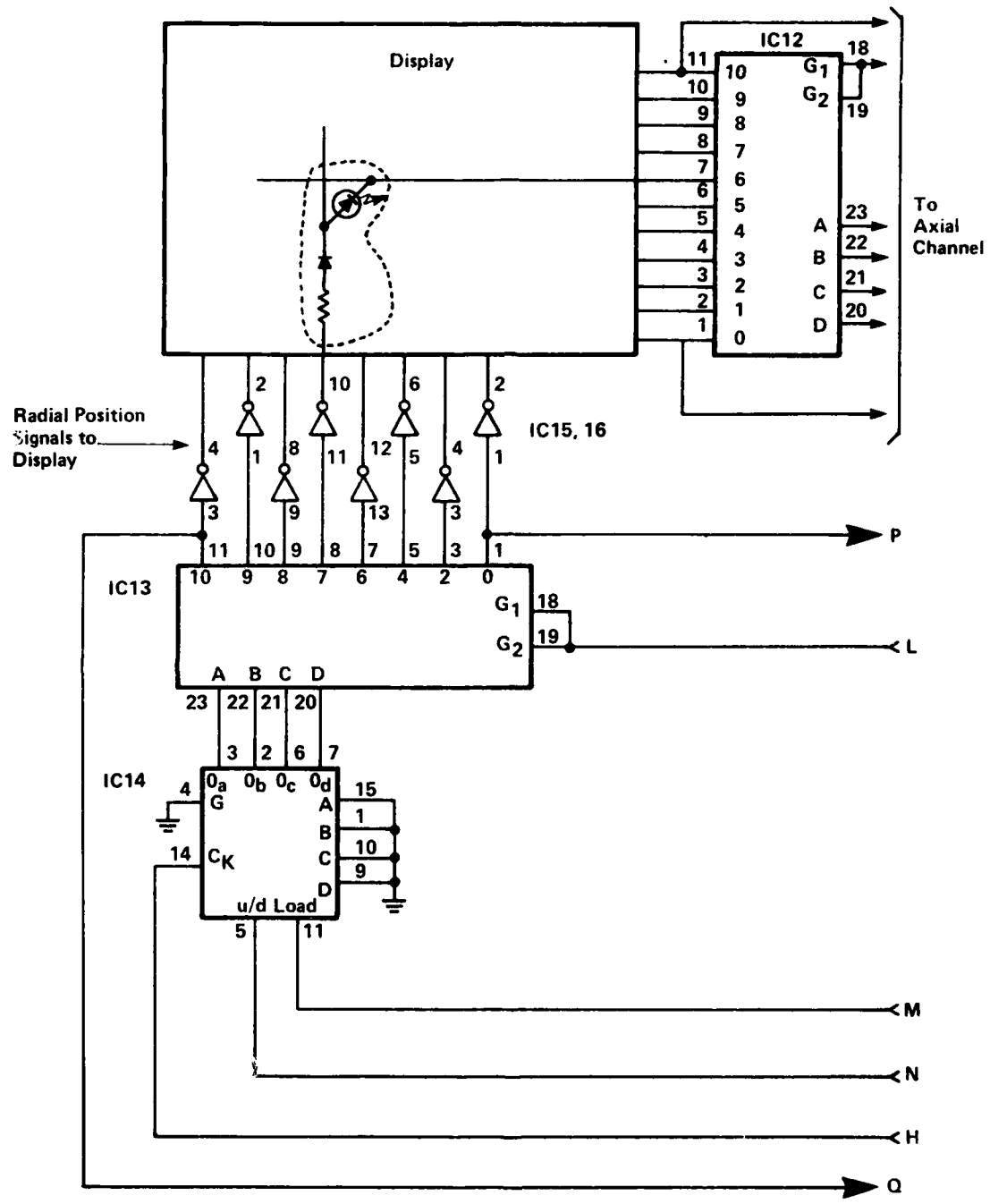


Fig. G-3 Sheet 3 of 4 Probe Position Control Unit

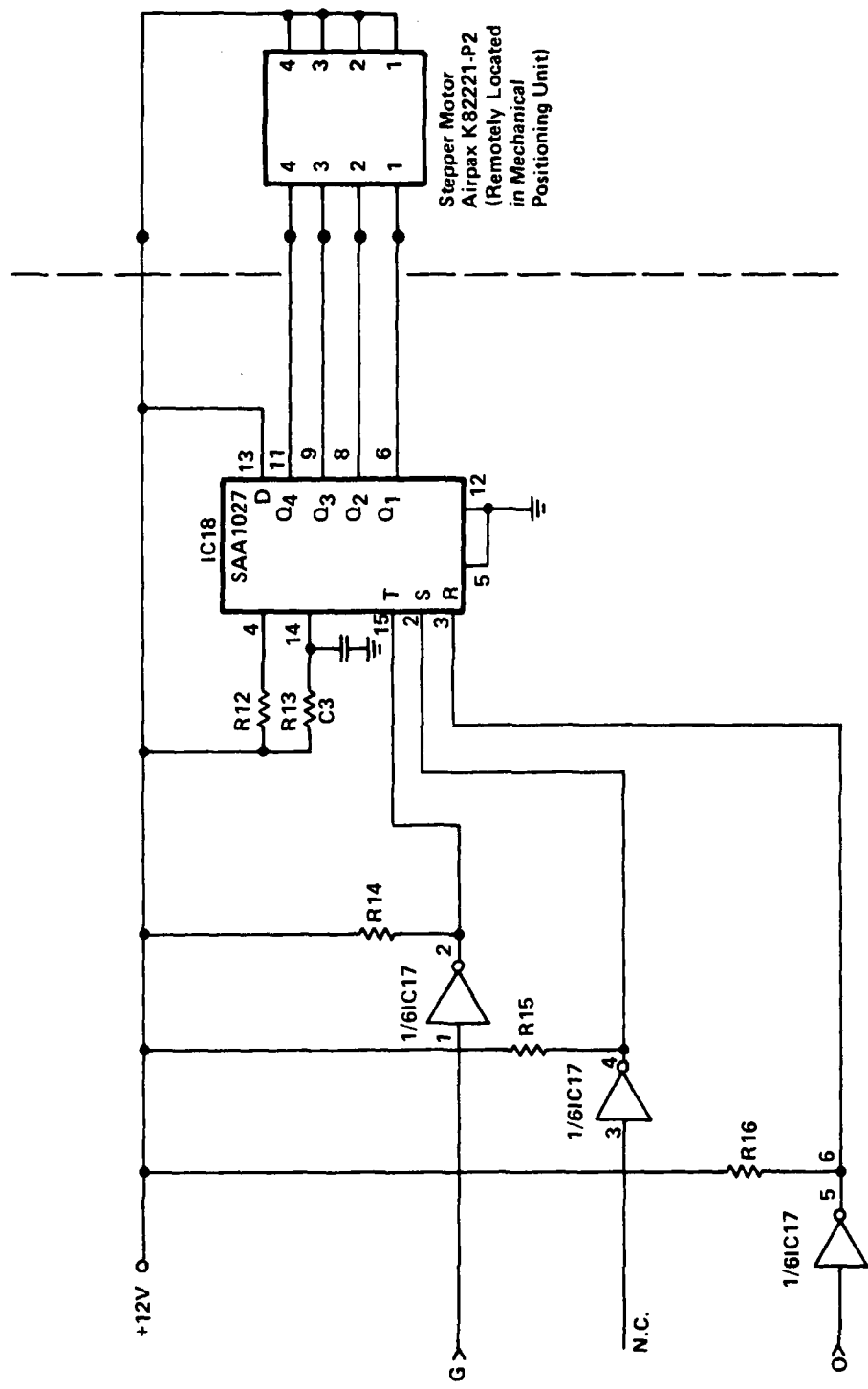


Fig. G-3 Sheet 4 of 4 Probe Position Control Unit

AD-A104 312 BELL NORTHERN RESEARCH LTD OTTAWA (ONTARIO) F/G 16/3
ELECTROMAGNETIC FIELD MAPPING OF CYLINDER AND MISSILE NOSEcone. (U)
JUL 81 R R GOULETTE, K E FELSKER F30602-79-C-0197

UNCLASSIFIED

RADC-TR-81-179

NL

3 or 3
401 A
401 A 2

END
DATE
JULY
10-81
DTIC

PARTS LIST

ELECTRIC FIELD PROBE

Diode	Zero-bias Schottky detector diode	Microwave Associates type MA 40230 Case style 120
Conductive Plastic	Polypenco Conductive TFE monofilament, 0.030" outer diameter. insulated with nylon sheath of 0.005" wall thickness	The Polymer Corp., Reading, Pa. 19603
Conductive Epoxy	ACME E-solder 3021 silver epoxy	ACME Chemicals and Insulation Co., Div. of Allied Products Corp., New Haven, Connecticut, 06505

PARTS LIST

MAGNETIC FIELD PROBE

Diode, conductive plastic,
and conductive epoxy materials are
identical to those listed for the
Electric Field Probe

Wire Used for Coil:

Belden #38 AWG
Magnet Wire

PARTS LIST

SIGNAL CONDITIONER

All fixed resistors are 1/4 watt, 2% tolerance,
film types, Corning Glass Works type FP55 or equivalent,
unless indicated otherwise.

R1	RESISTOR	FIXED	10	Mohm	1/2Watt, 2% IRC type CGH-1/2
R2	"	"	10	Mohm	
R3	"	"	91	ohm	
R4	"	"	3	Kohm	
R5	"	"	20	Kohm	
R6	"	"	20	Kohm	
R7	"	"	10	Kohm	
R8	"	"	10	Kohm	
R9	"	"	10	Kohm	
R10	"	VARIABLE	50	Kohm	Bourns Trimpot Model 3006P-1-503
R11	RESISTOR	FIXED	100	Kohm	
R12	"	"	6.8	Kohm	
R13	"	"	100	Kohm	
R14	"	"	3.3	Kohm	
R15	"	"	130	ohm	
R16	"	"	300	Kohm	
R17	"	"	20	Kohm	
R18	"	"	15	Kohm	
R19	"	"	20	Kohm	
R20	"	"	20	Kohm	
R21	"	"	10	Kohm	
R22	"	"	6.2	Kohm	
R23	"	"	22	Kohm	
R24	"	"	300	ohm	

C1	CAPACITOR, FIXED, CERAMIC, AXIAL LEAD	4700pf, 50v,	5%
C2	" " "	4700pf, 50v,	5%
C3	" " POLYSTYRENE	0.047μf, 60v,	2%
C4	" " "	0.047μf, 60v,	2%
C5	" " CERAMIC, RADIAL LEAD	.47μf, 50v,	10%
C6	" " "	.47μf, 50v,	10%
C7	" " "	.47μf, 50v,	10%
C8	" " "	.47μf, 50v,	10%
C9	CAPACITOR, FIXED, CERAMIC, AXIAL LEAD	800pf, 50v,	5%
C10	CAPACITOR, ALUMINUM ELECTROLYTIC	15μf, 50v,	20%

D1 DIODE, SILICON IN 914

D2 " " IN 914

D3 DIODE, LIGHT EMITTING HP 5082-4855

Q1 TRANSISTOR 2N3904

Q2 " 2N3904

1C1 DUAL BIFET OPERATIONAL AMPLIFIER LF353N

1C2 DUAL BIFET OPERATIONAL AMPLIFIER LF353N

1C3 OPERATIONAL AMPLIFIER MC 3403 P

1C4 VOLTAGE REGULATOR +15 VDC 7815

1C5 VOLTAGE REGULATOR -15 VDC 7915

1C6 VOLTAGE TO FREQUENCY CONVERTER,
ANALOG DEVICES 545

S1 SWITCH TOGGLE DPDT

S2 SWITCH TOGGLE DPDT

J1 CONNECTOR, BNC, MODIFIED

J2 JACK

J3 JACK

B1 BATTERY PACK 16 AA CELLS, NICKEL-CADMIUM
MALLORY TYPE NC-15

B2 BATTERY PACK 16AA CELLS, NICKEL-CADMIUM
MALLORY TYPE NC-15

PARTS LIST

OPTICAL LINK RECEIVER UNIT

NOTE:

(Resistors R1-R5 are Corning Glass Works Type FP55
or equivalent)

R1	RESISTOR,	FIXED,	FILM	430 Kohm, 1/4w, 2%
R2	"	"	"	430 Kohm, 1/4w, 2%
R3	"	"	"	430 Kohm, 1/4w, 2%
R4	"	"	"	130 ohm, 1/4w, 2%
R5	"	"	"	130 ohm, 1/4w, 2%
C1	CAPACITOR,	FIXED, CERAMIC, RADIAL LEAD,	0.47μf, 10%	
C2	"	"	"	0.47μf, 10%
D1	DIODE, SILICON ZENER			1N751A
D2	"	"	"	1N751A
D3	PHOTO DIODE	RCA		C30808
IC1	OPERATIONAL AMPLIFIER			MC3403
IC2	DUAL NAND SCHMITT TRIGGER			7413
S1	SWITCH, DPDT			
J1	JACK, SWITCHCRAFT			3501FP
B1	BATTERY, 9VDC ALKALINE			
B2	"	"	"	

PARTS LIST

FIBER OPTIC CABLE

Fiber Optic Link 20 Ft Length

Part No. LP-20

Instruments for Industry, Inc.

151 Toledo St.,

Farmingdale, N.Y.

11735

PARTS LIST

PROBE POSITIONING UNIT

QTY	DESCRIPTION	PART NO. AND SUPPLIER
2	Stepper Motor with 10:1 Reduction Gear Output Step Angle= 0.75 Degree	Airpax K-82221-P2 Cheshire Div., Cheshire Industrial Park, Cheshire, CT06410
4	Linear Motion Bearings for 1/4" DIA. Shaft. Outer Dia: 1/2" Length: 3/4"	Thompson Part No. A - 4812
1	Connector Plug 25 - Pin	Amphenol Part No. 17 - 90250-15
2	Connector Receptacle 25 - Pin	Amphenol Part No. 17-80250-15

PARTS LIST

PROBE POSITION CONTROL UNIT

C1	CAPACITOR, CERAMIC, AXIAL LEAD				0.01μf, 50v, 10%
C2	" " " "				0.01μf, 50v, 10%
C3	" " " "				0.1 μf, 50v, 10%
R1, 2	RESISTOR, FIXED FILM				470 Kohms, 1/4w, 2%
R3 - R9	" " "				1 Kohm, 1/4w, 2%
R14-R16	" " "				1 Kohm, 1/4w, 2%
R10,11	" " "				200 ohm, 1/4w, 2%
R12	" " "				390 ohm, 1/4w, 2%
R13	" " "				100 ohm, 1/4w, 2%
IC1	INTEGRATED CIRCUIT				LM555
IC2	" "				SN74279
IC3	" "				SN7408
IC4, 15, 16	" "				SN7404
IC5	" "				SN7474
IC6	" "				SN7476
IC7	" "				SN74151
IC8	" "				SN7427
IC9, 10, 11	" "				SN74193
IC12, 13	" "				SN74154
IC14	" "				SN74191
IC17	" "				SN7406
IC18	STEPPER MOTOR DRIVER	AIRPAX	SAA1027		
	+5v SUPPLY REGULATOR	MOTOROLA	78 H05		
	+12v. SUPPLY REGULATOR	MOTOROLA	7812		

NOTE: Resistors R1 to R 16 are Corning Glass Works
Type FP55 or equivalent

MISSION
of
Rome Air Development Center

RADC plans and executes research, development, test and selected acquisition programs in support of Command, Control Communications and Intelligence (C³I) activities. Technical and engineering support within areas of technical competence is provided to ESD Program Offices (POs) and other ESD elements. The principal technical mission areas are communications, electromagnetic guidance and control, surveillance of ground and aerospace objects, intelligence data collection and handling, information system technology, ionospheric propagation, solid state sciences, microwave physics and electronic reliability, maintainability and compatibility.